

Alma Mater Studiorum – Università di Bologna

DOTTORATO DI RICERCA IN
BIOLOGIA CELLULARE MOLECOLARE INDUSTRIALE

Ciclo XXV

Settore Concorsuale di afferenza: 05/F1

Settore Scientifico disciplinare: BIO/13

**HIF1 α REGULATES MITOCHONDRIAL BIOGENESIS AND CELLULAR SENESENCE
INDUCED BY GAMMA RADIATION**

Presentata da: **ANNA BARTOLETTI STELLA**

Coordinatore Dottorato

Relatore

Chiar.ma Prof.ssa Michela Rugolo

Chiar.ma Prof.ssa Michela Rugolo

Correlatore

Dott. Giuseppe Gasparre

Esame finale anno 2013

1. ABSTRACT	4
2. INTRODUCTION	5
2.1 MITOCHONDRIA and CANCER.....	5
2.1.1 Mitochondria origin and morphology	5
2.1.2 Mitochondrial function	7
2.1.3 Mitochondrial network	9
2.1.4 Mitochondrial genome.....	10
2.1.5 Levels of mitochondrial-nuclear communications.....	15
2.1.6 Mitochondria and diseases	22
2.1.7 Mitochondria and cancer	25
2.2 P53: LINK BETWEEN CANCER METABOLISM AND DNA DAMAGE RESPONSE	36
2.2.1 p53 and mitochondria.....	36
2.2.2 p53 and DNA Damage Response.....	37
3. AIMS of the STUDY.....	49
4. MATERIALS AND METHODS.....	50
4.1 Cell cultures.....	50
4.2 γ -rays treatment and HIF1 α compound-mediated stabilization	50
4.3 Western blotting.....	50
4.4 Nucleic acid extraction and reverse transcription	51
4.5 MtDNA sequencing.....	51
4.6 mtDNA copy number	52
4.7 Gene expression analyses via Real-Time PCR.....	52
4.8 Cellular and mitochondrial morphology	52
4.9 ATP synthesis evaluation.....	52
4.10 In silico promoter analyses.....	53
4.11 Chromatine immunoprecipitation.....	53
4.12 P53 PCR amplification and sequencing	54
4.13 TP53, MDM2, HIF1 α and HIF1 α TM cloning.....	54
4.14 Cells transfection.....	56
4.15 HIF1 α degradation evaluation	57
4.16 Senescence-associated β -galactosidase assay.....	57
4.17 Rectal biopsies collection	57
5. RESULTS.....	58
5.1 Effect of γ -rays on mitochondrial biogenesis.....	58

5.2	<i>Role of p53 in gamma-rays induced mitochondrial biogenesis.....</i>	64
5.3	<i>Role of HIF1α stabilization in γ-rays induced mitochondrial biogenesis activation</i>	72
5.4	<i>Role of HIF1α in gamma rays-induced cellular senescence</i>	83
5.5	<i>Evaluating the mtDNA copy number as a predictive marker of HIF1α stabilization after radiotherapy in vivo</i>	88
6.	DISCUSSION.....	91
7.	CONCLUSION.....	97
8.	REFERENCES	98
9.	APPENDIX A.....	108
10.	PUBBLICATION	109

1. ABSTRACT

Radiotherapy (RT) is one of the most effective non-surgical treatments of cancer patients with better functional preservation and less systemic influences. Resistance of tumor cells to RT is one of the most important causes of treatment failure, and the mechanism behind this process remains to be investigated in details. Cellular response to γ -rays is mediated by Ataxia telangiectasia mutated (ATM) kinase and the downstream effector p53. When p53 is phosphorylated, it can transactivate several genes to induce permanent cell cycle arrest (senescence) or apoptosis. Epithelial and mesenchymal cells as well as their derived tumor cells are more resistant to radiation-induced apoptosis and respond mainly by activating senescence. Hence, tumor cells in a senescent state might remain as “dormant” malignant cell and therefore represent a dangerous potential for tumor relapses. Through disruption of p53 function, cells may overcome growth arrest. A particular type of relapses after γ -rays was observed in patients with colorectal cancer, where oncocytic features were acquired in the recurring neoplasia after radiation therapy. Oncocytic tumors are characterized by aberrant biogenesis of nonfunctional mitochondria in their cells. They are mainly non-aggressive neoplasms and their low proliferation degree can be explained by chronic destabilization of HIF1 α , which presides to adaptation to hypoxia and mediates the progression of cancer cells towards malignancy. It has been demonstrated that HIF1 α acts as negative regulator of mitochondrial biogenesis and of oxygen consumption. Moreover, it also plays a pivotal role in hypoxia-related tumor radio-resistance since it is able to interfere with the signalling of p53, and hence to block the senescent program induced by γ -rays. The aim of this project was to verify whether mitochondrial biogenesis can be induced following radiation treatment, in relation of HIF1 α status, and whether such a mechanism is predictive of a senescence response. In this study was demonstrate that mitochondrial biogenesis parameters like mitochondrial DNA copy number could be used for the prediction of hypoxic status of tissue after radiation treatment. γ -rays induce an increase of mitochondrial mass and function, in response to a genotoxic stress that pushes cells into senescence. Mitochondrial biogenesis is only indirectly regulated by p53, whose activation triggers a MDM2-mediated HIF1 α degradation, leading to the release of PGC-1 β inhibition by HIF1 α . On the other hand, this protein blunts the mitochondrial response to γ -rays as well as the induction of p21-mediated cell senescence, indicating prevalence of the hypoxic over the genotoxic response. Finally *in vivo*, post-radiotherapy mtDNA copy number increase well correlates with lack of HIF1 α increase in the tissue, concluding this may be a useful molecular tool to infer the trigger of a hypoxic response during radiotherapy, which may lead to failure of activation of cell senescence.

2. INTRODUCTION

2.1 MITOCHONDRIA and CANCER

2.1.1 *Mitochondria origin and morphology*

Mitochondria have an endosymbiotic origin and retain many vestiges of their bacterial ancestry: a double membrane and a circular genome. Mitochondria resemble microbes in that they are typically about one micrometre in scale and constantly move, divide and fuse to form a dynamic network. Although mitochondria are referred to as semi-autonomous organelles, billions of years of expansive and reductive evolution accompanied by transfer of most of their genes to the nuclear genome have now effectively hard-wired these organelles within eukaryotic cells (Vafai 2012).

Human mtDNA contains only 13 protein-coding genes, as well as the 22 tRNA and 2 ribosomal RNA genes required for their translation. The remaining ~ 1100 proteins necessary for mitochondrial function and structure are encoded by nuclear genome. These nDNA-encoded mitochondrial proteins are translated on cytosolic ribosomes and selectively imported into mitochondrion through various mitochondrial protein import system (Wallace 2005).

Interestingly, mtDNA has a monophyletic origin, whereas the history of the mitochondrial proteome is far more complex. About 400 mitochondrial proteins have a proteobacterial origin, determined by sequence similarity to the closest living ancestral proteobacterial species, *Rickettsia prowazekii*, other 400 proteins were obtained from other bacterial organisms (estimated by determining the number of mitochondrial proteins with homologues in other prokaryotic organisms) and 300 proteins have no homologue in any prokaryotic organisms, and represent a eukaryotic innovation (Vafai 2012) (Fig. 1).

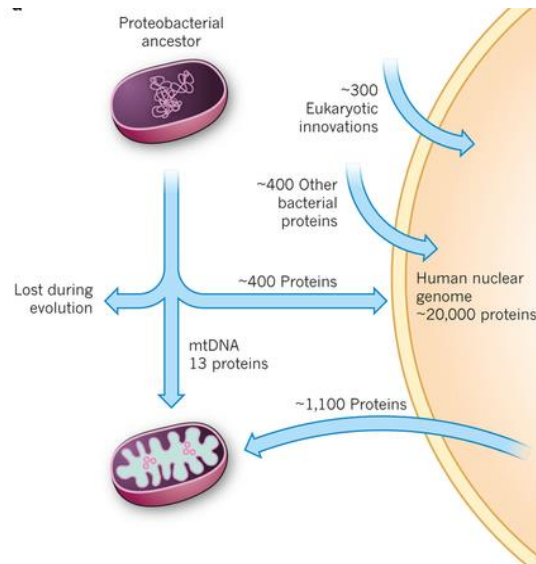


Fig. 1: Mitochondrial proteome evolution. The modern human mitochondrial proteome consists of 13 proteins, which are encoded by mitochondrial DNA (mtDNA) and are a vestige of the original proteobacterial genome, as well as at least 1,100 additional proteins that are known to be encoded by the nuclear genome (nuDNA) (Vafai 2012).

The presence in the mitochondria of both an inner and outer membrane leads to the formation of two aqueous compartments, the matrix and inter-membrane space. The inner mitochondrial membrane (IMM) is the site of oxidative phosphorylation (OXPHOS), as well as numerous other fundamental processes, including protein import and metabolite exchange (Benard 2009). The IMM of mitochondria contain invaginations called *cristae*. The cristae are not random folds in the membrane but rather micro-compartments that open through narrow tubular membrane segments into the peripheral region of the membrane (Mannella 2008). The outer mitochondrial membrane (OMM) is also required for various events related to ATP generation, including the regulation of metabolite transport. OMM is also involved in sensing and transduction of apoptotic stimuli, both in stressed cells and during development. The association of various apoptosis factors, including proteins from the Bcl-2 family, with the OMM, makes this mitochondrial compartment a major site in the apoptotic signal cascade transduction (Benard 2009). The matrix harbors the majority of proteins including various enzymes involved in metabolic processes, such as the tricarboxylic acid (TCA) cycle, fatty-acid oxidation, Fe-S biogenesis, and heme synthesis. The matrix also harbors a number of copies of mtDNA and the protein machinery involved in its maintenance and replication as well as components involved in transcription/translation (Ryan 2007) (Fig. 2).

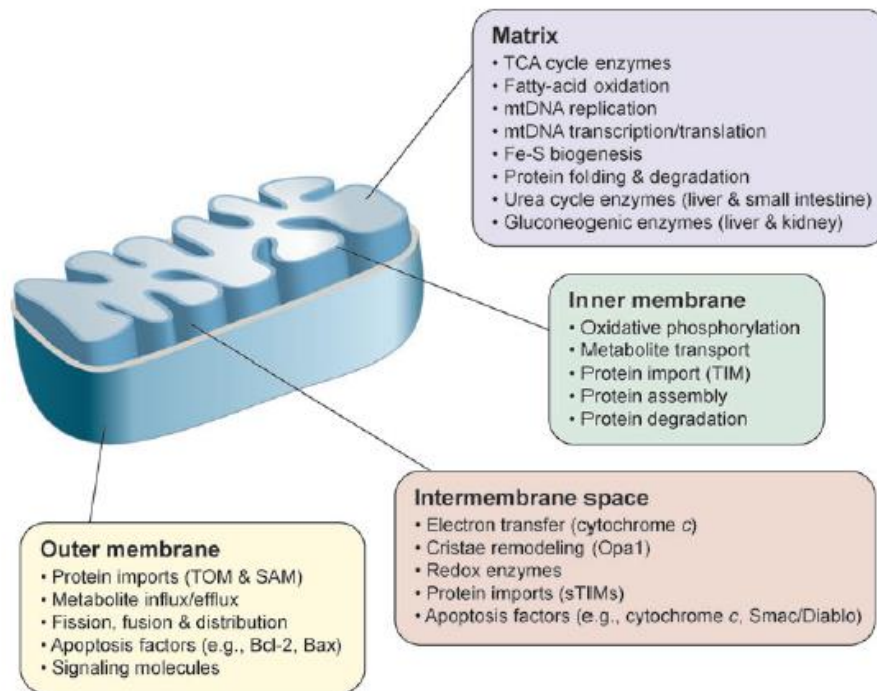


Fig. 2: The mitochondrial subcompartments. Examples of compartment specific processes and proteins within the mitochondrion (Ryan 2007).

2.1.2 Mitochondrial function

The mitochondria perform four central functions in the cell: they (I) provide the majority of the cellular energy in the form of ATP, (II) generate reactive oxygen species (ROS), (III) regulate cytosolic calcium (Ca^{2+}), and (IV) apoptosis through the mitochondrial permeability transition pore (mtPTP) (Wallace 2010).

Energetics in animals is based on the availability of reducing equivalents, consumed as carbohydrates and fats. Glucose is cleaved into pyruvate via glycolysis, and the pyruvate enters the mitochondrion via pyruvate dehydrogenase (PDH) resulting in acetyl-CoA, NADH^+ H^+ , and CO_2 . The acetyl-CoA then enters the TCA cycle which strips the hydrogens from hydrocarbons generating NADH^+ and H^+ . Fatty acids are oxidized within the mitochondrion by beta oxidation to generate acetyl-CoA, NADH^+ plus H^+ , and FADH_2 . Two electrons (reducing equivalents from hydrogen) are transferred from NADH^+ H^+ to the OXPHOS complex NADH dehydrogenase (complex I) or from FADH_2 containing enzymes such as the ETF dehydrogenase or succinate dehydrogenase (SDH, complex II) to reduce ubiquinone (coenzyme Q10, CoQ) to ubiquinol CoQH_2 . The electrons from CoQH_2 are transferred successively to complex III (bc1 complex),

cytochrome c, complex IV (cytochrome c oxidase, COX), and finally to oxygen ($\frac{1}{2}O_2$) to give H_2O . The energy that is released as the electrons flow down the ETC is used to pump protons out across the mitochondrial inner membrane through complexes I, III, and IV creating a proton electrochemical gradient. The potential energy is used for multiple purposes: to import proteins and Ca^{++} into the mitochondrion, to generate heat, and to synthesize ATP within the mitochondrial matrix. The energy to convert $ADP + P_i$ to ATP comes from the flow of protons through the ATP synthetase (complex V) back into the matrix. Matrix ATP is then exchanged for cytosolic ADP by the inner membrane adenine nucleotide translocators (ANTs) (Wallace 2007) (Fig. 3).

Mitochondria also regulate cellular levels of metabolites, amino acids, and cofactors for various regulatory enzymes, including chromatin-modifying histone deacetylases. Moreover, mitochondria play a central role in metal metabolism, synthesizing heme and Fe-S clusters, which are essential components of the major oxygen carrier, hemoglobin, as well as OXPHOS and DNA repair machinery (Nunnari 2012).

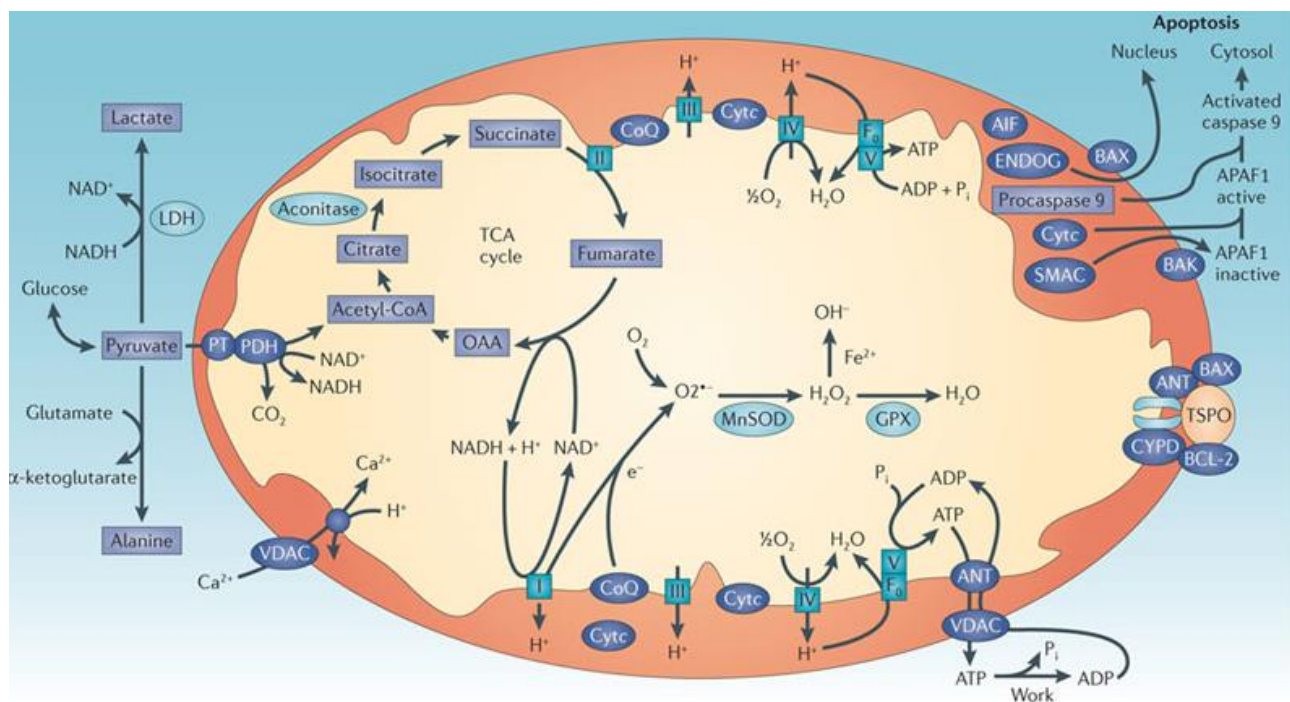


Fig. 3 Mitochondrial physiology. Mitochondria lie at the nexus of most biosynthetic pathways, produce much of the cellular energy through oxidative phosphorylation (OXPHOS), regulate mitochondrial and cellular redox status, generate most of the reactive oxygen species (ROS), regulate Ca^{2+} concentrations and can initiate apoptosis by the activation of the mitochondrial permeability transition pore (mtPTP). The mtPTP can be activated by a decreased membrane potential, high-energy phosphates (such as ADP), a more-oxidized redox status, and/or increased mitochondrial matrix Ca^{2+} and ROS concentrations (Wallace 2012).

2.1.3 Mitochondrial network

Mitochondrial form and function are intimately linked (Nunnari 2012). Mitochondrial morphologies vary widely among different cell types. Fibroblast mitochondria, for example, are usually long filaments (1 to 10 μm in length with a fairly constant diameter of ~ 700 nm), whereas hepatocyte mitochondria are more uniformly spheres or ovoids. Mitochondria shapes change continually through the combined actions of fission, fusion, and motility (Youle 2012). Large mitochondrial networks are frequently found in metabolically active cells. They consist of interconnected mitochondrial filaments and act as electrically united systems. These networks enable the transmission of mitochondrial membrane potential from oxygen-rich to oxygen-poor areas and thereby allow an efficient dissipation of energy in the cell. Similar to fusion, fission also plays a key role in cell life and death. As mitochondria are propagated by growth and division of pre-existing organelles, mitochondrial inheritance depends on mitochondrial fission during cytokinesis. Furthermore, mitochondrial division is important for several developmental and cellular differentiation processes, including the formation of synapses and dendritic spines in neurons and actively participates in the programmed cell death pathway (apoptosis) by inducing fragmentation of the mitochondrial network prior to cytochrome *c* release and caspase activation (Westermann 2008).

Mitochondrial fusion machinery is constituted by mitofusin 1 and 2 (MFN1, MFN2) and optic atrophy gene 1 (OPA1). The first proteins mediate mitochondrial outer-membrane fusion while OPA1 regulates the same process on inner-membrane. DRP1 is recruited at sites marked by endoplasmic reticulum tubules by mitochondrial fission factor (Mff) and mediates mitochondrial division (Nunnari 2012) (Fig. 4).

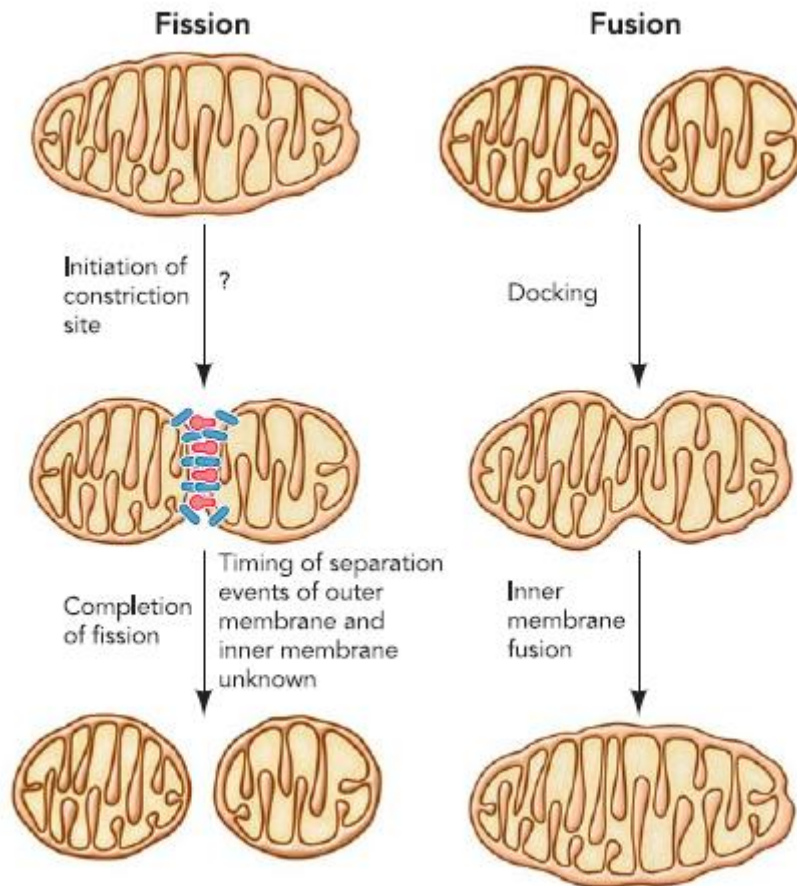


Fig. 4. Steps of mitochondrial fission and fusion Schematic representation of mitochondrial fusion and fission pathways (Dimmer 2006).

2.1.4 Mitochondrial genome

In the early 1950s, yeast geneticists reported cases where the transmission of some mitochondrial characters did not obey Mendelian rules and followed a “cytoplasmic inheritance pattern”. The carrier of this non-nuclear information was called ρ (rho) and remained unknown until the 1960s, when the existence of mitochondrial DNA (mtDNA) molecules was formally demonstrated (Malka 2006).

The human mtDNA is a circular molecule of approximately 16, 569 nucleotide pairs (nps). It retains the mitochondrial genes for the small (12S) and large (16S) ribosomal RNAs (rRNA) and the 22 transfer RNAs (tRNAs) necessary to translate the 13 mtDNA polypeptides. The 13 mtDNA proteins are all key components of OXPHOS and include seven (ND1, ND2, ND3, ND4L, ND4, ND5, ND6) of the approximately 46 polypeptides of OXPHOS complex I, one (cytochrome *b*, *cytb*) of the 11

proteins of complex III, three (COI, COII, COIII) of the 13 proteins of complex IV, and two (ATP6, ATP8) of the approximately 16 proteins of complex V (Wallace 2007).

In addition to the 37 structural genes, the mtDNA encompasses an approximately 1000 bp control region, D-Loop. This region contains the light (L)-strand and heavy (H)-strand promoters, HSP (H1 and H2) and LSP, respectively, the origin of H-strand replication, O_H , and of L-strand, O_L . The tRNAs punctuate the larger genes then fold in the transcripts are cleaved out to generate the transcripts which are then polyadenylated (Wallace 2005) (Fig. 5).

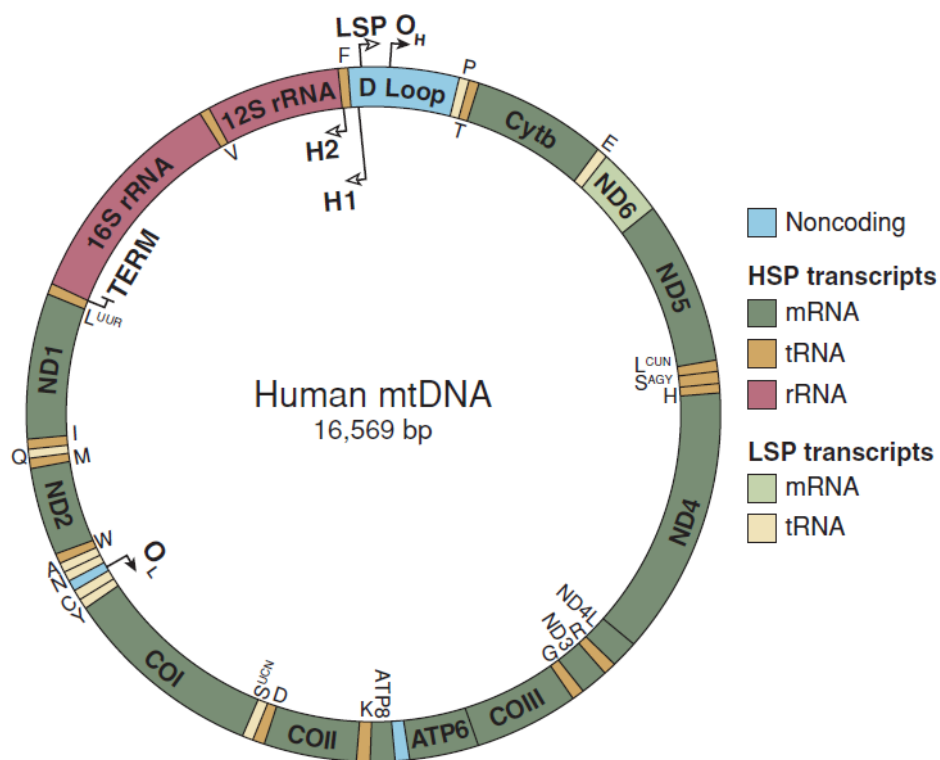


Fig. 5. The human mitochondrial genome. The 37 mitochondrial DNA (mtDNA) encoded genes include seven subunits of complex I (ND1, 2, 3, 4, 4L, 5 and 6), one subunit of complex III (cytochrome *b* (Cyt *b*)), three subunits of complex IV (Cyt *c* oxidase (COX) I, II and III), two subunits of complex V (A6 and A8), two rRNAs (12S and 16S) and 22 tRNAs (one-letter code). Also shown are the origins of replication of the heavy strand (O_H) and the light strand (O_L), and the promoters of transcription of the heavy strand (HSP) and light strand (LSP) (Falkenberg 2007).

The studies in the field of mitochondrial genetics have unraveled a series of peculiarities and differences compared to the nuclear genome:

(I) Cells are polyploid with respect to mtDNA: most mammalian cells contain hundreds of mitochondria and, in turn, each mitochondrion contains several (2–10) copies of mtDNA. In a given individual, all mtDNA copies are thought to be identical, a condition known as homoplasmy, but mutations can arise, be maintained or amplified to different levels and coexist with wild-type mtDNA, giving rise to the condition of heteroplasmy. At cell division mitochondria and their genomes are randomly distributed to daughter cells and hence, starting from a given heteroplasmic situation, different levels of heteroplasmy and even homoplasmy can arise in different cell lineages. As a consequence of this it is common to find a ‘threshold effect’ in mtDNA-linked human diseases; the mutation has to reach a certain percentage, usually higher than 60–80 %, in order to manifest pathological effects.

(II) The mitochondrial genome is maternally inherited; the few mitochondria from the sperm cell that could enter the oocyte during fertilization are actively eliminated by ubiquitin-dependent mechanism.

(III) The evolution rate of mtDNA is much faster than that of the nuclear genome. Several reasons are invoked to explain this fact: mtDNA is less protected by proteins, it is physically associated with the mitochondrial inner membrane where damaging reactive oxygen species (ROS) are generated, and it appears to have less-efficient repair mechanisms than the nucleus. This high mutation rate and the maternal inheritance pattern have made mtDNA sequence analysis an interesting tool in human population genetics and evolutionary studies.

(IV) Mitochondrial genes are translated using a genetic code with some differences from the universal genetic code (Fernández-Silva 2003).

It was early recognized that mtDNA does not distribute homogeneously within the mitochondrial compartment, but concentrates in structures that represent the dynamic and inheritable units of mtDNA and are called nucleoids (Malka 2006). A single nucleoid contains approximately one mtDNA genome packed in a space with a diameter of only 100 nm (Kukatt 2011) and a set of proteins involved in mtDNA replication and transcription in addition to several other metabolic proteins and chaperones (Bogenhagen 2008) (Fig. 6).

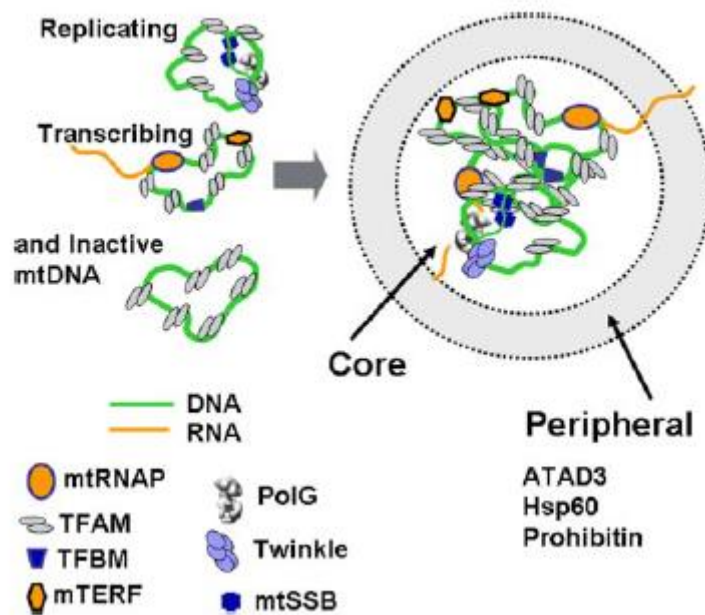


Fig. 6. Model for mtDNA nucleoid structure. Some individual mtDNA molecules within a nucleoid may be engaged in replication or transcription or may not be active in nucleic acid synthesis at any instant (Bogenhagen 2008).

2.1.4.1 Mitochondrial DNA transcription

Transcription originates from three promoters: two H strand promoters, called HSP1 and HSP2, and one L strand promoter, LSP. Transcripts emanating from HSP2 and LSP are long polycistronic products, some of which are nearly full-genome length. Excision of tRNAs from these polycistronic messengers is responsible for liberation of the mature mRNAs and rRNAs. In contrast to the other two promoters, transcription from HSP1 preferentially produces a relatively short message containing the two rRNAs and terminating at a specific site in the tRNA^{Leu} gene downstream of the 16S rRNA. Therefore, differential initiation at HSP1 and HSP2 determines the relative production of rRNAs and mRNAs from the H strand (Bonawitz 2006).

The transcription and translation of the mitochondrial genome is dependent upon a host of nucleus-encoded gene products. Mitochondrial DNA (mtDNA) transcription requires a single RNA polymerase (POLRMT), stimulatory transcription factors (Tfam, TFB2M, TFB1M), and a termination factor (MTERF1) (Scarpulla 2012).

Promoter recognition by the RNA polymerase is achieved by the insertion of a “specificity loop” into the DNA major groove at position –8 to –12 relative to the transcription start site. POLRMT may also play a role in the coordinated control of nuclear and mitochondrial transcription. In *S. cerevisiae*, there is a direct correlation between in vivo changes in mitochondrial transcript abundance and in vitro sensitivity of mitochondrial promoters to ATP concentration (Falkenberg 2007).

TFAM (mitochondrial transcription factor A) stimulates transcription through specific binding to the upstream enhancers on mtDNA. TFAM was first identified from human mitochondrial lysate fractions that stimulate the activity of crudely enriched mitochondrial RNA polymerase in LSP and HSP1 run off assays. This protein is highly conserved, and contains several well-defined domains, including an ~ 45 amino acid N-terminal mitochondrial targeting sequence (MTS), which is cleaved in a two-step reaction upon import to the matrix to reach a final mature product. TFAM generates RNAs corresponding to LSP and HSP1 initiation in these assays, which require the sequences immediately upstream of the transcription initiation sites. DNase I footprinting, which uses changes in nuclease sensitivity to map regions of protection and enhancement caused by protein binding, shows that TFAM binds specifically to sequences overlapping LSP and HSP1. Like other HMGB-related protein, TFAM can bind mtDNA also in aspecific manner and is a component of nucleoids (Campbell 2012).

The other two proteins essential for mtDNA transcription are TFB1M and TFB2M. Although TFB1M has about 1/10 the transcriptional activity of TFB2M, both proteins work together with TFAM and mitochondrial RNA polymerase to direct proper initiation from HSP and LSP. Both TFMs are also related to rRNA methyltransferases and TFB1M can bind *S*-adenosylmethionine and methylate mitochondrial 12S rRNA. Interestingly, TFB1M can also contact the carboxy-terminal domain of TFAM (Gleyzer 2005).

Transcription from HSP1 preferentially terminates just downstream of the two rRNA genes (forming a truncated H strand transcript that encodes only the 12S and 16S rRNAs, tRNA^{Phe}, and tRNA^{Val}), whereas transcription from HSP2 typically proceeds through this termination site to produce a near genome-length transcript (encoding all of the mRNAs, the two rRNAs, and most of the tRNAs). This termination event requires a 39 kDa transcription termination factor (mTERF) that contains three putative leucine-zipper motifs and binds a 28 bp sequence located downstream of the 16S rRNA gene in the tRNA^{Leu} gene (Bonawitz 2006).

2.1.4.2 Mitochondrial DNA replication

Transcription from the LSP is not only necessary for gene expression, but also produces the RNA primers required for initiation of mtDNA replication at the origin of H-strand DNA replication (OH). Two modes of DNA replication have been proposed to copy the mitochondrial genome, an asynchronous strand displacement model and a strand-coupled bidirectional replication model. In the asynchronous strand displacement model, mtDNA is replicated in an asymmetric fashion where DNA synthesis is primed by transcription through the H-strand origin within the D-loop. After two-thirds of the nascent H-strand is replicated, the L-strand origin is exposed, allowing initiation of nascent L-strand synthesis. In the strand-coupled model, bidirectional replication is initiated from a zone near OriH followed by progression of the two forks around the mtDNA circle (Kasiviswanathan 2012). MtDNA is replicated by an assembly of proteins in a replisome consisting of DNA polymerase γ (pol γ), the mitochondrial single-stranded DNA binding protein (mtSSB), mitochondrial DNA helicase, topoisomerases and RNaseH (Falkenberg 2007).

2.1.5 Levels of mitochondrial-nuclear communications

Mitochondrial-nuclear communications operate broadly at two levels. One mechanism involves a set of transcription factors, or coactivators, that regulate both nuclear and mitochondrial gene expression as occurs in response to changes in environmental temperatures, external stimuli such as changes in caloric intake, exercise, or changes in the levels of certain hormones such as thyroxine. In this mechanism, there is a change in the program of gene activation that results in the ability of mitochondria to undergo the synthesis and recruitment of mitochondrial and nonmitochondrial proteins.

The second mechanism involves cellular responses to changes in the functional state of the mitochondria itself, a process also called “retrograde regulation” (Ryan 2007).

2.1.5.1 Nuclear-mitochondrion communication: the mitochondrial biogenesis

Nucleus-encoded regulatory factors are major contributors to mitochondrial biogenesis and function. Several act within the organelle to regulate mitochondrial transcription and translation (example TFAM, POLG, POLRMT) while others direct the expression of nuclear genes encoding the respiratory chain and other oxidative functions (Scarpulla 2011).

2.1.5.1.1 Transcription factors and coactivator acting upon the nuclear genome

The nuclear respiratory factors, NRF-1 and NRF-2, were the first nuclear transcription factors implicated in the expression of multiple mitochondrial functions. NRF-1 is initially identified through its binding to the cytochrome c promoter and functions as a positive regulator of its transcription. It acts on genes encoding respiratory subunits as well as TFAM and both TFB isoform genes whose products are major regulators of mitochondrial transcription and ribosome assembly. Human NRF-2 was identified as a transcriptional activator of the cytochrome oxidase subunit IV (COXIV) promoter. Like NRF-1, NRF-2 participates in the expression of the mitochondrial protein import machinery with functional recognition sites in TOMM70 and TOMM20 (Fig. 7). Several additional nuclear transcription factors have been linked to the expression of the respiratory apparatus, including CREB, YY1 and c-myc (Scarpulla 2012 trends). The cAMP response element binding protein, CREB, along with NRF-1 is involved in the growth-regulated expression of cytochrome c and both factors participate in the induction of cytochrome c in response to serum stimulation of quiescent cells.

The initiator element binding factor, YY1, is engaged in both the positive and negative control of certain cytochrome oxidase subunit genes. YY1 recognition sites along with those for the NRFs were enriched among genes encoding OXPHOS subunits and assembly factors. However both YY1 and CREB showed less specificity for respiratory genes than NRF-1 or NRF-2. Nevertheless, YY1 has been identified as a target for the nutrient sensor mTOR and YY1 silencing in myotubules results in diminished mitochondrial gene expression. Finally, c-myc directs the expression of certain NRF-1 target genes and myc null fibroblasts are deficient in mitochondrial content (Scarpulla 2012 b). Interestingly, c-myc positively regulates mitochondrial biogenesis and the respiratory apparatus through PGC-1 β , an effect that is repressed by HIF1 α in the absence of the von Hippel-Landau tumor suppressor. This pathway may be part of a molecular switch from oxidative phosphorylation to aerobic glycolysis mediated by HIF1 α in certain cancers (Zhang 2008).

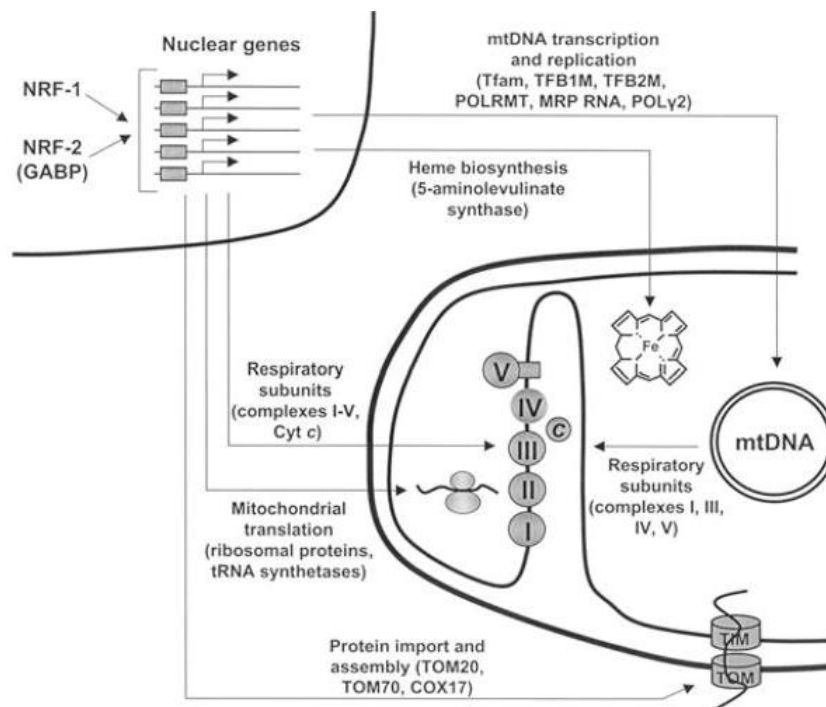


Fig. 7: Schematic representation of mitochondrial biogenesis network. Nuclear respiratory factors (NRF-1 and NRF-2) in the expression of nuclear genes governing mitochondrial respiratory function. NRFs act on the majority of nuclear genes that specify subunits of the five respiratory complexes of the mitochondrial inner membrane. In addition, they act on many other genes whose products direct the expression and assembly of the respiratory apparatus. Promoters for most of the nuclear genes encoding mtDNA transcription and replication factors have functional recognition sites for NRF-1, NRF-2, or both (Scarpulla 2008).

The PPAR γ coactivators 1 (PGC-1s) are a family of multifunctional transcriptional coactivators that have emerged as playing a central role in cellular and systemic metabolism. The first member of the PGC-1 family, PGC-1 α , was initially identified as a transcriptional coactivator driving mitochondrial function and thermogenesis in brown fat. The two other family members, PGC-1 β and PGC-1 related coactivator (PRC) were discovered using sequence homology searches (Girnun 2012) (Fig. 8). The PGC-1 coactivators contain a conserved N-terminal domain that interacts with proteins capable of remodeling chromatin, including histone acetyl transferases, such as CREB-binding protein, p300, and steroid receptor coactivator 1. This chromatin remodeling allows access to additional factors that enhance transcription.

The C-terminal domain of PGC-1 binds a second activating complex, consisting of the steroid hormone receptor-associated protein, TRAP/DRIP, and containing an RNA-binding domain that facilitates pre-mRNA splicing (Ryan 2007).

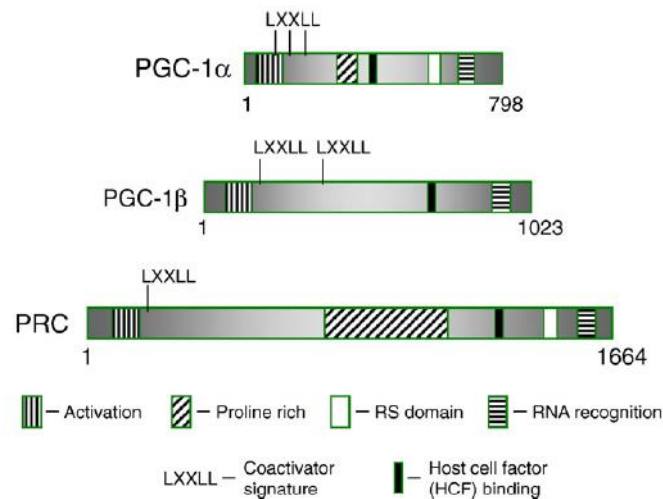


Fig. 8: PGC-1 family coactivator. Schematic comparison of PGC-1 α , PGC-1 β and PRC with the identities of the conserved sequence motifs shown in the key at the bottom. All three PGC-1 members are characterized by an N-terminal activation domain near leucine-rich LXXLL motifs that mediate interaction with nuclear receptors, an RNA recognition domain (RRM), and a host cell factor-1 (HCF) binding domain. In addition, PGC-1 α contains an RNA splicing domain (RS), the function of which has not been fully defined (Scarpulla 2012 c).

The three family members are differentially regulated by environmental cues governing pathways of thermogenesis, gluconeogenesis, muscle differentiation, and cell growth. The coactivators, in turn, implement programs of gene expression through direct interaction with transcription factor targets or through their indirect effects on transcription factor expression (Scarpulla 2008) (Fig. 9).

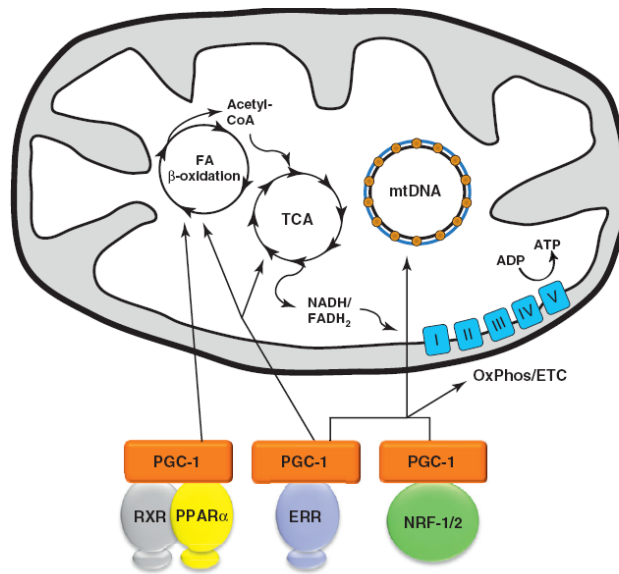


Fig. 9: Control of mitochondrial biogenesis by PGC-1. Interaction between PGC-1 and specific transcription factors orchestrates the major functions of mitochondria, including fatty acid b-oxidation, the tricarboxylic acid cycle (TCA), mtDNA replication and oxidative phosphorylation, and the electron transport chain (OxPhos/ETC), in addition to biogenesis of this organelle. PPAR α interacts with its binding partner, the retinoid X receptor (RXR), to control the expression of many fatty acid b-oxidation enzymes. NRF-1 and NRF-2 contribute to the maintenance of mtDNA and the expression of multiple components of the ETC. ERR members regulate the expression of virtually all functions of the mitochondria including those shown here (Scarpulla 2012).

PGC-1 α lacks histone-modifying enzymatic activities but it interacts, through a potent amino-terminal activation domain, with a number of coactivator complexes which contain intrinsic chromatin remodeling activities (SRC-1, CBP/p300 and GCN5). In addition PGC-1 α binds a large complement of transcription factors and nuclear hormone receptors. Among those directly associated with mitochondrial respiratory function are NRF-1, YY1, PPAR α and MEF2C. PGC-1 α can trans-activate NRF-1 target genes and a dominant negative allele of NRF-1 blocks the effects of PGC-1 α on mitochondrial biogenesis. The proposed role for PGC-1 α as a regulator of mitochondrial biogenesis is supported by gain of function experiments in both cultured cells and transgenic mice. In cultured cells, ectopic PGC-1 α expression increases COXIV and cytochrome c protein levels as well as the steady-state level of mtDNA. More recently, metabolic signaling through PGC-1 α was found to occur through post-translational modifications. For example, AMP-activated protein kinase (AMPK), an enzyme sensor that is activated upon energy depletion in muscle, phosphorylates PGC-1 α on specific serine and threonine residues. This results in increased mitochondrial gene expression supporting the idea that AMPK can mediate at least some of its effects through PGC-1 α (Scarpulla 2011).

A homologue of PGC-1 α was designated as PGC-1 β . PGC-1 α and β are closely related but PGC-1 β lacks the arginine/serine (R/S) domain that is associated with RNA processing. PGC-1 β appears identical to PGC-1 α in its functional interaction with NRF-1 and in its ability to promote the expression of nuclear respiratory genes and mitochondrial mass when expressed from viral vectors. Interestingly, despite the functional similarities between the two family members, PGC-1 β promotes a much higher level of coupled respiration than PGC-1 α , suggesting differences between the two in metabolic efficiency (Scarpulla 2011).

While PGC-1 β expression in distinct tissues is unaffected by physiological processes characterized by increased energy expenditure, such as cold exposure (in brown adipose tissue), fasting (in liver) or exercise (in muscle), PGC-1 α is highly regulated at the transcriptional level under similar physiological challenges. These data suggest that PGC-1 β likely controls basal mitochondrial biogenesis, whereas PGC-1 α controls stimulated or regulated mitochondrial activity. Moreover PGC-1 β is a regulator of mitochondrial fusion, promoting Mfn2 expression (Liesa 2008).

PRC was identified as a large cDNA with significant sequence similarities to PGC-1 α within the carboxy-terminal RS domain and RNA recognition motif. PRC shares with PGC-1 α and β the ability to bind NRF-1 both *in vitro* and *in vivo* and to use NRF-1 for the *trans*-activation of NRF-1 target genes. NRF-1-dependent *trans*-activation requires the PRC activation domain, suggesting that this domain shares function with PGC-1 α in recruiting chromatin-remodeling cofactors that drive transcription. PRC and PGC-1 α are indistinguishable in *trans*-activating promoters for cytochrome *c*, 5-aminolevulinate synthase, and both of the TFB isoforms, suggesting that PRC may participate in the expression of the respiratory chain. Maximal *trans*-activation by both coactivators requires the NRF-1 and NRF-2 binding sites within the proximal promoters of these genes. Although similar to PGC-1 α in these basic transcriptional properties, PRC mRNA is not enriched in brown versus white fat and is only slightly elevated in brown fat upon cold exposure, arguing against a major role for PRC in adaptive thermogenesis. Analysis of PRC expression in cultured fibroblasts revealed that PRC levels correlate with the cell proliferative cycle. The steady-state expression of PRC mRNA and protein is high in growing cells but markedly diminished upon exit from the cell cycle as a consequence of contact inhibition or serum withdrawal (Scarpulla2008).

The external stimuli, which influence mitochondrial function, are sensed in various ways by different tissues. This leads to the activation of signal transduction pathways that allow tissue-specific activation of PGC-1 transcription. For example, cold exposure leads to the activation of β -adrenergic receptors in brown adipose tissue cells, activating the cAMP pathway to transcriptional activation of PGC-1 α and downstream expression of UCP1, thereby leading to uncoupled thermogenesis. Long-term exercise in mice, by contrast, leads to chronic energy deficits, which are

sensed by AMP-activated protein kinase (AMPK), which in turn leads to mitochondrial biogenesis via calcium/calmodulin-dependent protein kinase (CaMK) and PGC-1 α . Nitric oxide was also implicated as a signaling molecule in PGC-1 α induction via a cGMP-dependent mechanism in a wide range of cell types. Transgenic mice with deficient epithelial nitric oxide synthase were deficient in mitochondrial biogenesis. Likewise, the transcription of PGC-1 α was regulated through the release of repression by p160 through p38 MAP kinase. Thyroid (T3) and glucocorticoid hormones also induce mitochondrial biogenesis and respiration (Ryan 2007). Interestingly, an increase of mitochondrial biogenesis was observed in cell treated with chemotherapeutic drugs (Fu 2008, Kluza 2004).

2.1.5.2 Mitochondrial-nuclear communication: the retrograde signal

Metabolic cues or other damage that occurs within mitochondria can culminate in wide range of changes in nuclear gene expression via retrograde signaling from the mitochondria to the nucleus. Altered nuclear gene expression in response to mitochondrial dysfunction in mammalian cells was suggested by studies showing increased mRNA levels coding for various mitochondrial proteins in different ρ^0 cell lines. Mitochondrial retrograde signaling in mammalian cells (also referred to as mitochondrial stress signaling) was described initially in C2C12 skeletal myoblasts (rhabdomyoblasts) and later confirmed in human lung carcinoma A549 cells. Mitochondrial stress was defined by altered mitochondrial membrane potential, $\Delta\psi_m$, induced either by treating cells with ethidium bromide to partially deplete their mtDNA content or with the mitochondria-specific ionophore, CCCP (carbonyl cyanide m-chlorophenyl hydrazone) (Butow 2004). These treatments result in the elevation of cytosolic Ca^{2+} and activation of CaMK and calcineurin-responsive genes. Such responses appear to be mediated through PGC-1 α . Thus, overexpression of CaMK in muscle of transgenic mice resulted in generalized increases in mitochondrial biogenesis and fatty-acid oxidation. In cultured myocytes, CaMK was capable of inducing PGC-1 transcription through a direct effect on the gene promoter. This activation is dependent on MEF2-responsive elements in the case of calcineurin A and on the CREB-binding site in the case of CaMK. The genes activated by these changes in Ca^{2+} levels include a number of genes involved in Ca^{2+} transport and storage as well as a large number of transcription factors. The general net effect of activation of this gene network is to facilitate recovery of physiological function (Ryan 2007) (Fig. 10).

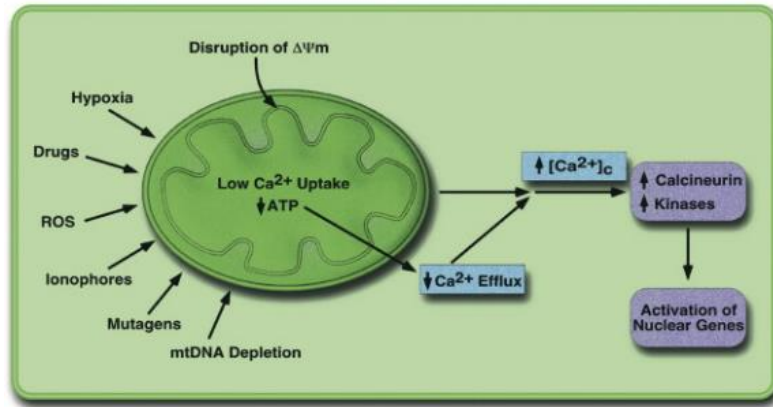


Fig. 10: Retrograde signaling in mammalian cells. Retrograde signaling in mammalian cells Occurs through Increased Cytosolic Ca^{2+} Disruption of $\Delta\Psi_m$ by various causes affects mitochondrial uptake of Ca^{2+} and reduced efflux into storage organelles or outside the cells due to reduced availability of ATP. Increased cytosolic Ca^{2+} in turn activates calcineurin and various Ca^{2+} -dependent kinases (Butow 2004).

Mitochondria also appear to have a stress response pathway superficially similar to the unfolded protein response in the endoplasmic reticulum. The accumulation of a mutant form of misfolded ornithine transcarbamylase (OTC) in the mitochondrial matrix induces a stress response that activates CEBP homology protein, CHOP, and induces expression of nuclear gene-encoded stress response proteins, Cpn60, Cpn10, mtDNAJ, and ClpP (Butow 2004).

2.1.6 Mitochondria and diseases

A broad spectrum of complex clinical phenotypes has been linked to mutations in nDNA and mtDNA mitochondrial genes. Very different gene mutations can cause a similar range of phenotypes, mutations in the same gene can give a range of different phenotypes, and the same mtDNA mutation at different levels of heteroplasmy can result in totally different phenotypes (Wallace 2010).

Accordingly, mitochondrial disorders are a complex dual genome disease that can be caused by molecular defects in both nuclear and mitochondrial genomes. The disease is genetically heterogeneous. Depending upon the primary defect, mitochondrial disorders may be autosomal recessive, autosomal dominant, X-linked, or maternally inherited (Wong 2010).

Most often, mitochondrial diseases are caused by molecular defects affecting OXPHOS system, i.e. electron transport chain complexes which perform oxidative phosphorylation (Fig. 11).

Oxidative phosphorylation subunits	mtDNA maintenance and expression	Oxidative phosphorylation biogenesis and regulation	Nucleotide transport and synthesis	Membrane dynamics and composition
Nuclear encoded				
Complex I: NDUFA1, NDUFA2, NDUFA9, NDUFA10, NDUFA11, NDUFA12, NDUFB3, NDUFB9, NDUFS1, NDUFS2, NDUFS3, NDUFS4, NDUFS6, NDUFS7, NDUFS8, NDUFV1, NDUFV2 Complex II: SDHA, SDHB, SDHC, SDHD Complex III: UQCRB, UQCRCQ Complex IV: COX4I2, COX6B1 Complex V: ATP5E	TWINKLE, MTFMT, GFM1, LRPPRC, MPV17, MRPS16, MRPS22, POLG, POLG2, TRMU, TSFM, TUFM, C12orf65, MTPAP, MRPL3, SARS2, YARS2, HARS2, MARS2, AARS2, RARS2, EARS2, DARS2, TACO1, MTO1, RMND1, PNPT1, PUS1	Complex I: NDUFAF1, NDUFAF2, NDUFAF3, NDUFAF4, NDUFAF5, NDUFAF6, ACAD9, FOXRED1, NUBPL Complex II: SDHAF1, SDHAF2 Complex III: BCS1L, HCCS, TTC19 Complex IV: COX10, COX15, ETHE1, FASTKD2, SCO1, SCO2, SURF1, COX14, COA5 Complex V: ATPAF2, TMEM70 Fe-S: ABCB7, FXN, ISCU, NFU1, BOLA3, GLRX5 Other: DNAJC19, GFER, HSPD1, SPG7, TIMM8A, AIFM1, AFG3L2	DGUOK, RRM2B, SLC25A3, ANT1, SUCLA2, SUCLG1, TK2, TYMP	ADCK3, AGK, COQ2, COQ6, COQ9, DRP1, MFN2, OPA1, PDSS1, PDSS2, TAZ, SERAC1
mtDNA encoded				
Complex I: ND1, ND2, ND3, ND4, ND4L, ND5, ND6 Complex III: CYTB Complex IV: COX1, COX2 Complex V: ATP6, ATP8	12S rRNA, tRNA ^{Tyr} , tRNA ^{Trp} , tRNA ^{Val} , tRNA ^{Thr} , tRNA ^{Ser1} , tRNA ^{Ser2} , tRNA ^{Arg} , tRNA ^{Gln} , tRNA ^{Pro} , tRNA ^{Asn} , tRNA ^{Met} , tRNA ^{Leu1} , tRNA ^{Leu2} , tRNA ^{Lys} , tRNA ^{Ile} , tRNA ^{His} , tRNA ^{Gly} , tRNA ^{Phe} , tRNA ^{Glu} , tRNA ^{Asp} , tRNA ^{Cys} , tRNA ^{Ile}			

Fig. 11: List of genes that are known to be mutated in respiratory chain disorders grouped by pathway (Shon 2012)

Although mitochondrial oxidative phosphorylation (OXPHOS) disorders are quite varied, they typically display a number of ‘canonical’ biochemical and morphological features. An obvious feature is respiratory chain deficiency, which typically manifests itself as reduced enzymatic function in one or more respiratory chain complexes, with a concomitant reduction in cellular oxygen consumption and ATP synthesis. In addition, patients often have increased resting lactic acid levels in the blood. Under normal conditions, pyruvate (the end product of anaerobic glycolysis) is transported into mitochondria for further oxidation in the TCA cycle to produce the reducing equivalents (namely, NADH and FADH₂) that are required for proton pumping by the respiratory chain. However, if the respiratory chain is compromised, NADH and pyruvate accumulate in the cytosol. Excess cytosolic pyruvate is converted to lactate by lactate dehydrogenase, thereby accounting for the increased lactic acid found in many mitochondrial diseases and especially in those affecting infants or young children. A prominent morphological feature of OXPHOS disease is the ragged red fibre (RRF), which reflects a massive proliferation of OXPHOS-defective mitochondria in muscle; this can be visualized with the modified Gomori trichrome stain (Schon 2012) (Fig. 12).

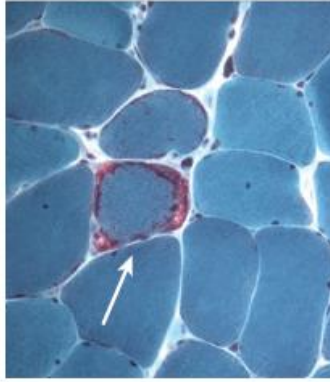


Fig. 12: Ragged red fibre seen on a modified Gomori-trichrome-stained skeletal-muscle section (Vafai 2012)

The vast majority of OXPHOS mutations impair the cell's ability to produce ATP in amounts that are sufficient for maintaining viability, but sometimes OXPHOS problems can leave ATP synthesis intact and yet can be deleterious by, for example, stimulating the overproduction of reactive oxygen species (ROS) or inducing an autoimmune response (Schon 2012).

Mitochondrial diseases are caused also by mutation in genes involved in mitochondrial biogenesis and mtDNA maintenance and expression (ex. POLG and mt-tRNA) , fusion and fission (ex. OPA1) (Wallace 2010).

Since mitochondria are the essential energy-producing organelles in animal cells, virtually all organ systems may be affected if there is a mitochondrial defect. However, the tissues with high-energy demand, such as muscle and nerve, are most susceptible. In general, neuromuscular symptoms are the major clinical features of mitochondrial diseases, including seizures, skeletal muscle weakness, exercise intolerance, cardiomyopathy, sensorineural hearing loss, optic atrophy, retinitis pigmentosa, ophthalmoplegia, diabetes mellitus, hypothyroidism, gastrointestinal reflux, renal dysfunction, and immunodeficiency (Wong 2010) (Fig. 13).

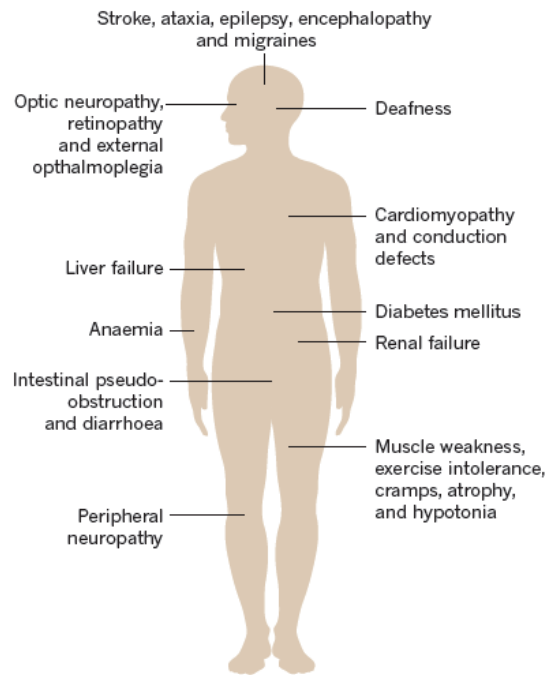


Fig. 13: Common clinical manifestations of mitochondrial disorders (Shown 2012).

2.1.7 *Mitochondria and cancer*

2.1.7.1 *Tumor metabolism*

In 2000, the Hanahan and Weinberg's groups proposed the hallmarks of cancer that comprised six biological capabilities acquired during the multistep development of human tumors. They include sustaining proliferative signaling, evading growth suppressors, resisting cell death, enabling replicative immortality, inducing angiogenesis, and activating invasion and metastasis. Underlying these hallmarks are genome instability, which generates the genetic diversity that expedites their acquisition, and inflammation, which fosters multiple hallmark functions. But, conceptual progress in the last decade has added two emerging hallmarks of potential generality to this list: evading immune destruction and reprogramming of energy metabolism (Hanahan 2011). The relation between metabolism and cancer dates back to 1924 when Otto Warburg observed that cancer cells metabolize glucose in a manner that is distinct from that of cells in normal tissues. Our current understanding of metabolic pathways is based largely on studies of nonproliferating cells in differentiated tissues. In the presence of oxygen, most differentiated cells primarily metabolize

glucose to carbon dioxide by oxidation of glycolytic pyruvate in the mitochondrial TCA cycle. This reaction produces NADH [nicotinamide adenine dinucleotide (NAD⁺), reduced], which then fuels oxidative phosphorylation to maximize ATP production, with minimal production of lactate. It is only under anaerobic conditions that differentiated cells produce large amounts of lactate. In contrast, most cancer cells produce large amounts of lactate regardless of the availability of oxygen and hence their metabolism is often referred to as “aerobic glycolysis.” Warburg originally hypothesized that cancer cells develop a defect in mitochondria that leads to impaired aerobic respiration and a subsequent reliance on glycolytic metabolism. However, subsequent work showed that mitochondrial function is not impaired in most cancer cells suggesting an alternative explanation for aerobic glycolysis in cancer cells (Vander Heiden 2009) (Fig. 14).

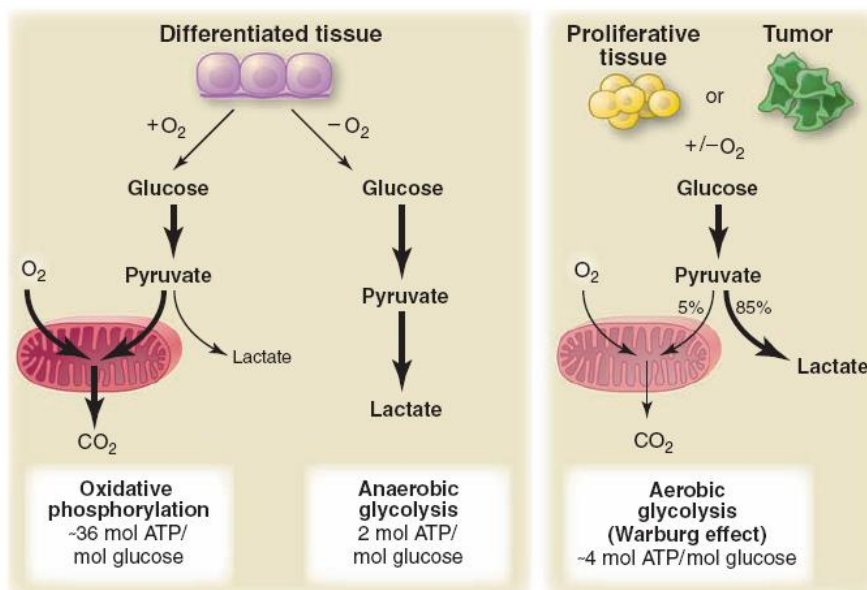


Fig. 14: Schematic representation of the differences between oxidative phosphorylation, anaerobic glycolysis, and aerobic glycolysis (Warburg effect). In the presence of oxygen, nonproliferating (differentiated) tissues first metabolize glucose to pyruvate via glycolysis and then completely oxidize most of that pyruvate in the mitochondria to CO₂ during the process of oxidative phosphorylation. Because oxygen is required as the final electron acceptor to completely oxidize the glucose, oxygen is essential for this process. When oxygen is limiting, cells can redirect the pyruvate generated by glycolysis away from mitochondrial oxidative phosphorylation or by generating lactate (anaerobic glycolysis). This generation of lactate during anaerobic glycolysis allows glycolysis to continue (by cycling NADH back to NAD⁺), but results in minimal ATP production when compared with oxidative phosphorylation. Warburg observed that cancer cells tend to convert most glucose to lactate regardless of whether oxygen is present (aerobic glycolysis). This property is shared by normal proliferative tissues. Mitochondria remain functional and some oxidative phosphorylation continues in both cancer cells and normal proliferating cells. Nevertheless, aerobic glycolysis is less efficient than oxidative phosphorylation for generating ATP. In proliferating cells, ~10% of the glucose is diverted into biosynthetic pathways upstream of pyruvate production (Vander Heiden 2009).

Cancer cells synthesize great amounts of nucleotides, macromolecules and lipids, and these biosynthesis require continuous production of NAD^+ , NADPH^+ and ATP. They consume at least 10 times more glucose than normal cells and produce lactic acid, even in the presence of oxygen. High rates of glucose uptake have been clinically used to detect tumours by positron emission tomography with a glucose analogue tracer (PET) (Icard 2012).

Glycolysis is inefficient in terms of ATP production, as it generates only two ATP molecules per molecule of glucose, whereas complete oxidation of one glucose molecule by oxidative phosphorylation can generate up to 36 ATP molecules. This raises the question of why a less efficient metabolism, at least in terms of ATP production, would be selected for in proliferating cells (Vander Heiden 2009).

Despite its low efficiency in ATP yield per molecule of glucose, aerobic glycolysis can generate more ATP than oxidative phosphorylation by producing ATP at a faster rate. Provided the glucose supply is abundant, an inefficient but faster pathway for ATP production may be preferred to meet the high demands of dividing cells. However, glycolysis is not the major contributor of ATP in most cells: a compilation of data for 31 cancer cell lines/tissues from studies that determined oxidative ATP production (by measuring O_2 consumption) and glycolytic ATP production (by measuring lactate excretion) shows that the average percentage of ATP contribution from glycolysis is 17%. This collection of data does not support the hypothesis that cancer cells exhibit aerobic glycolysis to generate ATP faster (Lunt 2011).

Advantages which glycolytic metabolism conveys to cancer cells include supply of nucleotides for DNA synthesis, lipids for membrane biogenesis and glutathione for redox regulation. Therefore, a main function of upregulated glycolysis in proliferating cells may be to maintain the levels of glycolytic intermediates needed to support biosynthesis (Icard 2012).

DNA and RNA, which are composed of nucleotides, account for a significant portion of cell mass. Each purine nucleotide (ATP, GTP, dATP, and dGTP) synthesized by the cell requires the assimilation of 10 carbon atoms from the extracellular environment. Half of the purine nucleotide carbons are derived from 5-phosphoribosyl- α -pyrophosphate (PRPP), an activated version of ribose-5-phosphate, which ultimately is derived from carbohydrate nutrients. Glucose is the major carbohydrate available to most animal cells. The activity of PRPP synthetase, an enzyme that converts ribose-5-phosphate to PRPP, increases two- to tenfold in lymphocytes following mitogen stimulation, which highlights the importance of increased PRPP generation for nucleotide biosynthesis during cell growth. In addition to serving as building blocks of nucleic acids, purines are necessary for cofactor biosynthesis, as adenine is present, for example, in FAD(H₂) (flavin adenine dinucleotide, reduced), NAD(H), NADP(H), and coenzyme A (CoA). Glycolysis is also a

major source of carbons for biosynthesis of pyrimidine nucleotides, as the majority (five out of nine) of the carbons comes from PRPP. In addition to supporting nucleotide biosynthesis, glycolysis is also a source of carbon for lipid precursors. The glycolytic intermediate dihydroxyacetone phosphate is the precursor to glycerol-3-phosphate, which is crucial for the biosynthesis of the phospholipids and triacylglycerols that serve as major structural lipids in cell membranes. Elevated levels of glycerol and glycerol-3-phosphate have been reported in human peripheral lymphocytes after mitogen stimulation, and elevated levels of choline phospholipids have been found in breast cancer (Lunt 2011) (Fig. 15).

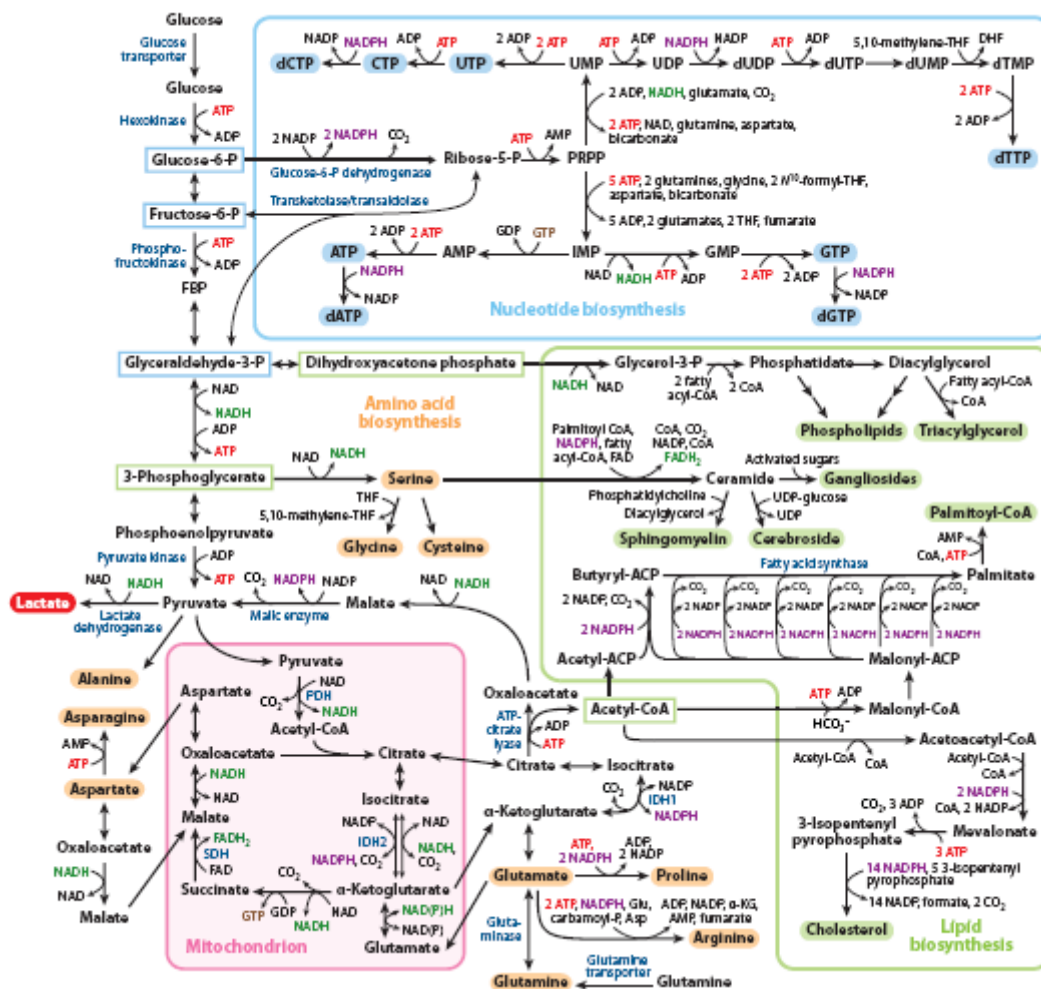


Fig. 15: Metabolic pathways active in proliferating cells. This schematic represents our current understanding of how glycolysis, oxidative phosphorylation, the pentose phosphate pathway, and glutamine metabolism contribute to biomass precursors. Enzymes that control critical steps and are often overexpressed or mutated in cancer cells are shown in dark blue. Nucleotides that can be incorporated into DNA and RNA are highlighted in light blue, representative lipids are highlighted in green, and nonessential amino acids are highlighted in orange (Lunt 2011)

Glutamine was recognized as another highly demanded cancer cell nutrient, sometimes indicated to be even more essential than glucose. Glutamine, which circulates with the highest concentration among amino acids, serves as a major bioenergetic substrate and nitrogen donor for proliferating cells. Glutamine enters into the TCA via its conversion to glutamate and then to α -ketoglutarate (aKG), a key TCA cycle intermediate that is also a cofactor for dioxygenases (Dang 2012). Despite the dependence of tumor on glucose and glutamine metabolism, the presence of functional mitochondria is essential for the cancer cell. This was confirmed by the elimination of mtDNA from various cancer cells through growth in ethidium bromide (Rho0 cells). The resulting Rho0 cancer cells have reduced growth rates, decreased colony formation in soft agar and markedly reduced tumor formation in nude mice (Wallace 2012).

2.1.7.2 Tumor microenvironment: hypoxia and HIF1 α

Together with elevated energy demand and building block requirements, the main selective pressure for metabolism regulation during any solid cancer progression is hypoxia. A critical difference between the tumor microenvironment and that of the surrounding normal tissue is the presence of intratumoral hypoxia (Semenza 2012). Hypoxia in tumors is primarily a pathophysiologic consequence of structurally and functionally disturbed microcirculation and the deterioration of diffusion conditions. Tumor hypoxia appears to be strongly associated with tumor propagation, malignant progression, and resistance to therapy and it has thus become a central issue in tumor physiology and cancer treatment (Höckel 2001).

Crucial mediators of the hypoxic response are the HIFs transcription factors, which transactivate a large number of genes including those promoting angiogenesis, anaerobic metabolism and resistance to apoptosis. HIFs are heterodimers comprising one of three major oxygen labile HIF α subunits (HIF1 α , HIF2 α or HIF3 α), and a constitutive HIF1 β subunit (also known as aryl hydrocarbon receptor nuclear translocator or ARNT), which together form the HIF1 α , HIF2 α and HIF3 α transcriptional complexes, respectively. Of the three α -subunits, HIF1 α and HIF2 α are the best studied. HIF3 α has high similarity to HIF1 α and HIF2 α in the basic helix–loop–helix (bHLH) and Per-Arnt-SIM (PAS) domains, but lacks the C-terminal transactivation domain (TAD-C). HIF3 α has multiple splice variants, the most studied being the inhibitory PAS domain protein (IPAS), which is a truncated protein that acts as a dominant negative inhibitor of HIF1 α . HIF1 α and HIF2 α have 48% amino acid sequence identity and similar protein structures, but are nonredundant and have distinct target genes and mechanisms of regulation (Fig. 16) (Koh 2012).

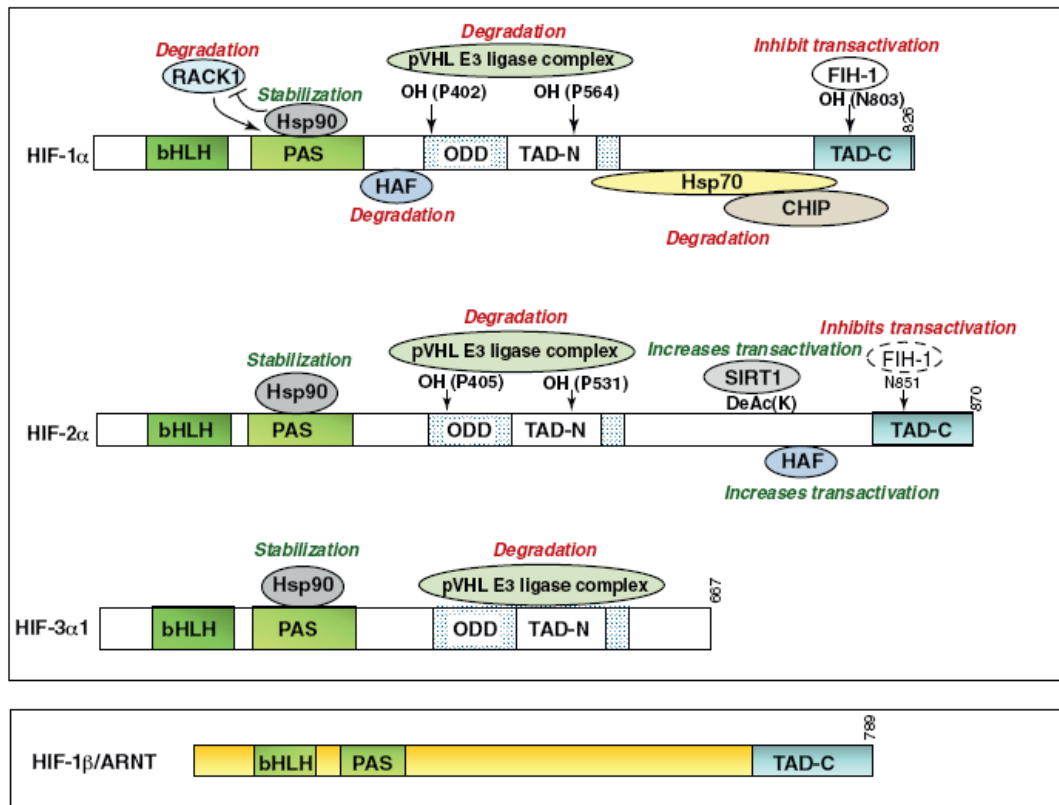


Fig. 16: The structural domains of hypoxia-inducible factor (HIF)-1/2/3 α and their transcriptional binding partner, HIF-1 β /ARNT (aryl hydrocarbon nuclear translocator), that together form the HIF1, HIF2 and HIF3 transcriptional complexes, respectively (Koh 2012).

Interesting, it appears that in some cell lines, HIF1 α is most active during short periods (2–24 h) of intense hypoxia or anoxia (<0.1% O₂), whereas HIF2 α is active under mild or physiological hypoxia (<5% O₂), and continues to be active even after 48–72 h of hypoxia. Hence, in certain contexts, HIF1 α drives the initial response to hypoxia, but during chronic hypoxic exposure, it is HIF2 α that plays the major role in driving the hypoxic response (Koh 2012).

Using molecular oxygen (O₂) and 2-oxoglutarate as substrates, hypoxia-inducible factor (HIF) prolyl-hydroxylase (PHD) enzymes hydroxylate two specific proline residues in the O₂-dependent degradation domain (ODD) of HIF α proteins. These hydroxylation events occur on Pro402 and Pro564 in HIF1 α , and Pro405 and Pro531 in HIF2 α , and are required for the von Hippel–Lindau (VHL) tumour suppressor protein (the recognition component of an E3 ubiquitin ligase complex) to bind and degrade HIF α subunits under normoxic conditions. Hypoxia inhibits PHD activity through various mechanisms, including substrate limitation, which results in HIF α subunit stabilization, heterodimerization with HIF1 β and increased HIF transcriptional activity. Hypoxic conditions also inhibit hydroxylation by factor inhibiting HIF (FIH) of a conserved carboxy-terminal asparagine residue in the HIF α subunits, an event that blocks the interaction between HIF α subunits and the

transcriptional co-activators p300 and CREB binding protein (CBP). Thus, whereas PHD-mediated hydroxylation destabilizes HIF α subunits, FIH-mediated hydroxylation inhibits their transcriptional activity (Keith 2011).

Under hypoxic conditions, PHD activity is inhibited, pVHL binding is abrogated, and HIF1 α and HIF2 α are stabilized. HIF1/2 α enter the nucleus, where they heterodimerize with HIF1 β and bind to a conserved DNA sequence known as the hypoxia responsive element (HRE), to transactivate a variety of hypoxia-responsive genes (Fig. 17) (Semenza 2003).

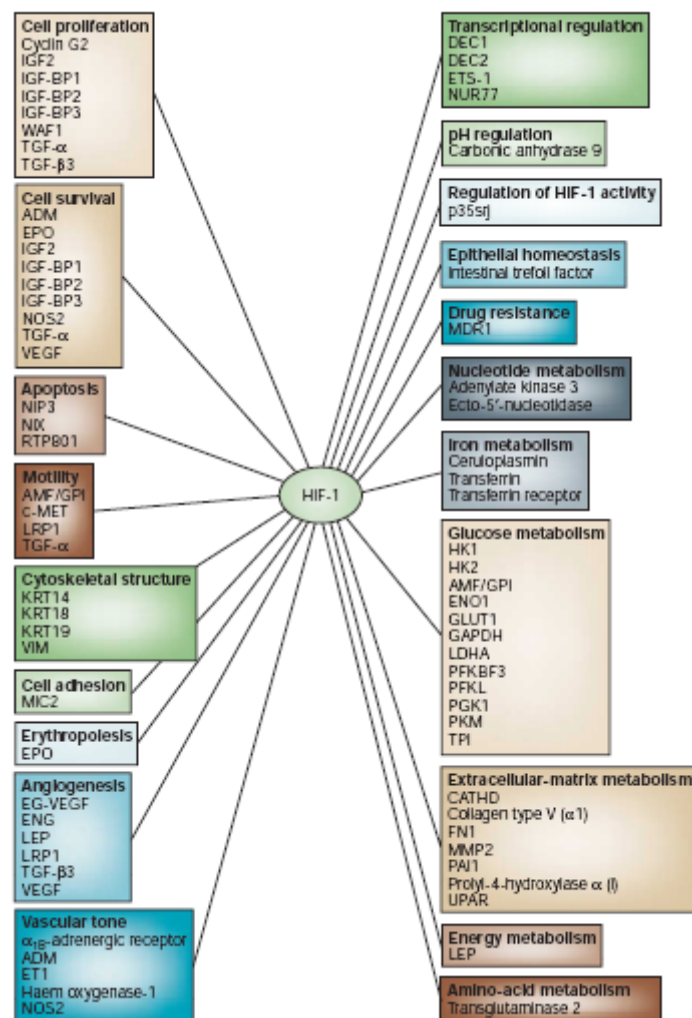


Fig. 17: Genes that are transcriptionally regulated by HIF (Semenza 2003).

Immunohistochemical analyses revealed that HIF1 α is overexpressed in many human cancers. Significant associations between HIF1 α overexpression and patient mortality have been shown in cancers of the brain (oligodendroglioma), breast, cervix, oropharynx, ovary and uterus (endometrial). In fact HIF1 α activity leads to upregulation of genes that are involved in many

aspects of cancer progression, including metabolic adaptation, apoptosis resistance, angiogenesis and metastasis (Fig. 17).

One way in which HIF1 α promotes cell survival under hypoxic conditions is by mediating a switch from oxidative to glycolytic metabolism. The transcription factor HIF1 α induces glycolysis under low oxygen tension through the upregulation of genes encoding glucose transporters, glycolytic proteins and angiogenic factors (such as erythropoietin and vascular endothelial growth factor (VEGF), and the inhibition of mitochondrial function. HIF1 α affects mitochondria by various mechanisms: it induces PDHK1, thus inhibiting PDH and retarding the conversion of pyruvate to mitochondrial acetyl-CoA; it induces the low oxygen tension subunit of complex IV, COX4-2; it upregulates the mitochondrial LON protease to degrade the normoxic subunit, COX4-1; it activates mitophagy to degrade existing mitochondria; and it inhibits MYC signaling that regulate the mitochondrial coactivator PGC-1 β . HIF1 α also upregulates the transcription of miR-210, which downregulates mitochondrial metabolism by inhibiting expression of the *ISCU1* and *ISCU2* genes which encode proteins involved in iron sulphur centre synthesis and genes for subunits of complex I (*NDUFA4*), complex II (*SDHD*) and complex IV (*COX10*). Finally, HIF1 α mediates the transcription of PKM2, but not PKM1, and PKM2 also serves as a co-transcriptional activator of HIF1 α . This is mediated by PHD3, which hydroxylates prolines 403 and 408 of PKM2, thus enhancing the binding of PKM2 to HIF1 α (Wallace 2012).

2.1.7.3 Role of mitochondria in tumorigenesis

As mitochondria play a critical role in numerous bioenergetic, anabolic and cell death-inducing biochemical pathways, it is not surprising that mitochondrial dysfunction contributes to the development of a plethora of human diseases, which range from highly tissue-specific conditions to generalized whole-body disorders including cancer. Several common features of established tumor cells can directly or indirectly result from mitochondrial deregulation. Moreover, mitochondria may be implicated in early tumorigenesis, as cancer progenitor cells appear, replicate and progressively acquire a malignant phenotype (Galluzzi 2010).

Although mutations in the mtDNA in cancer cells have been recognized for more than two decades, interest in the role of mitochondrial alterations in cancer came to general attention with the discovery of mitochondrial tricarboxylic acid (TCA) cycle gene mutations in cancer cells. Cancer cell defects are now well established in the genes for succinate dehydrogenase (SDH), fumarate hydratase (*FH*), and isocitrate dehydrogenase 1 (*IDH1*) and *IDH2* (Wallace 2012).

Specifically, mutations in fumarate hydratase were found in families afflicted with leiomyomatosis and kidney cancers, and mutations in succinate dehydrogenase were found in patients with pheochromocytoma and paragangliomas. These mutations cause a disruption of the TCA cycle with the accumulation of fumarate or succinate, both of which can inhibit prolyl hydrolases that mediate the degradation of HIFs proteins (Jones 2009). Heterozygous missense mutations in the two NADP⁺-dependent IDH enzymes, cytosolic IDH1 and mitochondrial IDH2, have been observed in gliomas, astrocytomas, chondromas and acute myeloid leukaemia (AML). IDHs are homodimer enzymes, and the cancer cell mutations identified to date create a neomorphic function. Like IDH3, IDH1 and IDH2 can oxidatively decarboxylate isocitrate to α -ketoglutarate. However, IDH1 and IDH2 reduce NADP⁺ instead of NAD⁺, and the NADP⁺-dependent reaction is reversible because NADPH can provide sufficient energy to drive the reductive carboxylation of α -ketoglutarate to isocitrate. However, the neomorphic IDH1-R132 and IDH2-R172 mutants use NADPH to reduce α -ketoglutarate to *R*(-)-2-hydroxyglutarate ((*R*)-2HG). As a result, IDH1 and IDH2 mutant cancers produce 10–100-fold increased levels of (*R*)-2HG64, which has been hypothesized to be an ‘oncometabolite’. (*R*)-2HG is associated with alterations in cellular genomic methylation and transcription patterns and is a potent inhibitor of the α -ketoglutarate-dependent Jumonji-C domain histone *N* ϵ -lysine demethylases (JMJD2A, JMJD2C and JMJD2D (also known as KDM4D)). Hence, (*R*)-2HG may act by altering chromatin modifications. The target genes showing marked changes include transforming growth factor- β (TGF β), RAS, epidermal growth factor receptor (EGFR), WNT and genes in angiogenesis pathways. As the WNT pathway, among others, has been implicated in the regulation of mitochondrial energy metabolism, such global changes in chromatin structure could accompany alterations in bioenergetics (Wallace 2012).

Genes encoded by mitochondrial DNA (mtDNA) have long been suspected to be actively involved in tumorigenesis when cells require high amounts of energy to grow and proliferate under few constraints (Gasparre 2011). Somatic and germline mtDNA mutations have been reported for a wide variety of cancers. These include renal adenocarcinoma, colon cancer cells, head and neck tumours, astrocytic tumours, thyroid tumours, breast tumours, ovarian tumours, prostate and bladder cancer (Fig. 18) (Chatterjee 2006). Ancient mtDNA population variants have also been correlated with cancer risk. For example, the macrohaplogroup N variant in the complex I, subunit ND3 gene (*ND3*; also known as *MTND3*) at nucleotide G10398A (resulting in a T114A amino acid change) has been associated with breast cancer risk in African American women, and the 16519 T to C mtDNA control region variant is associated with endometrial cancer. A mtDNA cytochrome *c* oxidase subunit 1 (*CO1*; also known as *MTCO1*) T6777C nucleotide variant has been linked with

epithelial ovarian cancer, along with variants in several nDNA mitochondrial genes (Wallace 2012). Furthermore, the mechanistic role played by these mutations is far from being elucidated

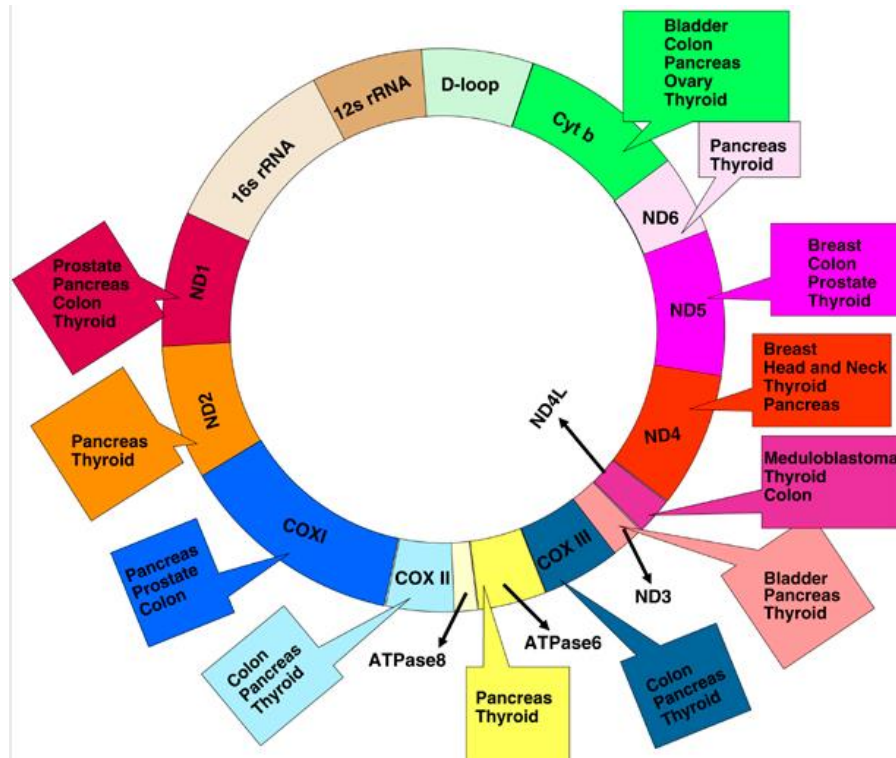


Fig. 18: The mitochondrial genome showing the various mutations summarized in this review. For mutations in complex I (*ND1*, *ND2*, *ND3*, *ND4*, *ND5*, *ND6* and *ND4L*), in complex III (*Cyt B*), in complex IV (*COX I*, *COX II* and *COX III*), mutations in complex V (ATPase 6) (Chatterjee 2006).

The most credited hypothesis is that they may foster tumor progression in various ways such as through effects on regulation of apoptosis, hypoxia-inducible factor-1 α (HIF1 α) stabilization, and reactive oxygen species (ROS) production and hence metastatic potential. Recently, Gasparre and colleagues have demonstrated that the oncogenic properties of a mtDNA encoded CI gene to influence tumor growth depend by the levels of heteroplasmy of such mutations.

2.1.7.4 Oncocytic tumors

Oncocytic tumors are a subset of neoplasia characterized by a major component of cells with aberrant mitochondrial hyperplasia (Fig. 18); they mainly originate from epithelial tissue and occur more frequently in endocrine organs such as the thyroid, kidney, parotid, parathyroid and pituitary glands (Gasparre 2010). Such peculiar type of cancer has been taken up as an excellent model to study the role of mitochondrial metabolism and of mitochondrial DNA (mtDNA) mutations in tumor progression. In fact, mitochondrial function is strongly hampered in oncocytic cells (Bonora 2007) and this has been ascribed to what is nowadays well ascertained to be the genetic hallmark of oncocytic tumors, namely the high frequency of deleterious mtDNA mutations, particularly in complex I genes (Gasparre 2007, Porcelli 2010).

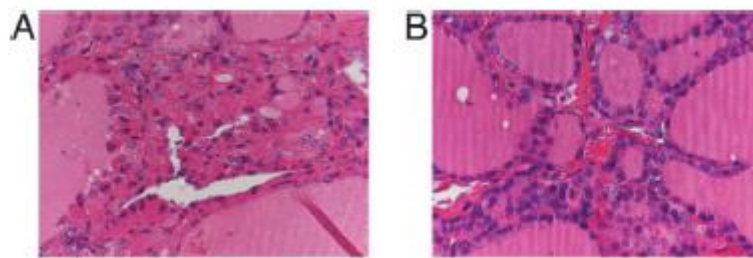


Fig. 19: Histologic appearance of the hyperplastic oncocytic nodule (A) and of one hyperplastic nodule without oncocytic change (B) (Gasparre 2007).

Upon the dissection of the functional consequences of such mutations, oncocytic tumors have revealed one of the determinants of their mostly benign behaviour, namely the setting in of a pseudonormoxic situation, i.e. a chronic hypoxia-inducible factor 1 α (HIF1 α) destabilization, due to an imbalance of α -ketoglutarate and succinate, two key Krebs cycle metabolites which regulate the prolyl-hydroxylases responsible for HIF1 α degradation (Porcelli 2010, Gasparre 2012). HIF1 α is well known to be the main transcription factor presiding to adaptation to hypoxia and mediating the progression of cancer cells towards malignancy (Semenza 2003), whose destabilization in oncocytic tumors may explain the low-proliferative and low-aggressive behaviour. In fact, oncocytic tumors are often considered benign entities, which may be in part due to the scarce ability to trigger neoangiogenesis, a feature that aids differential diagnosis, for instance, in renal oncocytoma (Gasparre 2010).

Recently, a parotid and a thyroid oncocytoma were described in patients with PTEN and FLCN mutation, causing autosomal dominant syndromes, respectively Cowden and Birt–Hogg–Dubè, (Pradella 2013), suggesting that there could be an alternative determinant to pathogenic mtDNA mutation in oncocytic phenotype in cancer cells.

Interestingly, oncocytic tumors have been described to be more resistant to radiotherapy than their non-oncocytic counterparts, consistently with the reports that rectal carcinoma patients undergoing radiotherapeutic treatment were observed to develop oncocytic relapses in the same anatomical site of the primary tumor (Rouzbahman 2006, Ambrosini-Spaltro 2006).

2.2 P53: LINK BETWEEN CANCER METABOLISM AND DNA DAMAGE RESPONSE

2.2.1 *p53 and mitochondria*

The tumor suppressor p53 can mediate growth arrest and initiate apoptosis. In addition to its traditional role of guardian of the genome, p53 appears to regulate various aspects of metabolism and mitochondrial biogenesis. It can be phosphorylated by AMP-activated protein kinase (AMPK) in response to energy limitation, thus activating cell cycle checkpoints. p53 also favours ATP production by OXPHOS and the decrease of cellular ROS production by inducing TP53-induced glycolysis and apoptosis regulator (TIGAR). TIGAR negatively regulates glycolysis by degrading fructose-2,6-bisphosphate, which is an allosteric activator of phosphofructokinase 1. This shifts carbon flux away from glycolysis and into the pentose phosphate pathway, which increases NADPH production and thus heightens antioxidant defences. p53 also negatively regulates phosphoglycerate mutase and AKT, thus further inhibiting glycolysis and upregulating OXPHOS complex IV by the induction of the cytochrome *c* oxidase (COX) Cu₂₊ chaperone, SCO2. Because the inhibition of glycolysis can redirect glucose-6-phosphate into the pentose phosphate pathway, this could increase antioxidant defences in conjunction with increased OXPHOS. Thus, the inactivation of p53 should decrease OXPHOS in favour of glycolysis, increase ROS production and inhibit apoptosis (Wallace 2012).

Moreover, the physical interaction of tumor suppressor with mtDNA, TFAM, POLG and the coactivator PGC-1 α was reported (Yoshida 2003, Achanta 2005, Bakhanashvili 2008), overall, these data suggest a positive control of p53 on mitochondrial biogenesis. Nevertheless, p53 has been recently called into play as negative regulator through its repressor activity at the promoters of murine homologues of the PGC-1 β family in the context of telomere dysfunction (Sahin 2011).

2.2.2 *p53 and DNA Damage Response*

At the end of the 1800 the German biologist Boveri suggested that the pathogenesis of cancer might be driven by a “specific and abnormal chromosome constitution”. A century later, genomic instability is recognized as a characteristic of most solid tumors and adult-onset leukaemias. In most cancers, the instability is obvious as alterations in chromosome number and structure, a phenotype termed chromosomal instability, and as changes to the structure of DNA, such as nucleotide substitutions, insertions and deletions. When they occur in crucial ‘driver’ genes these mutations can alter cell behavior, confer a selective advantage, drive the development of the disease and can also influence how the tumor will respond to therapy. Given the potentially devastating effects of genomic instability, cells have evolved an intricate series of interlocking mechanisms that maintain genomic integrity. The size of this task is daunting; the integrity of DNA is continually challenged by a variety of agents and processes that either alter the DNA sequence directly or cause mutation when DNA is suboptimal repaired (for example: ultraviolet component, ionizing radiation, cigarette smoke). The variety and frequency of DNA lesions are matched by the complexity of mechanisms that counteract these threats to genomic integrity. Collectively, these mechanisms are known as the DNA damage response (DDR) (Lord 2012).

Nuclear DNA is undoubtedly the most precious component of a cell. It is not surprising therefore that any kind of damage that introduces a discontinuity in the DNA double helix elicits a prompt cellular reaction. The DNA damage response has two distinct, but coordinated, functions: it prevents or arrests the duplication and partitioning of damaged DNA into daughter cells to impede the propagation of corrupted genetic information and it coordinates cellular efforts to repair DNA damage and maintain genome integrity (d’Adda di Fagagna 2008).

The DDR pathways consist of interconnected components that respond to DNA damage to allow repair and promote cell survival. The DNA repair pathways and downstream cellular responses have diverged in cancer cells compared with normal cells due to genetic alterations that underlie drug resistance, disabled repair and resistance to apoptosis. Consequently, abrogating DDR pathways represents an important mechanism for enhancing the therapeutic index of DNA-damaging anticancer agents (Al-Ejeh2012). In cancer cells, an important a potential cause of DNA damage is represented also by replication stress that can be caused by oncogene-induced hyper-replication that activates origins more than once per S phase, by nucleotide pool imbalance or by DNA damage; for example, by reactive oxygen species (Curtin 2012).

2.2.2.1 DDR signal transduction

A wide range of DNA lesions elicit the activation of DDR pathways and subsequent cell cycle checkpoints. Genetic lesions include DNA base damage or base misincorporation, DNA crosslinks and DNA single strand breaks or double strands breaks.

DDR pathways resemble the signaling paradigm established for growth factors, in which the cognate pathway comprises detection, signal transduction and effectors phases (Fig. 20).

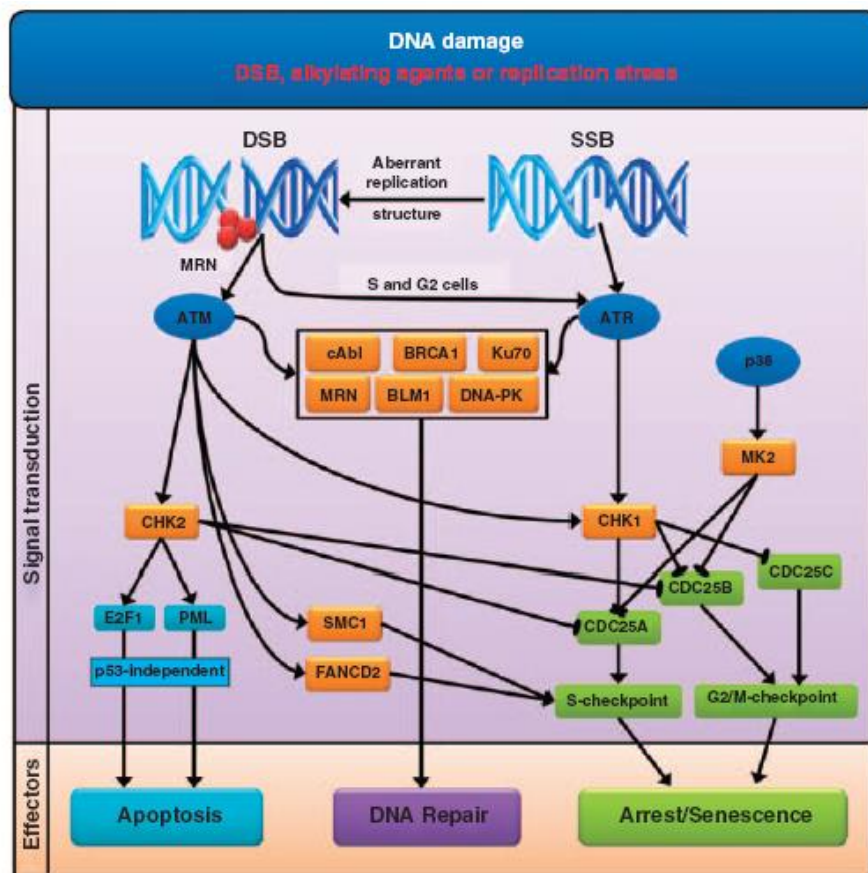


Fig. 20: DNA-damage response pathway. A set of targets lie downstream of ATM and ATR, including DNA repair proteins BRCA1, NBS1, BLM1, cAbl and 53BP1; cell cycle checkpoint proteins Chk1 and Chk2; and S-phase delay effectors FANCD2 and SMC1. In addition, downstream targets of ATM include p53 and MDM2, which are phosphorylated at Ser-15 and Ser-395, respectively. p53 is also phosphorylated by ATR at Ser-15. Furthermore, p53 is phosphorylated at Ser-20 by ATM-activated Chk2. Accumulation (by loss of MDM2 inhibition) and stabilization or activation of p53 (by phospho-Chk2 and phosphor-ATM-mediated phosphorylation) exert p53-dependent G1/S arrest or apoptosis.

The detectors of DNA-damage signaling activate signal transducers by recruiting them to sites of DNA damage and include the Mre11-Rad50-Nbs1 complex and replication protein A-coated single stranded DNA. The key signal transducers downstream of the detectors are the ataxia telangiectasia-mutated (ATM) and ATM-Rad3-related (ATR) protein kinases. ATM and ATR are Ser/Thr-Gln-directed protein kinases with overlapping substrate specificities. Whereas the ATM pathway is active during all phases of the cell cycle in response to double-strand breaks (DSBs), ATR acts primarily in S and G2 phases of the cell cycle in an ATM-dependent manner. The ATR pathway mainly responds to agents that interfere with the function of DNA replication forks (replication stress), such as ultraviolet light and gemcitabine, although it is now recognized that the ATR pathway can also activate downstream components of the ATM arm following replication fork stalling or ultraviolet treatment. In addition, DNA-alkylating agents can activate both pathways. Checkpoint proteins 1 and 2 (Chk1 and Chk2) are key downstream substrates of ATM and ATR. Chk1 or Chk2 phosphorylate several downstream substrates necessary for activating the DNA-damage checkpoints and subsequently halting the cell cycle. More recently, the p38MAPK/MAPKAP-K2 (MK2) complex has been characterized as an additional checkpoint transducer downstream of ATM and ATR. The effectors lie downstream of signal-transducing molecules and are involved in the inhibition of cell cycle progression, DNA repair activation and maintenance of genome stability. When damage is beyond repair, proteins in the DDR network mediate one of two effector functions: initiation of permanent cell cycle arrest (cellular senescence) or cell death. Characterizing these two outcomes will have important implications for understanding DDR signaling and improving the efficacy of DNA-damaging agents used in anticancer treatments. Although Chk1 and Chk2 proteins exhibit comparable cellular activities, Chk1 is important for checkpoint and replication arms of the DDR signaling, whereas Chk2 is more important for DNA-damage-induced apoptosis. However, as 50% of cancers lack functional p53, DDR signaling via the ATM/ATRChk2-p53 pathway is attenuated. Furthermore, while G1 arrest may be initiated independently of p53, it is not maintained owing to the lack of functional p53. Consequently, p53-mutant cancer cells are more resistant to apoptosis and rely on the S- and G2-phase checkpoints to repair DNA damage and promote cell survival (Al-Ejeh 2012).

2.2.2.1.1 *p53 as main effector of DDR*

The p53 signalling pathway is activated in response to a variety of stress signals, allowing p53 to coordinate transcription programmes that ultimately contribute to tumor suppression. Loss of p53 function, through mutations in p53 itself or perturbations in pathways signalling to p53, is a common feature in the majority of human cancers. More than 75% of the mutations result in the expression of a p53 protein that has (in most cases) lost wild-type functions and may exert a dominant-negative regulation over any remaining wild-type p53. Most interestingly, however, mutant p53 also acquires oncogenic functions that are entirely independent of wild-type p53 (Muller 2013).

In normal unstressed cells, p53 is a very unstable protein with a half-life ranging from 5 to 30 min, which is present at very low cellular levels owing to continuous degradation largely mediated by MDM2. Principally, MDM2 is an E3 ligase and promotes p53 degradation through a ubiquitin-dependent pathway on nuclear and cytoplasmic 26S proteasomes. Importantly, MDM2 itself is the product of a p53. Thus, the two molecules are linked to each other through an autoregulatory negative feedback loop aimed at maintaining low cellular p53 levels in the absence of stress (Fig. 21) (Moll 2003)

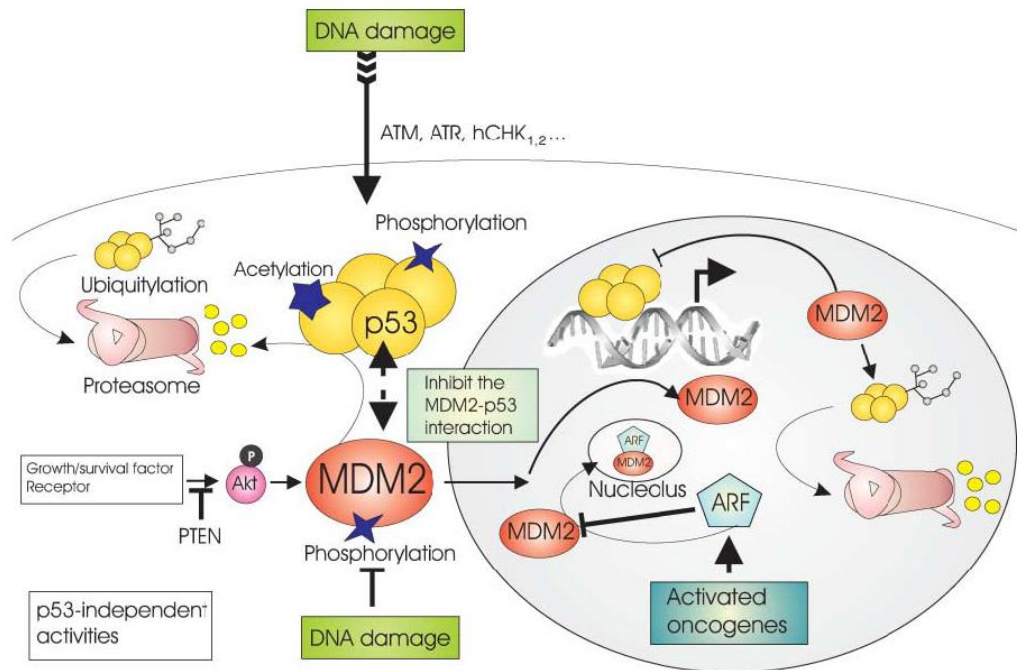


Fig. 21: Regulation of p53 by MDM2. p53 and MDM2 form an autoregulatory feedback loop. p53 stimulates the expression of MDM2; MDM2, in turn, inhibits p53 activity because it stimulates its degradation in the nucleus and the cytoplasm, blocks its transcriptional activity, and promotes its nuclear export. A broad range of DNA damaging agents or deregulated oncogenes induces p53 activation. DNA damage promotes phosphorylation of p53 and MDM2, thereby preventing their interaction and stabilizing p53. Likewise, activated oncogenes induce ARF protein, which sequesters MDM2 into the nucleolus, thus preventing the degradation of p53. Conversely, survival signals mediate nuclear import of MDM2 via Akt activation, which destabilizes p53 (Moll 2003).

There are multiple layers of regulation that connect MDM2 function with p53 stability during stress responses. A prominent physiological regulator of MDM2 is the tumor suppressor ARF. ARF interferes with the MDM2-p53 interaction, thereby acting to stabilize and activate p53. The low steady-state levels of ARF in normal cells are dramatically induced upon oncogenic stress. Interestingly, although the level of p53 is elevated in the absence of MDM2, p53 is still degraded in the cells of MDM2 null mice, suggesting the existence of alternative, MDM2-independent pathways for p53 degradation *in vivo*. Indeed, the recently discovered E3-ligases COP1, Pirh2, Arf-BP1, and others have clearly been shown to contribute to the efficient control of p53 levels in tissue culture and *in vitro* biochemical experiments. Nevertheless, the precise roles of MDM2-independent degradation in stress-induced p53 stabilization remain to be elucidated (Kruse 2009).

Phosphorylation of p53 is classically regarded as the first crucial step of p53 stabilization. p53 can be modified by phosphorylation by a broad range of kinases, including ATM/ATR/DNAPK, and Chk1/Chk2. Phosphorylation of serine residues within the N-terminal p53 transactivation domain

was among the first posttranslational modifications of p53 identified and has been extensively investigated in vitro biochemical assays, in tissue culture studies, and recently by using sitespecific knockin animals. N-terminal phosphorylation at Ser15 (mouse Ser18) and Ser20 (mouse Ser23) have been generally thought to stabilize p53 by inhibiting the interaction between p53 and MDM2 (Fig. 22). Ser15 and Ser20 are phosphorylated after DNA damage and other types of stress by ATM, ATR, DNA-PK, Chk1, and Chk2. Although it remains unresolved which of the different kinases perform the phosphorylation of these N-terminal regulatory sites in response to the varying stress signals, and to which extent N-terminal phosphorylation affects the p53-MDM2 interaction, the general consensus remains that their phosphorylation occurs rapidly in response to various stress stimuli to activate p53 (Kruze 2009).

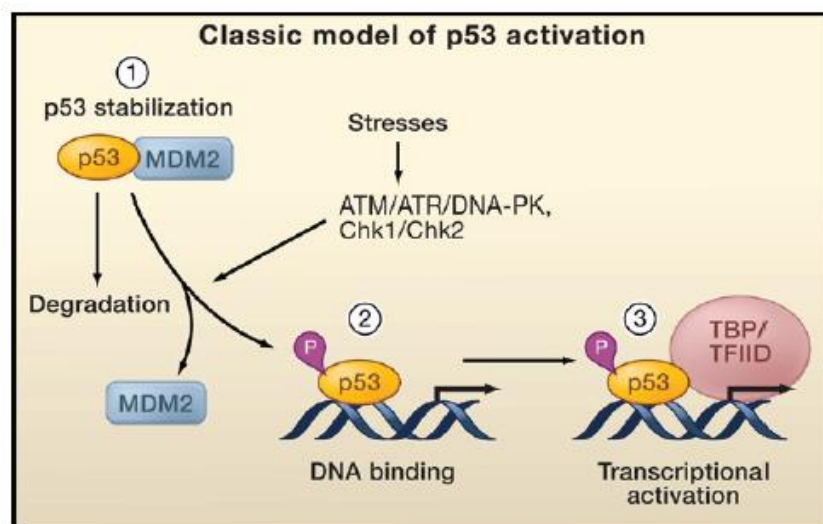


Fig. 22: Classical Model of p53 Activation. The classical model for p53 activation generally consists of three sequential activating steps: (1) stress-induced stabilization mediated by phosphorylation (P), (2) DNA binding, and (3) recruitment of the general transcriptional machinery. During normal homeostasis, p53 is degraded after Mdm2-mediated ubiquitination (left), while stress signal-induced p53 phosphorylation by ATM, ATR, and other kinases stabilizes p53 and promotes DNA binding. DNA-bound p53 then recruits the transcriptional machinery to activate transcription of p53 target genes (Kruze 2009).

Once stabilized, p53 exerts tumor-suppressive functions by inducing the expression of effector genes by interaction with specific DNA sequence within the promoter regions of target genes and through posttranslational modification like acetylation.

As a transcription factor, p53 recognizes its target genes by binding to a consensus response element located proximal to the transcription start site either at the gene promoter, the first intron or even further downstream of the gene. The canonical p53 consensus response element (p53RE) was originally defined as two tandem copies of a decamer motif “RRRCWWGYYY” separated by a 0–13 bp spacer, where “R” represents purines, “W” represents adenine or thymine, and “Y” represents pyrimidines. The initial description of the decamer half-site with a “CWWG” core as “C(A/T)(T/A)G” greatly facilitated the identification of many p53 target genes. Conversely, mutant p53 derived from tumors failed to bind to the canonical p53RE, leading to a loss of function that is characteristic of a tumor suppressor (Wang 2010).

Histone acetyltransferases (HATs) provide an important layer of p53 regulation, particularly in transcription. p53 is acetylated by the histone acetyltransferase CBP/p300, and CBP/p300 mutations are found in several types of human tumors. The acetylation is critically important both for the efficient recruitment of cofactors and for the activation of p53 target genes in vivo. Once localized at promoter regions, CBP/p300 can enhance transcription by acetylating histones in the vicinity of target genes, thereby establishing a more accessible chromatin conformation, and by bridging transcription factors to the pol II holoenzyme (Kruse 2009).

Two large subsets of p53 target genes have been identified: (I) negative regulators of cell cycle progression, such as the p21 cyclin-dependent kinase inhibitor 1A (*CDKN1A*), *14-3-3 σ* , and growth arrest and DNA damage-inducible gene (*GADD45a*); and (II) apoptosis-promoting genes, such as p53 upregulated modulator of apoptosis (*PUMA*) as well as the BH domain proteins Bcl-2-associated protein X (*BAX*) and Bcl-2 antagonist/killer (*BAK*). Mutational inactivation of p53 allows the uncontrolled proliferation of damaged cells. By contrast, the expression of dominant active forms of p53, leading to constitutive expression of downstream genes, results in degenerative phenotypes and premature aging (Reinhardt 2012) (Fig. 23).

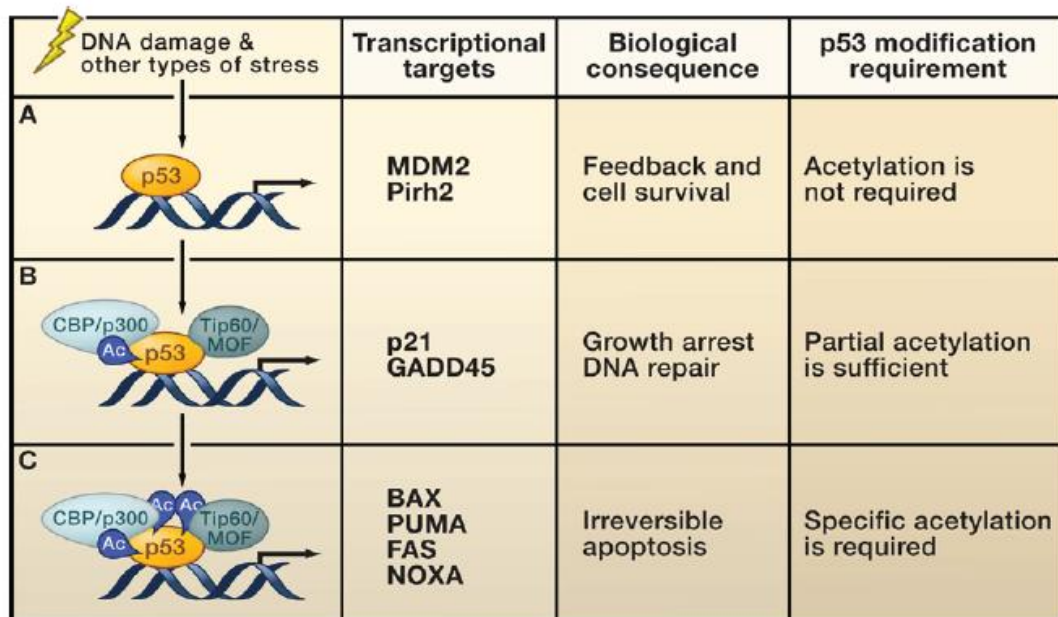


Fig. 23: p53 Acetylation and Target Gene Regulation. Upon stress-induced p53 activation, different sets of p53 target genes have different requirements for p53 posttranslational modifications. (A) A number of promoters can be activated by unacetylated p53. This class of p53 target genes protects cells from excessive p53 activation. These target genes include Mdm2, Pirh2, and others. (B) The activation of genes involved in DNA repair and cell cycle control requires recruitment of specific histone acetyltransferases (HATs) and partial acetylation (Ac), acting at least in part by antirepression. (C) Full acetylation of p53 is required for the activation of proapoptotic genes. Activation of these targets induces a program to ensure efficient apoptosis (Kruse 2009).

2.2.2.2 Cellular senescence as DNA damage response

The impact of DDR activation may be different: if the DNA damage that is generated in proliferating cells is promptly and properly fixed, cells will quickly resume normal proliferation. By contrast, when DNA damage is particularly severe, cells may undergo programmed cell death (apoptosis), a cellular form of suicide that removes damaged cells from a cell population. However, an additional outcome is also possible: cells may initiate cellular senescence, a naturally irreversible cell-cycle arrest that is induced by DDR signalling. It is still unclear what determines the choice between apoptosis and senescence, but determinants may include cell type and the intensity, duration and nature of the damage. In contrast to quiescence, senescence cannot be reversed by altering the cellular environment, by removing cell contact inhibition or providing abundant nutrients *in vitro*. (d'Adda di Fagagna 2008).

The first description of 'cellular senescence' dates to 1965 when Leonard Hayflick observed that cells undergo a replicative senescence in culture. It is now well established that premature forms of cellular senescence can be triggered by DNA damage agents, and through either the activation of

oncogenes (a type of senescence that is termed oncogene-induced senescence (OIS) or the loss of tumour suppressor genes, including *PTEN*, *RBI*, *NF1* and *INPP4B* (Fig. 24) (Nardella 2011).

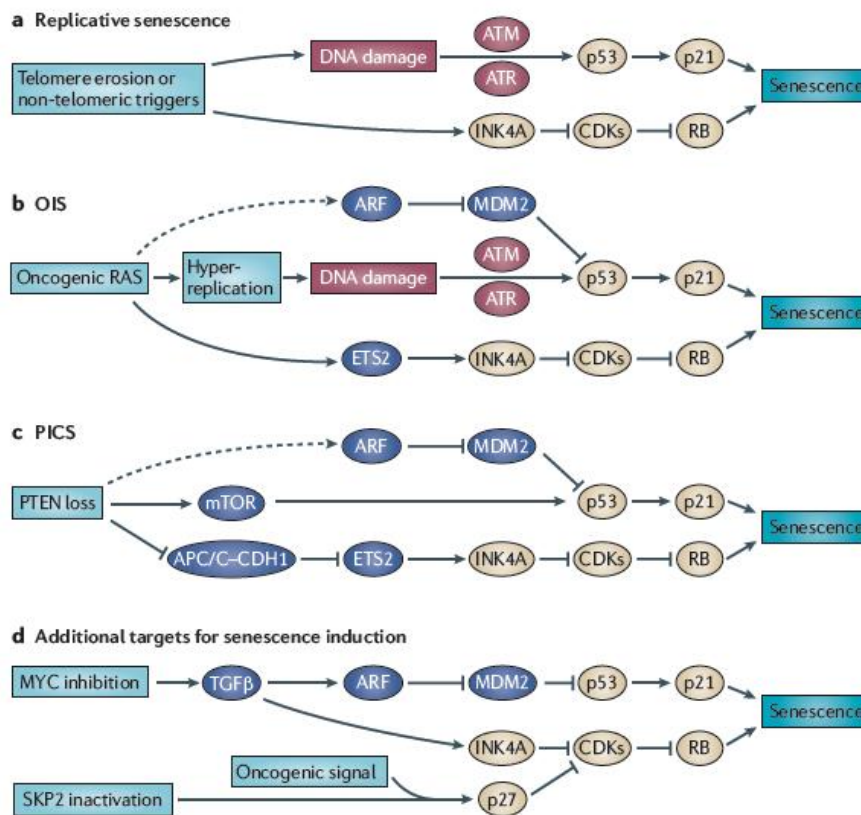


Fig. 24: Differential senescence responses. Several independent stimuli have the capacity to induce senescence through various common effectors. These differential stimuli can be categorized as replicative senescence, oncogene-induced senescence (OIS) and PTEN loss-induced cellular senescence (PICS). Upstream effectors are shown in dark blue, DNA damage transducers in red and downstream effectors in yellow. **a** Replicative senescence is driven by multiple stimuli, including telomere erosion, and can result in activation of INK4A (also known as p16) expression and can trigger DNA damage pathways resulting in p53 induction. **b** In OIS, the activation of p53 is driven by two main mechanisms. First, it is stabilized through phosphorylation by the DNA damage response (DDR) and second, by ARF-mediated stabilization.. **c** By contrast, p53 upregulation in PICS is mainly mediated through translational mechanisms that are controlled by mTOR. In addition, the ETS2–INK4A pathway is also required for senescence induction. Although RAS–MAPK signalling directly promotes ETS2 activity³⁴, PICS-mediated activation of ETS2 occurs through the deregulation of ETS2 degradation by the CDH1-containing anaphase-promoting complex (APC/C (also known as the cyclosome)–CDH1). **d** Senescence induction can also be achieved through targeting key inhibitors of senescence. For example, MYC inactivation can result in the restoration of transforming growth factor-β (TGFβ) signalling pathways resulting in senescence, and the inhibition of S phase kinase-associated protein 2 (SKP2) in combination with additional oncogenic events (Nardella 2011).

Despite the different modes of activation, all senescent cells present common features. Senescent cells differ from other nondividing (quiescent, terminally differentiated) cells in several ways, although no single feature of the senescent phenotype is exclusively specific. Hallmarks of senescent cells include (Rodier 2011) (Fig. 24):

(I) The senescence growth arrest is permanent and cannot be reversed by known physiological stimuli.

(II) Senescent cells increase in size, sometimes enlarging more than twofold relative to the size of nonsenescent counterparts (Hayflick 1965).

(III) Senescent cells express a senescence-associated β -galactosidase (SA- β -gal) (Dimri 1995), which partly reflects the increase in lysosomal mass

(IV) Most senescent cells express p16INK4a, which is not commonly expressed by quiescent or terminally differentiated cells. In some cells, p16INK4a, by activating the pRB tumor suppressor, causes formation of senescence-associated heterochromatin foci (SAHF), which silence critical proliferative genes. p16INK4a, a tumor suppressor, is induced by culture stress and as a late response to telomeric or intrachromosomal DNA damage. Moreover, p16INK4a expression increases with age in mice and humans and its activity has been functionally linked to the reduction in progenitor cell number that occurs in multiple tissues during aging.

(V) Cells that senesce with persistent DDR signaling harbor persistent nuclear foci, termed DNA segments with chromatin alterations reinforcing senescence (DNA-SCARS). These foci contain activated DDR proteins, including phospho-ATM and phosphorylated ATM/ataxia telangiectasia and Rad3 related (ATR) substrates, and are distinguishable from transient damage foci. DNA-SCARS include dysfunctional telomeres or telomere dysfunction-induced foci.

(VI) Senescent cells with persistent DDR signaling secrete growth factors, proteases, cytokines, and other factors that have potent autocrine and paracrine activities.

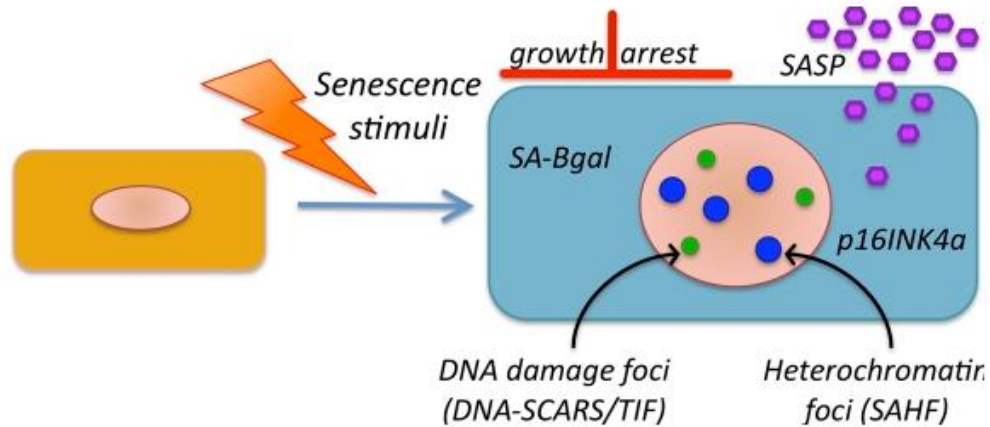


Fig. 24: Hallmarks of senescent cells. Senescent cells differ from other nondividing (quiescent, terminally differentiated) cells in several ways, although no single feature of the senescent phenotype is exclusively specific. Hallmarks of senescent cells include an essentially irreversible growth arrest; expression of SA-Bgal and p16INK4a; robust secretion of numerous growth factors, cytokines, proteases, and other proteins (SASP); and nuclear foci containing DDR proteins (DNA-SCARS/TIF) or heterochromatin (SAHF). The pink circles in the nonsenescent cell (left) and senescent cell (right) represent the nucleus.

Studies of human tissues and cancer-prone mice argue strongly that cellular senescence suppresses cancer *in vivo*. Premalignant human nevi and colon adenomas contained cells that express senescence markers, including SA- β -gal and DDR signaling; however, senescent cells were markedly diminished in the malignant melanomas and adenocarcinomas that develop from these lesions. Likewise, in mouse models of oncogenic Ras expression or Pten deletion, senescent cells were abundant in premalignant lesions, but scarce in the cancers that eventually developed. Further, dismantling the senescence response by inactivating p53 caused a striking acceleration in the development of malignant tumors (Rodier 2011). The concept of pro-senescence therapy has emerged over the past few years as a novel therapeutic approach to treat cancers. However, unlike the field of apoptosis, which was embraced with great fervor in its promise to cure cancer by cell suicide, there has been little excitement surrounding the use of senescence as a cancer therapy strategy. This scepticism mostly arose from the prevailing dogma that senescent cells were not cleared by the immune system, but remained part of the tissue. (Nardella 2011). Second, senescent cells develop a secretory phenotype (SASP) that can affect the behavior of neighboring cells. Strikingly, many SASP factors are known to stimulate phenotypes associated with aggressive cancer cells. For example, senescent fibroblasts secrete amphiregulin and growth-related oncogene (GRO) α , which, in cell culture models, stimulate the proliferation of premalignant epithelial cells. Senescent cells also secrete high levels of interleukin 6 (IL-6) and IL-8, which can stimulate

pre-malignant and weakly malignant epithelial cells to invade a basement membrane. Further, senescent fibroblasts and mesothelial cells secrete VEGF, which stimulates endothelial cell migration and invasion (a critical step in tumor-initiated angiogenesis), and senescent fibroblasts and keratinocytes secrete matrix metalloproteinases (Rodier 2011). Hence, cancer cells in a senescent state might remain as 'dormant' malignant cells, and therefore represent a dangerous potential for tumor relapses, since through disruption of p53 and p21 function they may escape senescence (Brown 1997, Beausejour 2003).

3. AIMS of the STUDY

Radiotherapy (RT) is one of the most effective non-surgical treatments of cancer patients with better functional preservation and less systemic influences. Cellular response to γ -rays is mediated by Ataxia telangiectasia mutated (ATM) kinase and the downstream effector p53. When p53 is phosphorylated, it can transactivate several genes to induce permanent cell cycle arrest (senescence) or apoptosis. Epithelial and mesenchymal cells as well as their derived tumor cells are more resistant to radiation-induced apoptosis and respond mainly by activating senescence. Hence, tumor cells in a senescent state might remain as “dormant” malignant cell in fact through disruption of p53 function, cells may overcome growth arrest. A particular type of relapses after γ -rays was observed in patients with colorectal cancer, where oncocytic features were acquired in the recurring neoplasia after radiation therapy. Oncocytic tumors are characterized by aberrant biogenesis of nonfunctional mitochondria in their cells. They are mainly non-aggressive neoplasms and their low proliferation degree can be explained by chronic destabilization of HIF1 α , which presides to adaptation to hypoxia and mediates the progression of cancer cells towards malignancy. Moreover, it also plays a pivotal role in hypoxia-related tumor radio-resistance since it is able to interfere with the signalling of p53, and hence to block the senescent program induced by γ -rays. The aim of this project was to verify whether mitochondrial biogenesis can be induced following radiation treatment, in relation of HIF1 α status, and whether such a mechanism is predictive of a senescence response. To this purpose, *in vitro* and *in vivo* studies have been designed, in order to assess:

1. the molecular mechanisms involved in mitochondrial biogenesis due to radiation treatment;
2. whether p53 is a key regulator of mitochondrial biogenesis;
3. the role of HIF1 α in regulating mitochondrial biogenesis and senescence induced by γ -rays;
4. whether mitochondrial biogenesis parameters could be utilized as prognostic markers to predict the stabilization of HIF1 α after radiation treatment.

4. MATERIALS AND METHODS

4.1 Cell cultures

Human colorectal carcinoma cell line HCT116, their genetically modified derivatives lacking TP53 (Bunz 1998), HCT116^{TP53-/-}, and the osteosarcoma cell line HPS11 were grown in Dulbecco's Modified Eagle's Medium (DMEM) supplemented with 10% foetal bovine serum (FBS), 100units/mL penicillin, 100µg/mL G-streptomycin and 2mmol/L L-glutamine. RPE1 (non-tumor human retinal epithelial cell line) were cultured in DF12 medium [DMEM/nutrient mixture F-12 ham (Sigma-Aldrich)] supplemented with 10% FBS and 100units/mL penicillin, 100µg/mL G-streptomycin. Cell lines were maintained in a humidified incubator at 37 °C with 5% CO₂.

4.2 γ -rays treatment and HIF1 α compound-mediated stabilization

Treatment was optimized to (I) use γ -rays doses close to those currently used in radiotherapy, (II) maintain cells viable and (III) eliminate dead cells from the population. 200.000 cells were seeded per 25cm² flask (T0). The following day flasks were submitted to a dose of 4 Gray (Gy), specifically 2 Gy/min with the biological irradiator IBL437C (89-294). The treatment was repeated after exactly 24 hours for 4 days (IR). Alternatively, cells were allowed to recovery for 120 hours before harvesting (REC). The medium was changed after the last dose of irradiation. HIF1 α was stabilized by adding the inhibitor of proline hydroxylase dimethylxallylglycine (DMOG, 1µM) or the iron chelator desferrioxamine (DFO, 250nM) (Sigma-Aldrich) to the culture medium for the entire duration of the radiation treatment.

4.3 Western blotting

Proteins were extracted from snap-frozen tissue using RIPA Lysis Buffer [TrisHCl (50mM), NaCl (150mM), SDS (0.1%), Triton (1%), EDTA (1mM, pH 7.6)]. Total lysates (80µg) were denatured for 5min at 99°C in Laemli Buffer [SDS (4%), beta-Mercaptoethanol (10%), Glycerol (20%), Tris (125mM, pH 6.8), bromo-phenol-blue (0.25%)] and separated by SDS-PAGE (10%). Hybond-ECL nitrocellulose membranes (GE Healthcare) were incubated with antibody against beta-actin (1:20000, Sigma), HIF1alpha (1:1000, Bethyl Laboratories, Montgomery, TX, USA) γ -tubulin (Sigma), p53, p21, p16 (Santa Cruz biotechnologies), OPA1 (Bioscience), TFAM (AbCam), SDHA, SDHB, NDUFA9, NDUFS3 (MitoSciences), ATP5 β (BioVision), VDAC

(Millipore), Core II (Invitrogen) and MDM2 (Calbiochem). Western Breeze Kit (Invitrogen) was used for blocking, secondary antibody and chemiluminescent substrate incubations.

4.4 Nucleic acid extraction and reverse transcription

DNA from cell lines and snap-frozen mouse tumors was extracted using QIAamp DNA Mini Kit (Qiagen, Hilden, Germany). RNA extraction was performed using the Trizol reagent (*Invitrogen*) according to the manufacturer protocol. Cells are first pelleted at 1500 rpm for 5', then the pellet are washed twice in PBS buffer. The pellet is suspended in 300 μ L of Trizol Reagent and transferred in a new tube. Follows an incubation a RT for 5'. 60 μ L of chloroform are added to separated the two phases. The tube is shaker 15'' in hands and then incubated at RT for 2-3'. Then the tube is centrifugated at 12.000g for 15' at 4°C. The aqueous phase is removed avoid drawing any of the interphase or organic layer, and transferred to a new tube and the RNA isolation phase begins. 200 μ L of isopropanol is added and the mix is incubated 10' at RT. Then is centrifugated at 1200g for 10' at 4°C. The supernatant is removed to leave only the pellet in the tube. The pellet is washed by adding 200 μ L of ethanol (70%) and centrifugated at 7500g at 5'. Finally the ethanol is removed and the pellet is air dried and resuspended in 20-40 μ L of RNAase-free water and incubated for 10' at 55°C-60°C to help resuspension. The integrity of the RNA is verified on electrophoresis gel at 1%. For the quantification is utilized the Nanodrop (*Thermo Scientific*). cDNA was prepared by retrotranscription of 1 μ g of total RNA with High Capacity cDNA Reverse Transcription Kit (Life Technologies).

4.5 MtDNA sequencing

Whole mtDNA resequencing was performed with MitoAll (Applied Biosystems) as previously described (Bonora 2006). Electropherograms were analyzed with Sequencing Analysis version 2.5.1 software and inspected with SeqScape version 2.5 software (Applied Biosystems). Sequencing was performed with Big Dye v3.1 (Applied Biosystems, Foster City, CA, USA) in 10 μ l final volume, according to the manufacturer's instructions and run on a 3730 DNA Analyzer (Applied Biosystems).

4.6 mtDNA copy number

Mitochondrial DNA content was evaluated by a Real Time-PCR multiplex assay based on hydrolysis probe chemistry. Briefly, a mtDNA fragment (*MTND2* gene) and a nuclear DNA fragment (*FASLG* gene) were co-amplified in the same PCR reaction. The concentration of mtDNA normalized on nuclear DNA in the samples was extrapolated from a standard curve of serial dilution of a vector in which the templates for the two amplifications were cloned tail to tail, to have a ratio of 1:1. Primers, probe and conditions were previously published (Cossarizza 2003). About 2ng of DNA extracted from cells and tissues were analysed using the LightCycler® 480 Probes Master Mix (Roche) and the LightCycler® 480 (Roche) instrument.

4.7 Gene expression analyses via Real-Time PCR

Quantitative Real-time PCR (qRT-PCR) for MT-ND5, p21, GADD45 α , BAX, PGC-1 β , HIF1 α , and TUBB1 was performed on cDNA diluted 1:50. The qRT-PCR reaction was performed with GoTaq® qPCR Master Mix (Promega) and run in 7500 Fast Real-Time PCR System (Life Technologies), using following conditions: 95°C 5min; 45 cycles of 95°C 15sec and 60°C 45sec. The calculations were performed following $2^{-\Delta\Delta CT}$ method. Primer sequences were designed using Primer3 software (Rozen 2000). Primer sequences are listed in Appendix A.

4.8 Cellular and mitochondrial morphology

Cellular and mitochondrial morphology was assessed after cell staining with 100nM calcein-acetoxymethyl ester (calcein-AM, Life Technologies) and 10nM MitoTracker Red (MTR - Life Technologies) for 30min at 37°C. Images were acquired with a digital imaging system using an inverted epifluorescence microscope with 63X/1.4 oil objective (Diaphot, Nikon, Japan) and a back-illuminated Photometrics Cascade CCD camera system (Roper Scientific, Tucson, AZ, USA). Images were captured and analyzed using the Metamorph software (Universal Imaging Corp., Downingtown, USA).

4.9 ATP synthesis evaluation

The amount of cellular ATP was determined by using the luciferin/luciferase assay as previously described (Zanna 2005). The measurements of mitochondrial ATP synthesis were done in cells grown in DMEM-glucose according to Manfredi (Manfredi 2002), with minor

modifications. Briefly, after trypsinization, cells were resuspended ($7 \times 10^6/\text{ml}$) in buffer A [KCl (10mmol/L), Tris-HCl (25mmol/L), EDTA (2mmol/L), bovine serum albumin (0.1%), potassium phosphate (10mmol/L), MgCl_2 (0.1mmol/L, pH 7.4)], kept for 15min at room temperature, and then incubated with 50 $\mu\text{g}/\text{mL}$ digitonin for 1min. After centrifugation, the cells pellet was resuspended in buffer A and aliquots were taken to measure ATP synthesis, protein content (Bradford 1976), and citrate synthase activity (Trounce 1996). Cell aliquots were incubated with Complex I substrates malate (5mmol/L) plus glutamate (5mmol/L) in the presence or absence of oligomycin (10 $\mu\text{g}/\text{mL}$), or with the Complex II substrate succinate (10mmol/L) plus rotenone (2 $\mu\text{g}/\text{mL}$), and ADP (0.2mmol/L) for 1 and 3min. The amount of ATP was measured as described 140. The rate of ATP synthesis was expressed as a ratio of citrate synthase activity (Trounce 1996). Dichlorodihydrofluorescein diacetate was obtained from Molecular Probes (Invitrogen) and ATP monitoring kit from BioOrbit (Turku, Finland).

4.10 *In silico promoter analyses*

The promoter and 5'UTR regulatory regions of the PGC-1 β gene were scanned to verify the presence of one or more p53 responsive elements (p53REs) using the PatSearch algorithm implemented in the DNafan tool (Gisel 2004, Grillo 2003). The syntax pattern of the p53RE is made up of two tandem repeated decamers complying with a specific consensus corresponding to the 5'-PuPuPuC(A/T)(T/A)GPyPyPy-3' sequence, allowing at most 3 mismatches. The decamers can be spaced by 0 to 13 nt. The *in silico* analysis revealed the presence of one p53RE at position -2732; -2706 (promoter region) upstream the Transcription Start Site (TSS) of the PGC-1 β gene (GRCh37 - Entrez Gene ID:133522).

4.11 *Chromatine immunoprecipitation*

After treatments, proteins were cross-linked to DNA in living nuclei by adding formaldehyde directly to the cell culture medium to a final concentration of 1%. Cross-linking was allowed to proceed for 10 min at 37°C. Cross-linked cells were washed with phosphate-buffered saline, scraped off the plates and resuspended in 20mM Tris-chloride pH=8.3, 3mM MgCl_2 , 20 mM KCl, 1mM phenylmethylsulfonyl fluoride, 1 $\mu\text{g}/\text{ml}$ leupeptin, 1 $\mu\text{g}/\text{ml}$ aprotinin. Nuclei were pelleted by microcentrifugation and lysed by incubation in nuclear lysis buffer (1% sodium dodecyl sulphate, 10mM EDTA, 50mM Tris-chloride pH=8.1, 1mM phenylmethylsulfonyl fluoride, 1 $\mu\text{g}/\text{ml}$ leupeptin, 1 $\mu\text{g}/\text{ml}$ aprotinin). The resulting chromatin solution was sonicated in order to generate 300-1000bp DNA fragments. After microcentrifugation, the supernatant was diluted with dilution

buffer (0.01% sodium dodecyl sulphate, 1.1% Triton X-100, 1.2mM EDTA, 16.7mM Tris-chloride pH=8.1, 167mM NaCl, 1mM phenylmethylsulfonyl fluoride, 1µg/ml leupeptin, 1µg/ml aprotinin) and precleared with protein A-Agarose/salmon sperm DNA and divided into aliquots. Five micrograms of p53 and HIF1 α antibodies (Santa Cruz) or any antibody (as negative control), was added to the chromatin solution and incubated on a rotating platform O.N. at 4°C. In parallel, we added acetylated H4-histone antibody (UpstateTM) or any antibody (as negative control) to a small fraction of the chromatin solution. Antibody-protein-DNA complexes were precipitated with protein A-Agarose/salmon sperm DNA. After centrifugation, the beads were washed and the protein-DNA complexes were eluted with 1% sodium dodecylsulphate, 100 mM Sodium Carbonate. DNA-protein cross-links were reversed by heating at 65°C for 4 hours and DNA was phenol extracted and ethanol precipitated. DNA fragments were analyzed by Real Time q-PCR using SybrGreen and primers specific for the CDKN1A (p21), as p53 activation-positive control, and PGC-1 β .

4.12 P53 PCR amplification and sequencing

All 10 coding exons of *TP53* and exon-intron boundaries of the gene were amplified using Fast Start Taq DNA Polymerase (Roche). PCR amplification was performed in a final volume of 25µl in a 9700 thermal cycler (Life Technologies), and PCR products were purified with Multiscreen PCR clean-up Filter Plates (Millipore). Primer sequences are listed in Appendix A. Sequencing was performed with BigDye v1.1 (Life Technologies) on both strands according to the manufacturer's instructions. Briefly, 0.32µM of primer were used in 10µl final reaction, together with 0.5µl of BigDyev1.1 and 2µl of Buffer (2x). Upon cycling (4 minute elongation) the amplicons were precipitated and run in a ABI3730 Genetic Analyzer automated sequencing machine (Life Technologies). Electropherograms were analyzed using Chromas Lite v.2.01 (Technelysium).

4.13 TP53, MDM2, HIF1 α and HIF1 α TM cloning

Plasmid for overexpression of p53 was previously done. The full length cDNA of MDM2 and HIF1 α was amplified by total cDNA obtain from RNA of RPE1 cells using the follow primer:

Bst1107I_Mdm2_fw: TGCGTATACCCACCATGGTGAGGAGCA

BamHI_Mdm2_rv: ACGGATCCCTAGGGGAAATAAGTTA

BspeI_HIF1_fw: CGTCCGGAGCCACCATGGAGGGCG

BamHI_HIF1_rv: GACGGATCCTAGTAACTGATCCAAAG

The PCR product is first cloned in pGEM-T Easy vector system (*Promega*) for the amplification. DH5 α competent cells were transformed with the plasmid: pGEM_HIF1 or pGEM_MDM2 and selected on Luria-Bertani medium containing ampicillin (100 μ g/mL) and 5-bromo-4-chloro-3-indolyl-h-D-galactopyranoside (3%). White colonies were picked and grown at 37°C in Luria-Bertani medium/ ampicillin (100 μ g/mL). DNA was extracted using in-house suspension [Tris (15mM, pH 8.0), EDTA (10mM), RNaseA (100 μ g/ml)], lysis [NaOH (0.2M), SDS (1%)] and neutralization [KAc (3M, pH 5.5)] buffers and the presence of the insert was verified using Sanger sequencing. The full length cDNA of HIF1 α and MDM2 present in pGEM_HIF1 and pGEM_MDM2 was inserted in pcDNA3.1 vector (Invitrogen) after digestion with restriction enzyme (Bst1107I and BamHI for MDM2; BspEI and BamHI for HIF1 α). The complete sequence of these plasmids was verified using Sanger sequencing.

To generate a form of HIF1 α that is not subjected to proline hydroxylase degradation, HIF1 α TM, aminoacids P402, P564 and P803 of HIF1 α were replaced with alanine residues. In normoxic conditions, O₂-dependent hydroxylation of proline (P) residues 402 and 564 in HIF1 α by the enzymes PHD (prolyl hydroxylase-domain protein) 1–3 is required for the binding of the von Hippel–Lindau (VHL) and next degradation. O₂ also regulates the interaction of HIF-1 α with transcriptional co-activators. O₂-dependent hydroxylation of asparagine (N) residue 803 in HIF1 α by the enzyme FIH-1 (factor inhibiting HIF-1) blocks the binding of p300 and CBP to HIF-1 α and therefore inhibits HIF-1-mediated gene transcription. Under hypoxic conditions, the rate of asparagine and proline hydroxylation decreases. VHL cannot bind to HIF-1 α that is not prolyl-hydroxylated, resulting in a decreased rate of HIF-1 α degradation. By contrast, p300 and CBP can bind to HIF1 α that is not asparaginyl-hydroxylated, allowing transcriptional activation of HIF-1 target genes (Fig. 25) (Semenza 2003).

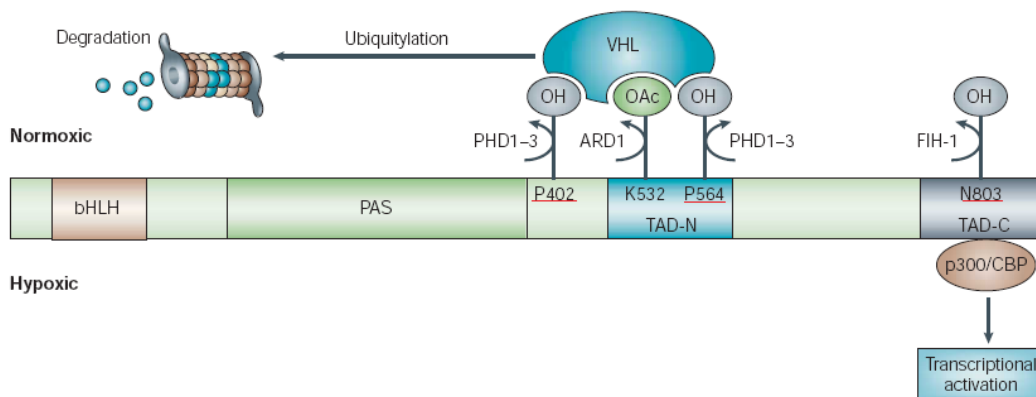


Fig. 25 O₂-dependent regulation of HIF1 α activity. The residue underline in red are those that was replaced with alanine residues (Semenza 2003).

Aminoacids P402, P564 and P803 of HIF1 α were replaced with alanine using QuikChange Site-Directed Mutagenesis Kits (Agilent) with the following primers:

P402A5'-ACTTTGCTGGCCGCAGCCGCTGGAG-3'

P402A_antisense5'-CTCCAGCGGCTGCGCCACAAAGT-3'

P564A5'-TAGACTTGGAGATGTTAGCTATATCCCAATGGATGATG-3'

P564A_antisense5'-CATCATCCATTGGGTATAGCTAACATCTCCAAGTATA-3'

N803A5'-CACAGCTGACCAGTTATGATTGTGAATTGCTGCTCCTATAACAAGG-3'

N803A_antisense5'-CCTTGTATAGGAGCAGCAACTTCACAATCATAACTGGTCAGCTGT-3'

The stabilization of HIF1 α TM in presence of oxygen was verified through western blot analysis performed on HCT116 cells trasfected with the plasmid pcDNA3.1_HIF1 α TM (Fig. 26).

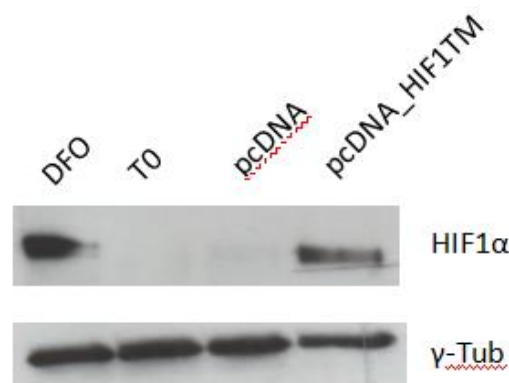


Fig. 26: Western blot analysis of HCT116 cells trasfected with pcDNA_HIF1TM. Cells treated with DFO were used as positive controls for the stabilization of HIF1 α .

4.14 Cells transfection

Cells were seeded the day before in concentration that allow to reach the 70-90% of confluence in 24 h. The transfection reaction was performed using the *X-treme GENE HP DNA Transfection Reagent (Roche)*, following the manufacturer protocol. At 600 μ l of serum free medium; 6 μ g of vector and 18 μ l of transfection reagent were added. This mix was added in the medium of the cells. The cells were incubated at 37°C for 48h and then utilized for the following experiments.

4.15 *HIF1 α degradation evaluation*

For protein stability analysis, the cells were treated with 10 μ M cycloheximide, an inhibitor of protein biosynthesis in eukaryotic organisms, and then whole cell lysates were prepared after different time of incubation. The lysates (30 μ g) were then subjected to Western blot analysis to identify the HIF1 α . Treatments with cycloheximide (50 μ g/ml) were performed at 24h after MDM2 transfection and cells collected after 0, 10 and 20 minutes of incubation.

4.16 *Senescence-associated β -galactosidase assay*

Increased β -Gal activity was determined following a protocol previously described (). The assay was performed on irradiated cells after recovery. Cells were washed twice with PBS and then incubated for 7 min with a fixation solution (2% formaldehyde and 0.2% glutaraldehyde in PBS). Cells were washed five times with PBS and incubated with a staining solution (40mM citric acid/Na phosphate buffer pH6, 1mg/ml X-gal, 5mM K₄[Fe(CN)₆]3H₂O, 5mM K₃[Fe(CN)₆], 150mM NaCl and 1mM MgCl₂ in ddH₂O) at 37°C until β -Gal staining became visible. Cells were finally washed five times with PBS.

4.17 *Rectal biopsies collection*

The study included 32 male patients, 18 years of age and older with prostate cancer. All patients underwent three-dimensional conformal radiotherapy and, by using 4-5-field techniques, a minimum energy of 6 MV was applied on linear accelerators. A computed tomography scan was performed before radiotherapy in order to enhance the reliability of the rectal dose-volume histogram. Dosing schedules followed the institutional protocols. During the treatment, patients laid in the supine position and were immobilised at the pelvis. Over 6-7 weeks period, using daily fractionation of 2Gy for 5 days a week, patients received a total dose of external-beam radiation ranging from 66 to 74Gy, given in 33-37 fractions. The radiation dose was prescribed to the isocentre (Fuccio 2011). During the examination by rectosigmoidoscopy, bioptic sampling was performed from the anterior wall of the rectum, 10cm above the anal verge, prior to and one month after the radiotherapy. Samples were snap frozen and kept at -80°C until the molecular analysis was performed. Patients were enrolled following internal ethical committee procedures.

5. RESULTS

5.1 *Effect of γ -rays on mitochondrial biogenesis*

Radiotherapy (RT) is one of the most effective non-surgical treatments of cancer patients with better functional preservation and less systemic influences. Tumor cells may escape the lethal effects of radiation and result in disease relapse (Kim 2005). Cellular response to γ -rays is mediated by ATM and the downstream effector p53. When p53 is phosphorylated, it can transactivate several genes to induce permanent cell cycle arrest (senescence) or apoptosis (Kruse 2009). A particular type of relapses after γ -rays was observed in patients with colorectal cancer, where oncogenic features were acquired in the recurring neoplasia after radiation therapy (Rouzbahman 2006, Ambrosini-Spaltro 2006). It has been demonstrated that genotoxic stress induced by γ -radiation increase mtDNA copy number, an index of mitochondrial biogenesis, in spleen and brain of total-body irradiated mouse (Malakhova 2005).

In order to test the effect of γ -rays commonly used in radiotherapy on mitochondrial biogenesis, a radiation treatment were optimized in order to: (i) use γ -rays doses close to those currently used in radiotherapy, (ii) maintain cells viable, (iii) eliminate dead cells from the population.

Different cell lines were submitted to a dose of 4 Gray (Gy) every 24 hours for 4 days (IR). Alternatively, cells were allowed to recovery for 120 hours before harvesting (REC).

The first experiments were conducted on TP53 wild type cell lines, namely non-tumor immortalized retinal epithelial, RPE1, to understand what is the response of non-tumor cell to γ -rays in term of mitochondrial biogenesis and colorectal tumor-derived cancer cell line, HCT116, since oncogenic relapses have been observed in rectal tissues.

Both cell lines survived to radiation treatment and were able to proliferate until the recovery (Fig. 27), and the significant increase upon irradiation of p53 demonstrated the activation of genotoxic response, (Pandita 2000). It was further confirmed by increased expression of p53 target gene p21, a cyclin-dependent kinase inhibitor that plays essential roles in the DNA damage response by inducing cell cycle arrest and direct inhibition of DNA replication (Jung 2010) (Fig. 28).

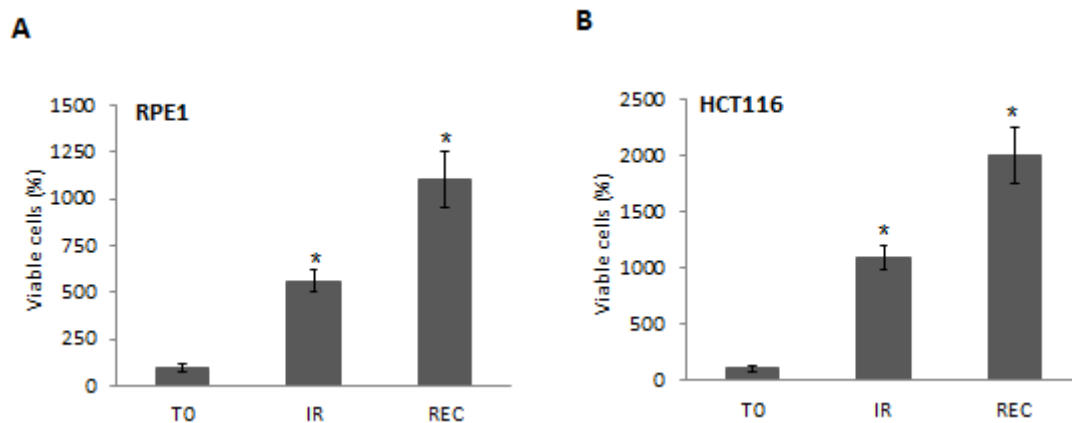


Fig. 27 Cells viability of RPE1 (A) and HCT116 (B) cell during radiation treatment at the last day of radiation treatment (IR) and after 120h of recovery (REC). Data are mean \pm SD (n=4, t-test, *P <0.05 vs T0)

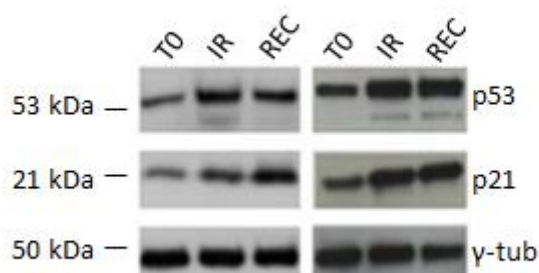


Fig. 28 Activation of genotoxic response after γ -rays treatment. Western blot analysis of p53 and p21 in RPE1 and HCT116 cells at the last day of irradiation (IR) and after 120-h of recovery (REC). Gamma-tubulin was used as a loading control. One representative experiment of three is shown

To establish the effect of genotoxic stress on mitochondrial biogenesis, mtDNA copy number was first evaluated in irradiated cells. Both RPE1 and HCT116 cells showed an increase of mtDNA copy number both at the last day of irradiation and after 120h recovery in culture following irradiation, suggesting the copy number increase is an ongoing process starting with the initial genotoxic stimulus and proceeding beyond stimulus withdrawal. In agreement with the coupling between the processes of mtDNA replication and transcription (Bonawitz 2006), the latter was also observed to increase following irradiation, even at 120h from stimulus withdrawal (Fig. 29).

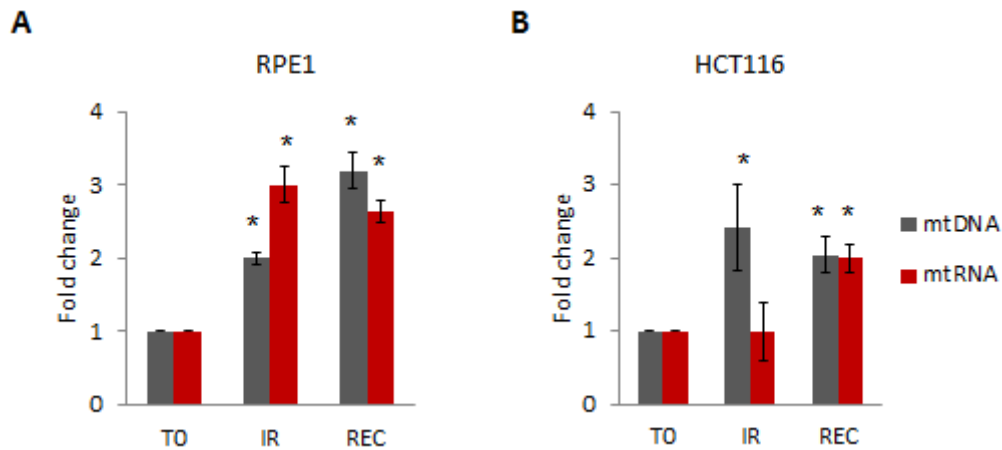


Fig. 29 Relative mtDNA copy number and mtRNA transcription in RPE1 (A) and HCT16 (B) cells after radiation treatment. Data are mean \pm SD (n=3, *P<0.05 vs T0).

The entire mtDNA was sequenced in both cell lines after irradiation and no differences from control cells were found.

In parallel to an increase of mitochondrial DNA replication and transcription, a number of mitochondrial proteins, nuclear encoded, showed an increased expression after γ -rays treatment in both cell lines. In fact, regulatory protein like TFAM and OPA1 increased from the last day of radiation treatment, which remained constant at 120h after stimulus withdrawal. The same trend was observed for VDAC1, an indicator of mitochondrial mass. Similarly, expression of mitochondrial respiratory complexes subunits (complex V ATP5 α , complex II SDHA and SDHB and complex I NDUFA9, and NDUFS3 and complex III core II) displayed to increase at the last day of irradiation and further increase or remained unchanged at recovery (Fig. 30).

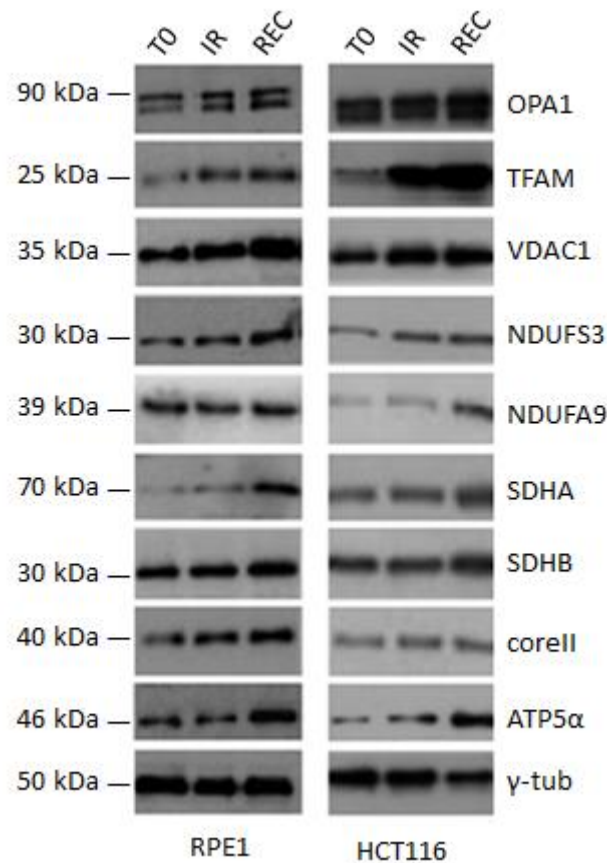


Fig. 30 Western blot analysis of mitochondrial proteins at T0, IR and REC in RPE1 and HCT116 cells. Gamma-tubulin was used as a loading control. One representative experiment of three is shown

The increase of mtDNA copy number, its transcription as well as the increased expression of different mitochondrial proteins, regulatory, structural and of the respiratory chain, suggested an activation of mitochondrial biogenesis. One of its main regulators is the coactivator PGC-1 β , whose levels have been already shown to be dependent on oncogenic stimuli such as C-MYC and HIF1 α (Liesa 2008, Zhang 2007). Gene expression evaluation of PGC-1 β after γ -rays treatment indicated a radiation-dependent increase in both RPE1 and HCT116 up to 2- and 3-fold respectively (Fig. 31). Expression of the other mitochondrial biogenesis regulator belonging to the same family of PGC-1 β , namely PGC-1 α , was undetectable in both RPE1 and HCT116, consistently with the knowledge that it is expressed at high levels in tissues where oxidative metabolism is active, such as brown adipose tissue, the heart, and skeletal muscle (Puigserver 1998).

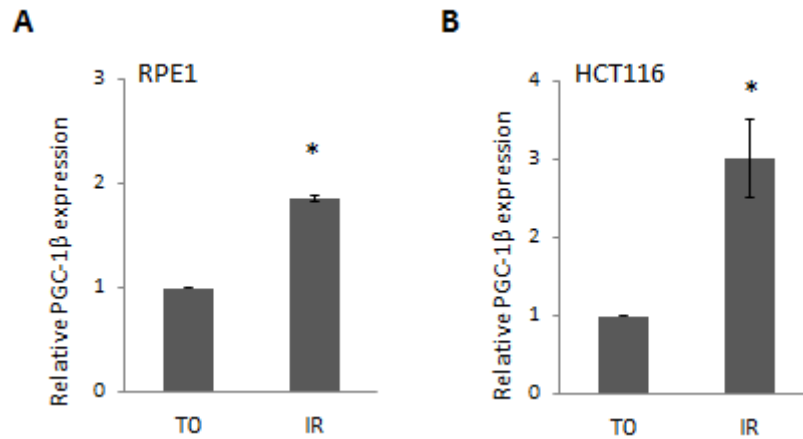


Fig. 31 Relative mRNA quantification of PGC-1 β in RPE1(A) and HCT116 (B) cells upon irradiation. Data are mean \pm SD (n=3, *P<0.05 vs T0).

These data suggested an overall increase in mitochondrial mass. This was demonstrated by loading cells with Mitotracker Red, a fluorescent dye that is accumulated by mitochondria of live cells as a function of membrane potential. After irradiation, RPE1 and HCT116 showed an increase of fluorescence. In parallel, calcein-AM staining, used to highlight cell morphology, demonstrated an increase of cell size together with the mitochondrial mass (Fig. 32).

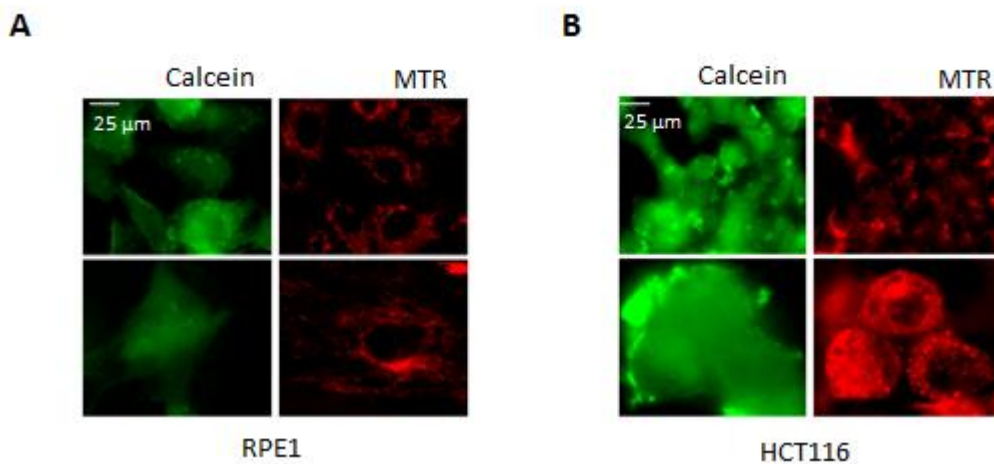


Fig. 32 RPE1 and HCT116 stained with Mitotracker Red (MTR) to evaluate mitochondrial mass and network morphology. Calcein-AM staining was used to highlight cells morphology. One representative experiment of 3 is shown. Magnification 63X/1.4. Bar: 25 μ M.

In order to understand whether such increase in mitochondrial biogenesis was due to a compensatory effect following damage, the bioenergetics competence of both cell lines was evaluated. Following irradiation, both complex I- and II-driven ATP synthesis were shown to be significantly increased over twofold in RPE1 and HCT116 alike. The same result was obtained

upon evaluation of the activity of citrate synthase (CS), an enzymatic marker of mitochondrial mass (Fig. 33A). When ATP synthesis and CS activity were normalized over protein content, no changes were observed (Fig. 33B), suggesting that the induced mitochondrial biogenesis may not be a compensatory mechanism for some radiation-induced mitochondrial damage, and that cells remained metabolically active.

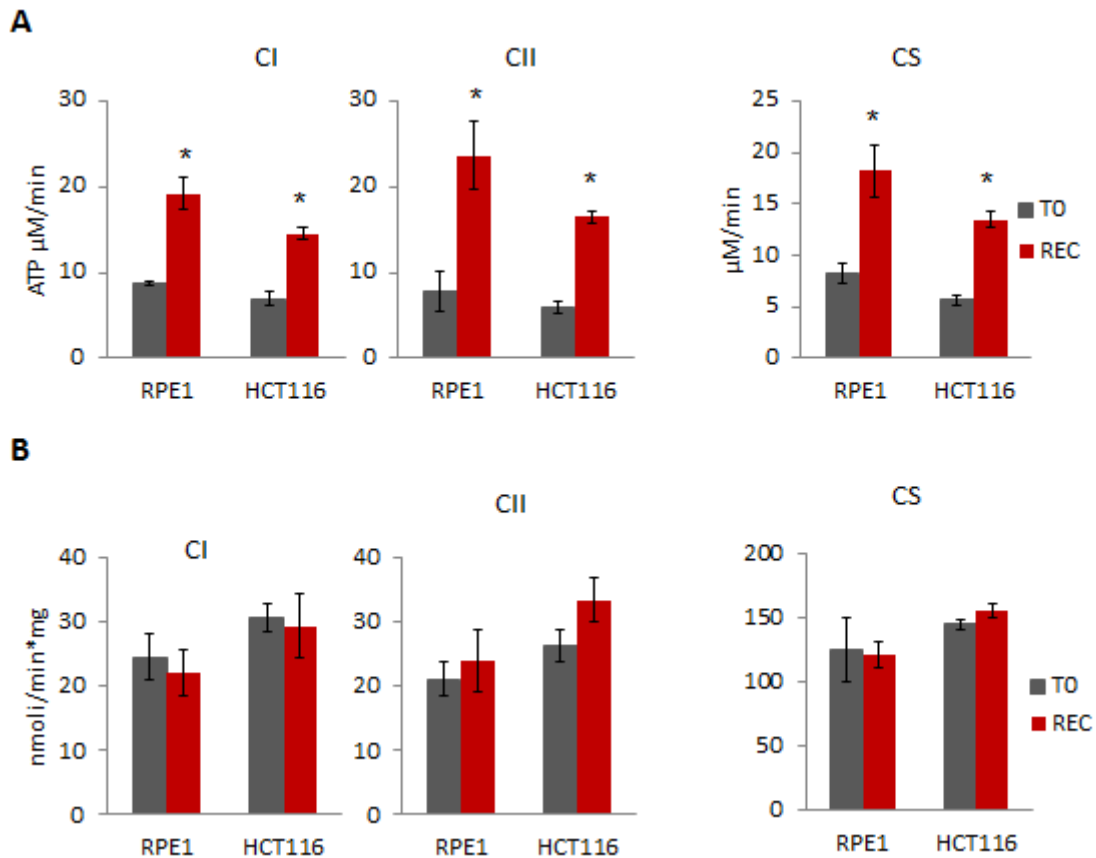


Fig. 33 (A) The rate of mitochondrial ATP synthesis driven by complex I (CI) and complex II (CII) substrates, and cytrate synthase activity (CS) in RPE1 and HCT116 cells after irradiation. Data are mean±SD (n=3, *P<0.05 vs T0). **(B)** ATP synthesis driven by CI and CII and CS activity normalized over protein content.

5.2 Role of p53 in gamma-rays induced mitochondrial biogenesis

Despite the response to DNA damage may be different (quiescence, senescence, apoptosis) it is mediated by the ATM-p53 axis (Kruse 2009). In addition to its traditional role of guardian of the genome, p53 appears to regulate various aspects of mitochondrial biogenesis, in fact its physical interaction with mtDNA, TFAM, POLG and the coactivator PGC-1 α was reported (Yoshida 2003, Achanta 2005, Bakhanashvili 2008). Moreover p53 may transactivate genes involved in oxidative metabolism, such as cytochrome oxidase deficient homolog 2 (*SCO2*) (Matoba 2006), or in glycolytic pathway, the TP53-induced glycolysis and apoptosis regulator gene (*TIGAR*) (Bensaad 2006). Nevertheless, the tumor suppressor p53 has been recently called into play as a negative regulator of mitochondrial biogenesis through its repressor activity at the promoters of murine homologues of the PGC-1 β family in the context of telomere dysfunction. It has been shown that overexpressed p53 binds its specific responsive elements on both murine PGC-1 α and PGC-1 β gene promoters to reduce expression of both regulators (Sahin 201).

PGC-1 β appeared to be the main driver of the increased mitochondrial biogenesis induced by γ -rays, but, simultaneously, an activation of p53 was observed in both cell lines, RPE1 and HCT116. In order to rule out a potential role for p53 activated by DNA damage response in triggering the mitochondrial effect induced by γ -rays, a potential role of activator or repressor of mitochondrial biogenesis was examined.

In order to verify if p53 can influence the transcription of PGC-1 β , specific p53 responsive elements were looked in the promoter of human PGC-1 β , and two close decamers were detected, starting at position -2732; -2706 (GRCh37 - Entrez Gene ID:133522), the first decamer differ from two nucleotide from the canonical sequence, the second from only one base. The two decamers are separate by spacer of 6 nucleotides (Fig. 34).

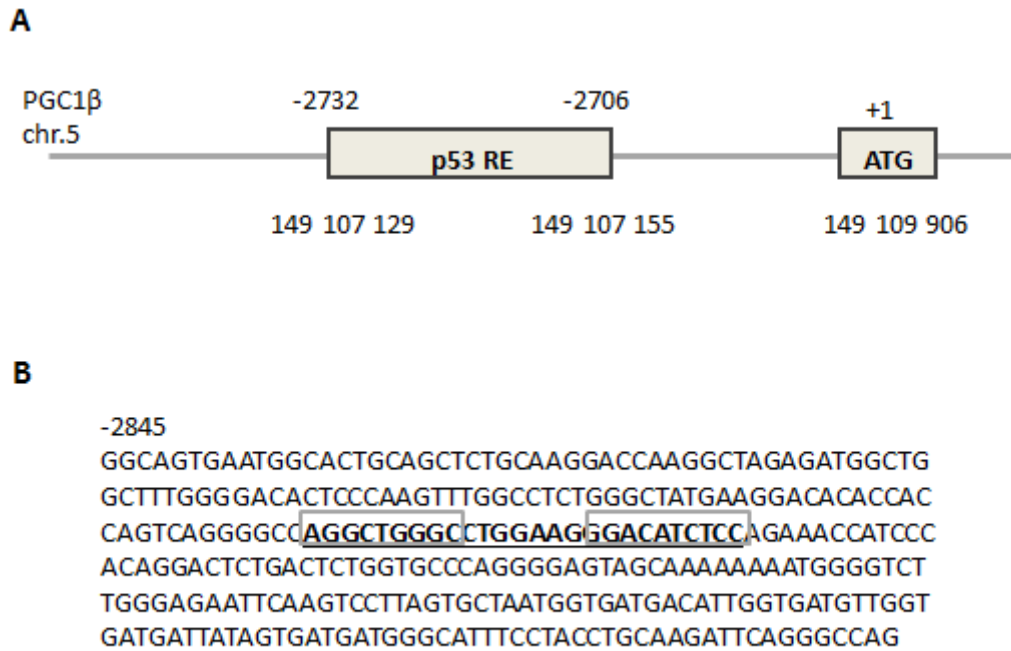


Fig. 34 (A) Schematic representation of the genomic location of the p53-responsive elements (RE) within the promoter region of PGC-1 β . The genomic coordinates are relative to the human genome build hg19. **(B)** Promoter region of human PGC-1 β , stretching from -2845 to -2542 with respect to ATG. The putative p53-RE is underlined and the two decamers are within the gray rectangles.

To check if p53 is able to prevent the transcription of PGC-1 β after radiation treatment, the expression of coactivator was evaluated in the syngenic HCT116 cell line knock-out for *TP53*, namely HCT116^{TP53}, and in the same cells complemented with wild-type p53, HCT116^{p53}. The cell lines HCT116^{TP53} and HCT116^{p53} were submitted to a dose of 4 Gray (Gy) every 24 hours for 4 days. The activation of complemented p53 upon irradiation in HCT116^{p53} was confirmed by p21 expression (Fig. 35).

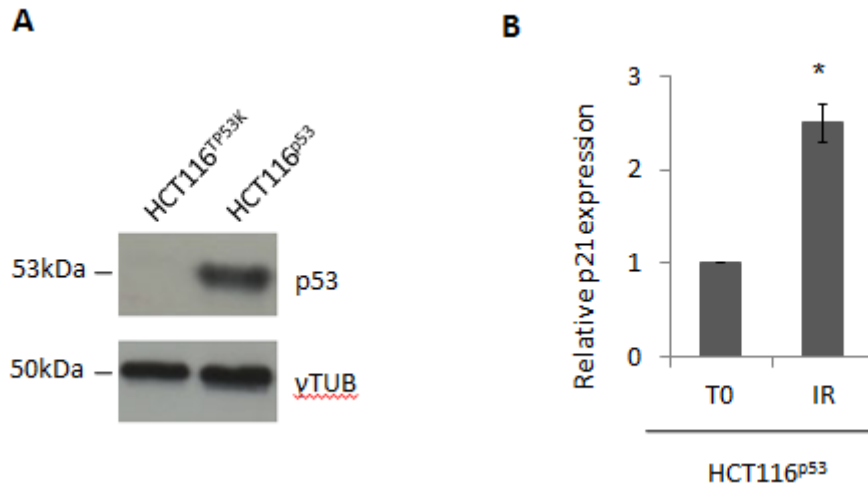


Fig. 35 (A) Western blot analysis of p53 after HCT116^{TP53KO} complementation with wild-type p53. Gamma-tubulin was used as a loading control. (B) Relative expression of p21 in HCT116^{p53} (T0) e HCT116^{p53} after irradiation (IR). Data are mean±SD (n=3, *P<0,05 vs T0).

Complementation with wild-type p53 did not prevent PGC-1β expression increase following irradiation, similarly to what occurred in mock HCT116 knock-out cells, in fact in both cell lines γ-rays induced an increase of 2 fold of the level of the mitochondrial coactivator (Fig. 36).

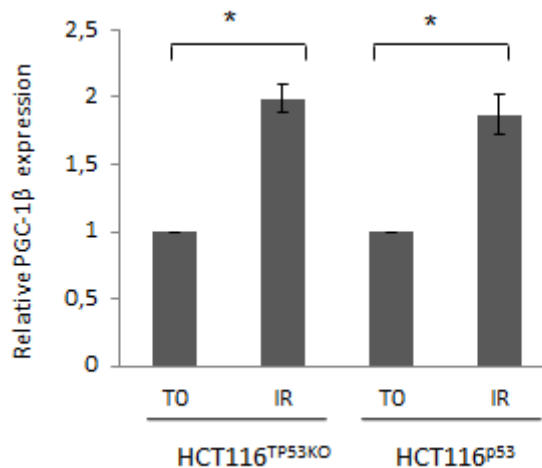


Fig. 36 Expression of PGC1β both in HCT116^{TP53KO} and in HCT116^{p53} upon IR. Data are mean±SD (n=3, *P<0,05 vs T0).

Consistently, p53 did not bind to its PGC-1β weak responsive elements, both in control cells and after irradiation. The occupancy of p53 and histone H4 on p21 promoter were used as positive control of chromatin immunoprecipitation experiment. Both protein significantly bound p21 promoter after radiation treatment (Fig. 37).

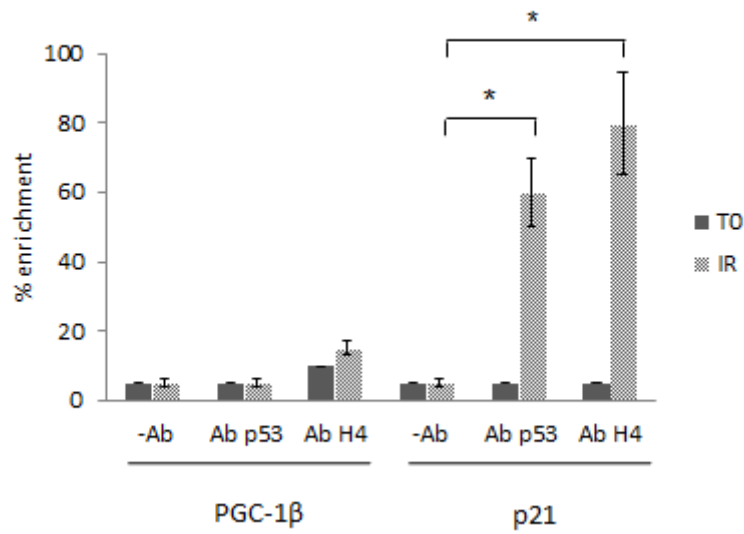


Fig. 37 p53 and histone H4 occupancy at the promoter of PGC-1β in RPE1 cells upon IR. Data are mean±SD. The occupancy of p53 and H4 at the promoter of p21 in the same cells is used as positive control. (n=2, *P<0.05).

In order to rule out a potential role for p53 activation in triggering the mitochondrial effects induced by γ -rays, mitochondrial biogenesis parameters were evaluated in a cell line knock-out for *TP53* gene, HCT116^{TP53KO}, and in an osteosarcoma-derived cell line, HPS11, whose *TP53* harbours a hemizygous mutation within the exon 4, i.e. the c.13055G>C. This mutation cause a replacement of arginine to proline in the DNA binding domain of the protein, i.e. p.156R>P (Fig. 38).

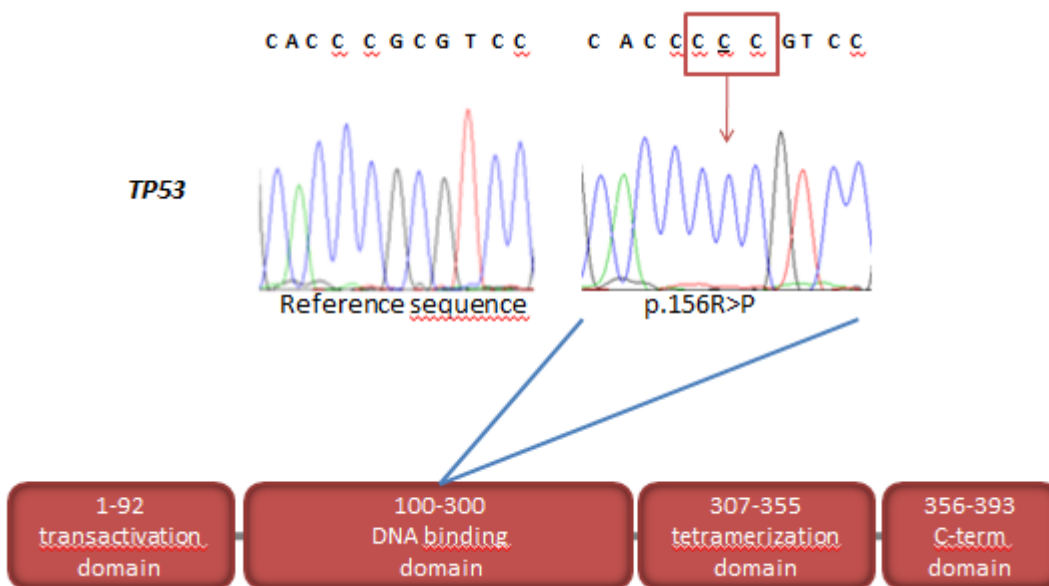


Fig. 38 Electropherogram of the HPS11 cells inactivating *TP53* mutation (p.156R>P) and reference sequence within the DNA binding domain of the protein.

Complementation of HCT116^{TP53KO} cells with a p.156R>P-mutated p53 confirmed that the presence of such mutation impairs the transcriptional activity of p53 that was unable to activate one of its target gene, p21, compared to HCT116^{TP53KO} complemented with wild-type p53 (Fig. 39), as previously observed (Youlyouz-Marfak 2008).

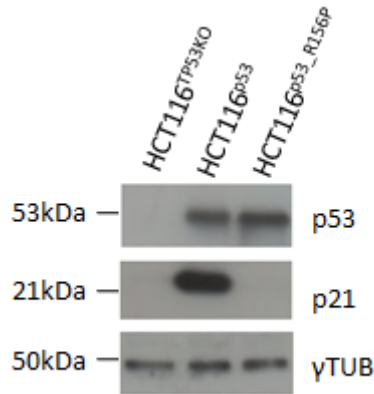


Fig. 39 Western blot analysis of p53 and its target gene p21 in HCT116^{TP53KO}, HCT116^{TP53KO} complemented with wild-type p53 (HCT116^{p53}) and with p.156R>P mutated p53 (HCT116^{p53_R156P}). Gamma-tubulin was used as a loading control. One representative experiment of three is shown.

Both HPS11 and HCT116^{TP53KO} were more sensitive to radiation treatment compared to RPE1 and HCT116, not surviving beyond the fourth dose of radiation, likely because of their inability to undergo senescence (Fig. 40). For this reason, the mitochondrial parameters were measured after the last doses of radiation.

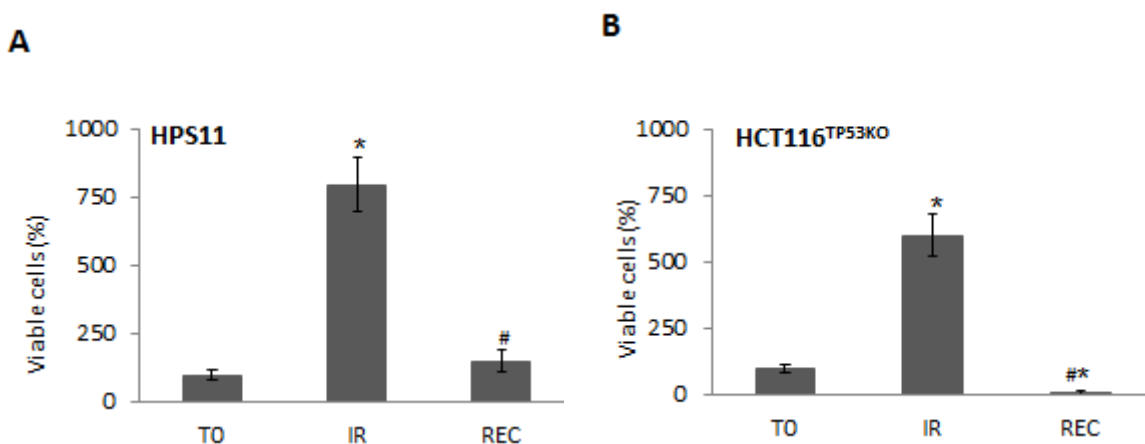


Fig. 40 Viability of (A) HPS11 and (B) HCT116^{TP53} cells at last day of radiation treatment (IR) and after 120h of recovery (REC). Data are mean±SD (n=4, t-test, *P <0.05 vs T0; #P <0,05 vs IR).

Despite the absence of p53 or the mutation in the DNA binding domain, both HCT116^{TP53KO} and HPS11 displayed a 2.5-fold increase of mtDNA copy number after irradiation, similar to that occurring in *TP53* wild-type cells, RPE1 and HCT116 (Fig. 3). MtDNA transcription increased concordantly with mtDNA replication, both cell lines shown an increase of 2-fold. (Fig. 41).

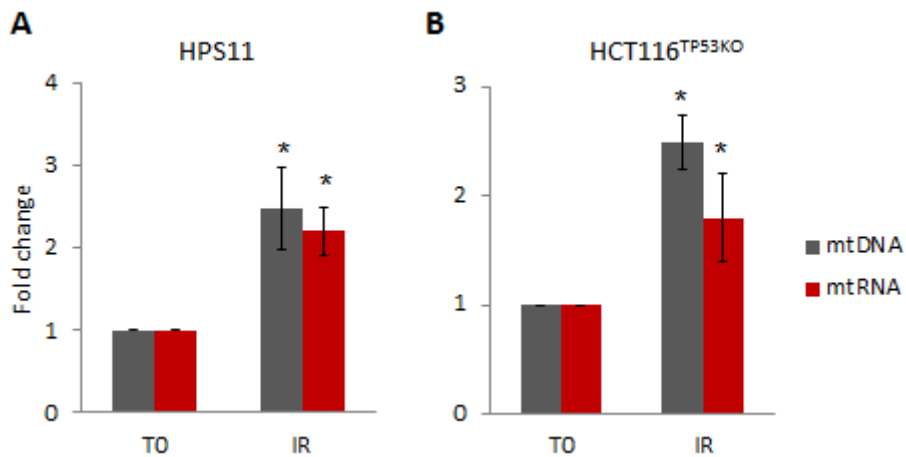


Fig. 41 Relative mtDNA copy number and mtRNA transcription, in HPS11 and HCT116^{TP53KO} cells upon irradiation (IR). Data are mean±SD (n=3, *P<0.05 vs T0).

The expression of both regulatory (TFAM and OPA1) and oxidative phosphorylation (NDUFA9, SDHA, SDHB, ATP5 β , coreII) mitochondrial proteins showed to markedly increase upon irradiation (Fig. 42).

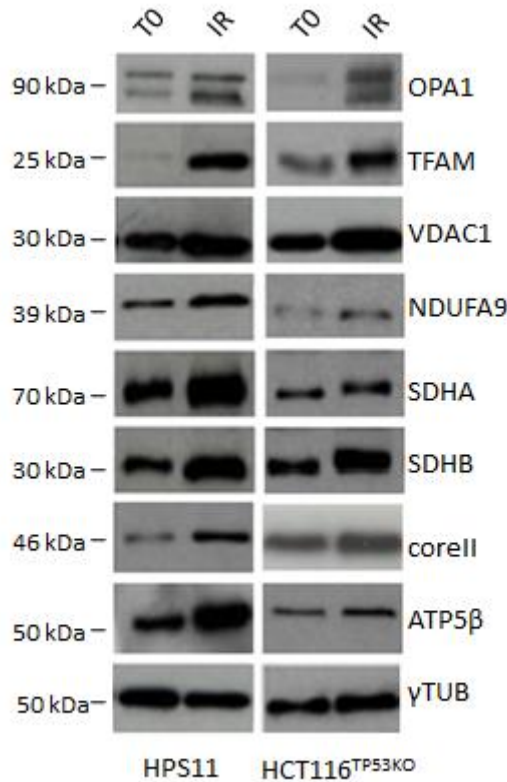


Fig. 42 Western blot analysis of mitochondrial proteins upon IR in HPS11 and HCT116^{TP53KO} cells.

In *TP53* wild type cells, RPE1 and HCT116, the coactivator PGC-1β appeared to be the main driver of the increased mitochondrial biogenesis induced by γ -rays, and, as previously demonstrated, the p53 protein activated by gamma-rays is not involved in the transcriptional regulation of PGC-1β. In HCT116^{TP53} and HPS11, PGC-1β increased respectively 2- and 4-fold after irradiation (Fig. 43).

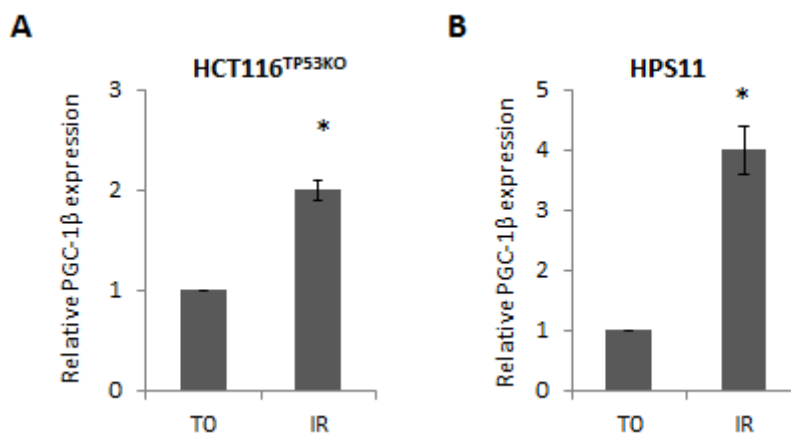


Fig. 43 Relative mRNA quantification of PGC-1β in HPS11 and HCT116^{TP53KO} after irradiation. Data are mean±SD (n=3, *P<0.05 vs T0).

The increase of mtDNA replication and transcription, the levels of expression of PGC-1 β and mitochondrial protein after radiation treatment were concordant with mitochondrial mass increase, as demonstrated also by Mitotracker staining. The calcein-AM staining displayed a parallel increase of cell size (Fig. 44).

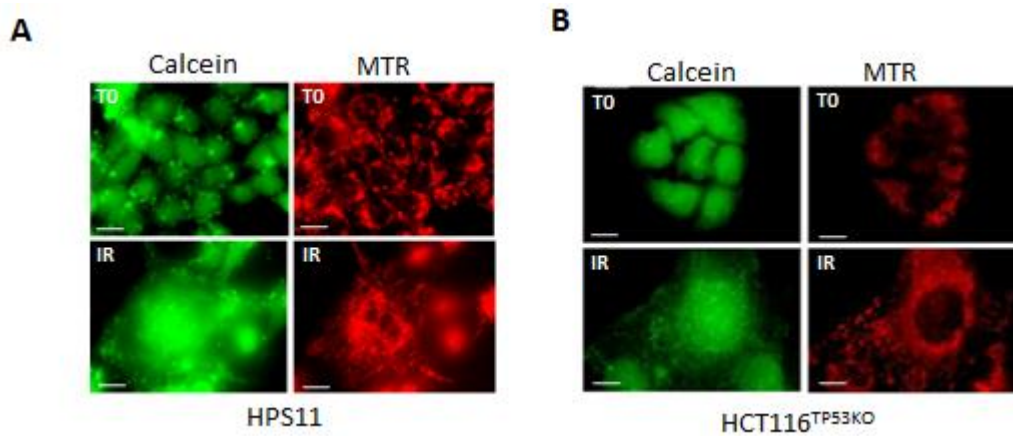


Fig. 44 Mitotracker Red (MTR) and Calcein-AM staining of HPS11 (A) and HCT116^{TP53KO} (B) to evaluate mitochondrial mass and network morphology prior and after irradiation (IR). Magnification 63X/1.4. Bar=25 μ M.

Altogether, these findings point to a lack of involvement of p53 in orchestrating the cell response to γ -rays in terms of activation of mitochondrial biogenesis.

5.3 Role of HIF1 α stabilization in γ -rays induced mitochondrial biogenesis activation

Solid tumors contain heterogeneous populations of cells due to in part to a limited blood supply that leads to lowered oxygen concentrations, acidic conditions and glucose starvation (Achison 2003). This hypoxic condition, a pathophysiologic characteristic of solid malignancies, interferes with the DNA damage induced by ionizing radiation and is therefore a major cause of resistance to irradiation.

On the other hand, p53 pathway is activated by various stresses, and is one of the principal effectors of DNA damage response due to gamma rays (Kruse 2009).

The mutual relationship between hypoxia and genotoxic response as well as their main effectors HIF1 α and p53 has been subject of several studies, but the underlying mechanism remain ill defined (Sermeus 2011). It was reported that the loss of p53 in HCT116 cell line enhances HIF1 α levels and augments HIF1 α dependent transcriptional activation in response to hypoxia (Ravi 2000). Again, HIF1 α dependent transcription in a panel of prostate cell lines increased from low in normal epithelial to high in highly metastatic cell, and this observation was related to decreasing p53 activity in the same direction (Salnikow 2000). Vice versa, the effect of HIF1 α on the stabilization of p53 seems to be more complicated: hypoxia has been frequently described to be a p53 inducer, however, in some cases, hypoxia, alone or in combination with other stresses, has no effect or even decreases p53 protein level (Sermeus 2011). Therefore the relationship between p53 and HIF1 α is far from being elucidated and it has never been put within the contest of mitochondrial biogenesis regulation. Instead, it has been demonstrated that HIF1 α acts as negative regulator of mitochondrial biogenesis. The transcription of PGC-1 β is c-MYC dependent. HIF1 α is able to inhibit c-MYC, by encoding a repressor or by promoting a proteasome-dependent degradation (Zhang 2007).

It is plausible that HIF1 α stabilization may repress mitochondrial biogenesis induced by radiation treatment and p53-dependent genotoxic could indirectly foster mitochondrial biogenesis by blunting the hypoxic one.

For this purpose, HIF1 α expression was analyzed during the radiation protocol. Following irradiation, HCT116 cells showed to have a time-dependent HIF1 α decrease in terms of stabilized protein, which was highest at recovery (Fig. 45), and therefore antithetically followed p53 activation and stabilization (Fig. 28).

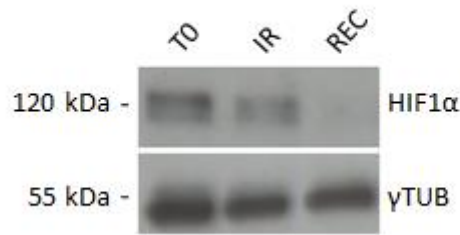


Fig. 45 Western blot analysis of HIF1 α in HCT116 at irradiation (IR) and after 120h of recovery (REC); gamma-tubulin was used as a loading control. One representative experiment of 3 is shown.

The decrease of HIF1 α observed after treatment with gamma radiation may be due to an increased degradation or to its decreased expression. Since HIF1 α mRNA was even shown to increase at recovery (Fig. 46), where the relative protein product level was the lowest, it is plausible that such decrease was a post-transcriptional effect.

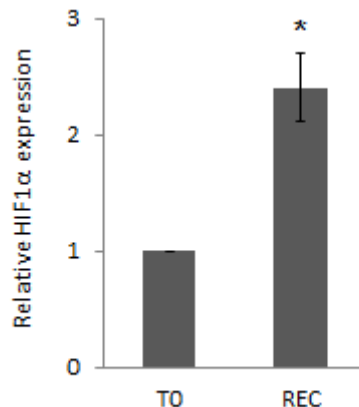


Fig. 46 Relative expression of HIF1 α in HCT116; data are mean \pm SD (n=3, *P<0.05 vs T0).

The degradation of HIF1 α at normal oxygen tension, is mediated by the E3-ubiquitin protein ligase von Hippel Lindau (VHL). The hydroxylation of two proline residues Pro⁴⁰² and Pro⁵⁶⁴ by PHD2 is required for the binding of VHL, which leads to HIF1 α ubiquitination and proteasomal degradation (Semenza 2009). In order to verify if VHL is involved in the degradation of HIF1 α after radiation treatment also in presence of normal oxygen concentration, its expression was analysed at recovery, but any differences were observed between control and irradiated HCT116 cells (Fig. 47).

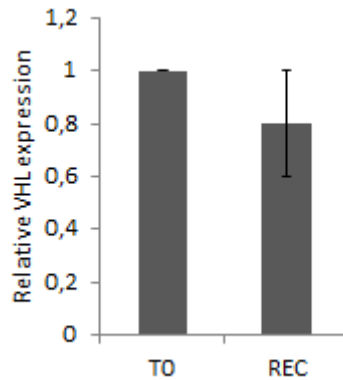


Fig. 47 Relative expression of VHL after irradiation in HCT116; data are mean±SD (n=3, *P<0.05 vs T0).

Interestingly, another E3 ubiquitin protein ligase canonically involved in p53 regulation, MDM2, is able to promote HIF1 α proteasomal degradation (Ravi 2000). To validate such a mechanism in case of gamma radiation treatment, the expression of MDM2 was first analysed in HCT116 after irradiation. MDM2 increased at IR and further increased at recovery (Fig. 48). This expression pattern was antithetical to HIF1 α (Fig. 45).

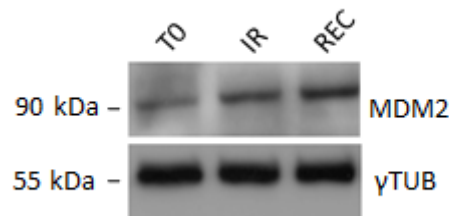


Fig. 48 Western blot analysis of MDM2 in HCT116 after irradiation; Gamma-tubulin was used as a loading control. One representative experiment of 3 is shown.

To demonstrate that MDM2 is involved in the degradation of HIF1 α , the cell line HCT116 transfected with plasmid expressing HIF1 α wild type, HCT116^{HIF1 α} , was used.

The degradation of HIF1 α was followed after blocking protein translation with cycloheximide (chx) treatment in HCT116^{HIF1 α} and HCT116^{HIF1 α} co-transfected with a plasmid expressing MDM2. HIF1 α was shown to be rapidly degraded only when MDM2 was in excess within the cells.

In HCT116^{HIF1 α} the degradation of HIF1 α began after 20 minutes of chx treatment, whereas in presence of MDM2 the decrease was evident already after 10 minutes of incubation with chx and levels diminished further after 20 minutes (Fig. 49).

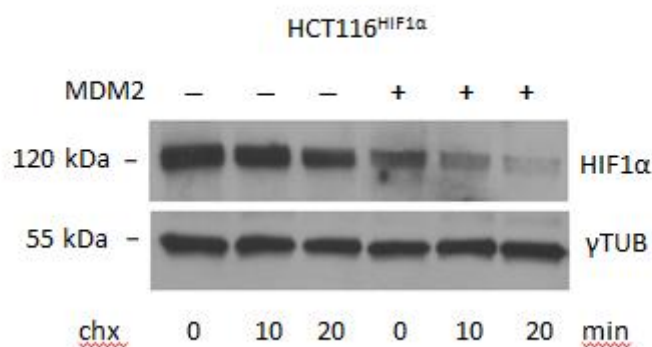


Fig. 49 Western blot analysis of HIF1 α in HCT116 over-expressing HIF1 α (HCT116^{HIF1 α}) upon over-expression of MDM2 (+) compared to clones not over-expressing MDM2 (-). Degradation of HIF1 α was evaluated by treating cells with 50 μ g/ml of cycloheximide (chx) for 0, 10 and 20 minutes.

HIF1 α showed to be rapidly degraded only when MDM2 was in excess within the cells, even without a radiation stimulus, indicating that a basal MDM2-dependent HIF1 α degradation occurs in HCT116.

VHL is able to degrade HIF1 α only in presence of oxygen, when the proline residues Pro⁴⁰² and Pro⁵⁶⁴ are hydroxylated (Semenza 2009). The co-transfection of MDM2 in HCT116 cell line overexpressing a HIF1 α mutated on the two residues responsible for hydroxylation by PHDs and in residue N803, also subject to hydroxylation in the presence of oxygen, HCT116^{HIF1 α TM}, did not induce the degradation of HIF1 α , indicating these residues to be essential. The necessity for PHDs to mediate MDM2-dependent degradation was further confirmed when the potent HIF1 α stabilizer dimethylxallylglycine (DMOG), a specific inhibitor of prolyl-hydroxylase (PHD) activity, was used. In such conditions, HIF1 α protein did not decrease upon chx treatment (Fig. 50).

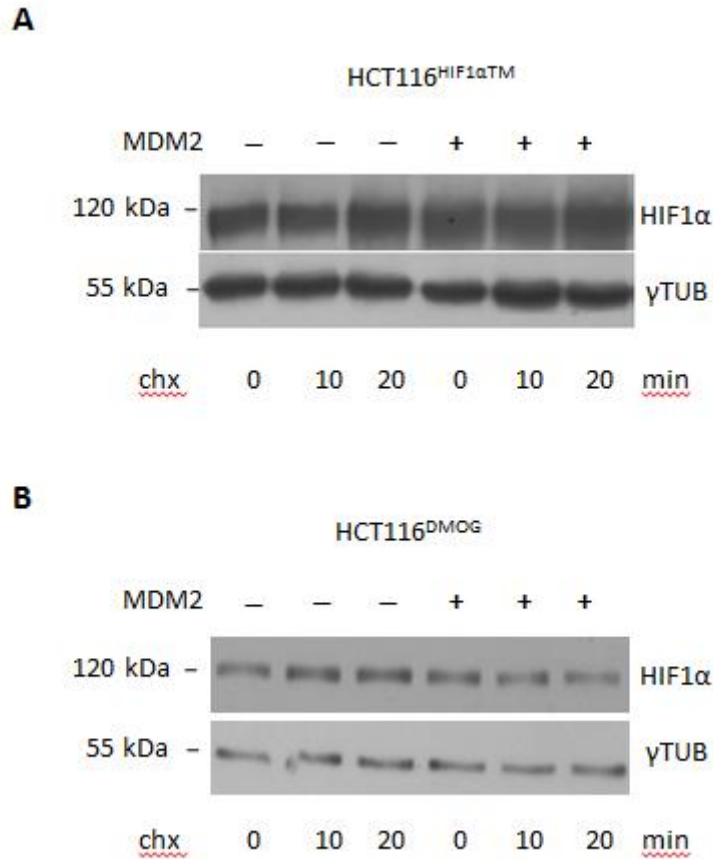


Fig. 50 (A) Degradation evaluation of HIF1α mutated on the three residues responsible for hydroxylation by PHDs (HIF1αTM), in presence and absence of over-expressed MDM2. Degradation of HIF1α was evaluated by treating cells with 50μg/ml of cycloheximide (chx) for 0, 10 and 20 minutes. (B) Degradation evaluation of HIF1α in presence and absence of over-expressed MDM2, upon forced pharmacological HIF1α stabilization by 1μM DMOG. Degradation of HIF1α was evaluated by treating cells with 50μg/ml of cycloheximide (chx) for 0, 10 and 20 minutes.

MDM2 is a transcriptional target of p53 (Manfredi 2010), but mitochondrial biogenesis activation occurs also in absence of functional tumor suppressor. The decreased expression after irradiation of HIF1α was observed also in HPS11 (Fig. 51). Like in cell line wild type for *TP53*, HCT116, the genotoxic stress induced an increase of MDM2.

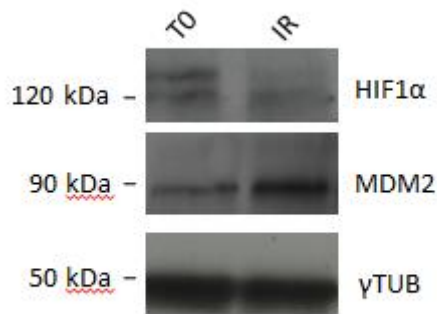


Fig. 51 Western blot analysis of HIF1 α and MDM2 in HPS11 after irradiation; Gamma-tubulin was used as a loading control. One representative experiment of 3 is shown.

The genotoxic response and hypoxia are closely interrelated. Under normal oxygen tension, when HIF1 α can be degraded by the ubiquitin-proteasome system, the genotoxic response activated by gamma rays treatment prevails the hypoxic (Semenza 2009).

Subsequently, hypoxic response was forced concomitantly to genotoxic one, with the aim to reveal if mitochondrial biogenesis would be activated according to the prevalence of one or the other response.

The specific inhibitor of PHD activity, dimethylallyl-glycine (DMOG), was used to stabilize HIF1 α . DMOG was added to the culture medium the day before the first dose of radiation and was maintained for the entire duration of irradiation. HCT116 cells shown to respond well in terms of toxicity, in fact survived and remained able to proliferate despite the combined treatment. DMOG-treated cells presented HIF1 α stabilized for the entire duration of the radiation treatment and increased expression of canonical HIF1 α -responsive genes lactate dehydrogenase A (*LDHA*) and BCL2/adenovirus E1B 19 KDa interacting protein 3-like (*BNIP3L*) (Fig. 52).

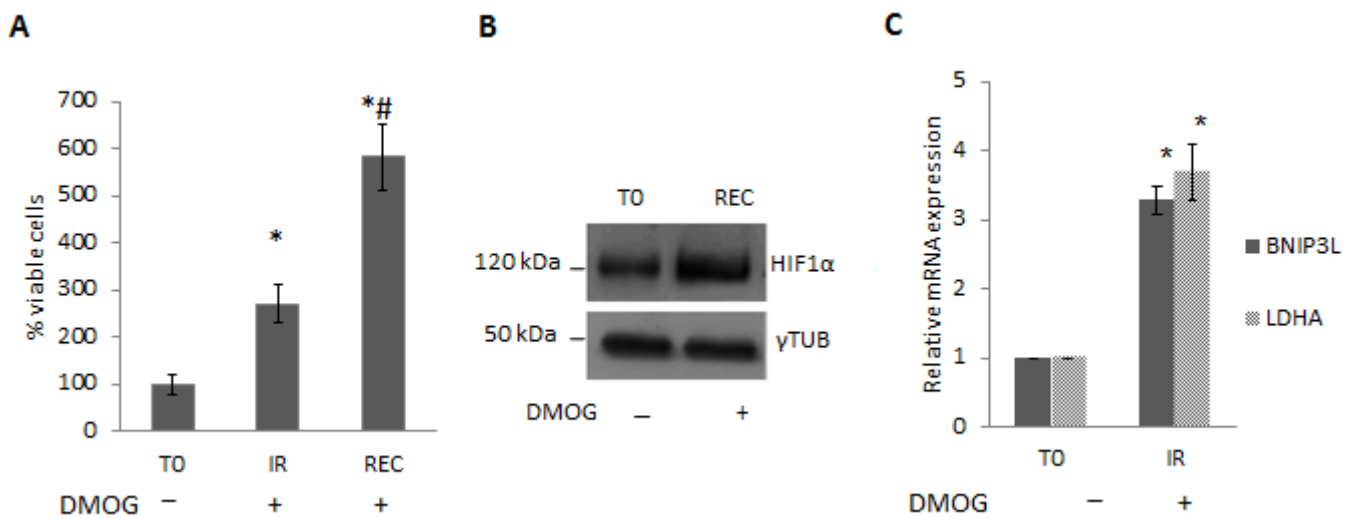


Fig. 52 (A) Viability of HCT116 irradiated and treated with 1 μ M DMOG, Data are mean \pm SD (n=4, t-test, *P <0.05 vs T0; #P<0,05 vs IR). (B) Western blot analysis of HIF1 α in HCT116 irradiated and treated with 1 μ M DMOG, Gamma-tubulin was used as a loading control. One representative experiment of 3 is shown. (C) Relative expression of BNIP3L and LDHA in RPE1 cells before and after treatment with 1 μ M DMOG and irradiation. Data are mean \pm SD (n=3, t-test, *P<0.05).

HCT116 with HIF1 α stabilized did not display increase in mtDNA copy number irradiation. The same finding was obtained when cells were treated with another HIF1 α stabilizer, the iron chelator desferrioxamine (DFO) (Fig. 53).

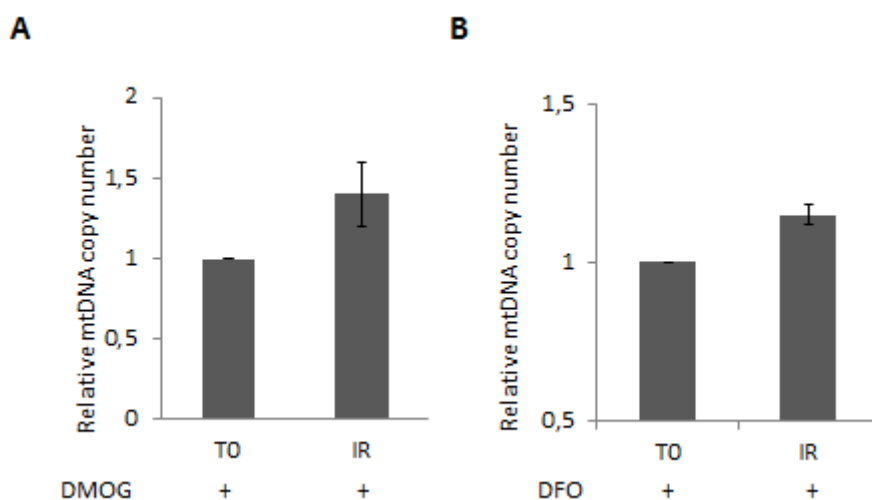


Fig. 53 Relative mtDNA copy number HCT116 cells with stabilized HIF1 α after 1 μ M DMOG treatment (A) or 250nM DFO (B) and irradiated. Data are mean \pm SD (n=3, *P<0.05 vs T0).

Concordantly with mtDNA copy number and with a repressive effect of HIF1 α on mitochondrial biogenesis already demonstrated (Zhang 2009), PGC-1 β expression after irradiation was not increased in DMOG-treated cells (Fig. 54).

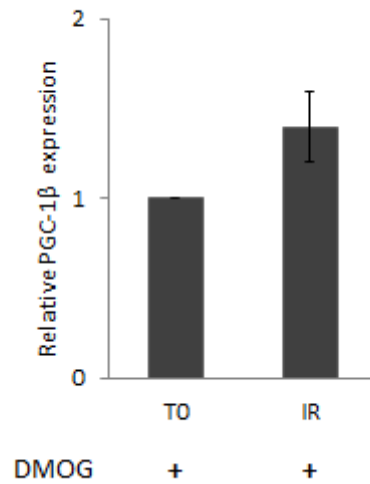


Fig. 54 PGC1 β expression after irradiation in HCT116 cells with stabilized HIF1 α after 1 μ M DMOG treatment. Data are mean \pm SD (n=3, *P<0.05 vs T0).

Accordingly, neither mtDNA maintenance proteins (OPA1 and TFAM), nor respiratory complexes subunits (SDHA, SDHB, coreII, NDUFA9 and ATP5 β) were shown to increase after irradiation in DMOG-treated cells displaying a chronically stabilized HIF1 α (Fig. 55).

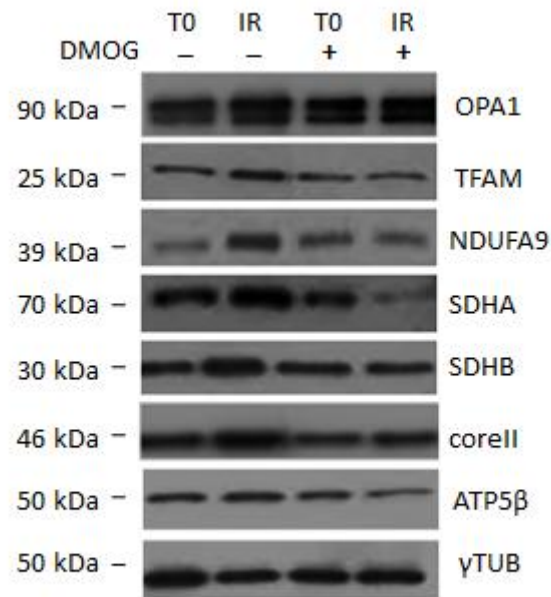


Fig. 55 Western blot analysis of mitochondrial proteins in HCT116 treated with DMOG and irradiated. γ -tubulin was used as a loading control. One representative experiment of 3 is shown.

Overall, no increase of mitochondrial mass was observed, as evaluated by Mitotracker staining, despite a net cell mass increase as observed in all other cell lines irradiated, as evidenced by calcein-AM staining (Fig. 56).

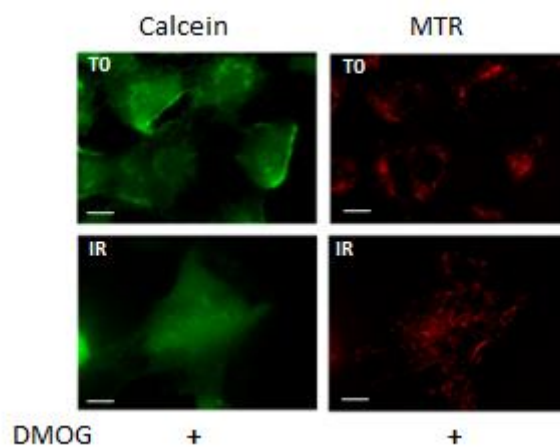


Fig. 56 Staining with Mitotracker Red (MTR) and Calcein-AM to evaluate mitochondrial mass and network morphology in HCT116 treated with DMOG and irradiated . Magnification 63X/1.4. Bar=25 μ M.

Analogous findings were obtained when the cell line RPE1 was treated with DMOG and irradiated. Also in these cells, the stabilization of HIF1 α prevented the activation of the mitochondrial biogenesis induced by radiation, in fact, when the cells were treated with DMOG there was no difference between control and irradiated, both in terms of mitochondrial DNA copy number and PGC-1 β expression (Fig. 57).

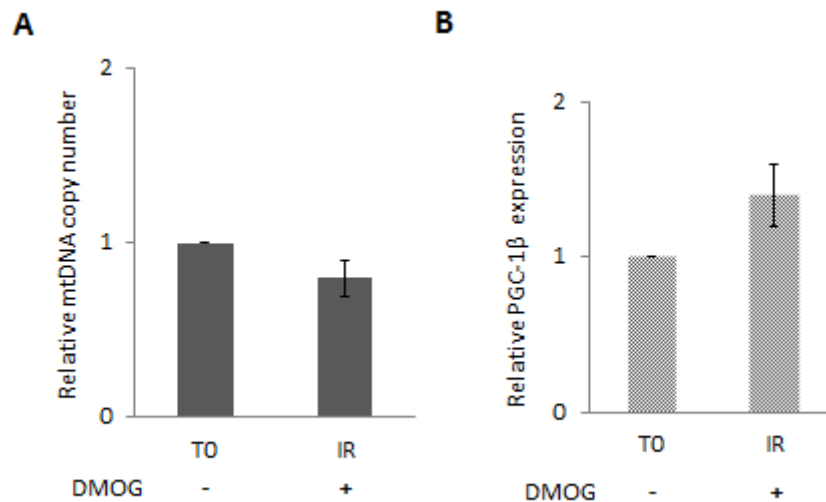


Fig. 57 (A) Relative mtDNA copy number. Data are mean \pm SD (n=3, t-test, *P<0.05) and (B) relative PGC-1 β expression after γ -rays treatment in RPE1 with HIF1 α stabilized by DMOG treatment. Data are mean \pm SD (n=3, t-test, *P<0.05).

Concordantly, mitochondrial protein like TFAM and some subunits of the respiratory chain did not increase after irradiation in RPE1 treated with DMOG (Fig. 58).

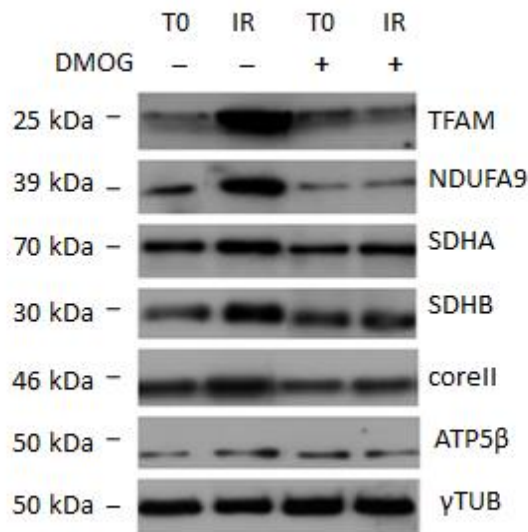


Fig. 58 Western blot analysis of mitochondrial proteins in RPE1 with HIF1 α stabilized by DMOG treatment. One representative experiment of 3 is shown.

Mitochondrial DNA copy number, the main parameter used to evaluate mitochondrial biogenesis, was also measured in HCT116^{TP53KO} irradiated and treated with DMOG. Like in others cells, the stabilization of HIF1 α prevented the activation of gamma rays-induced mitochondrial biogenesis (Fig. 59).

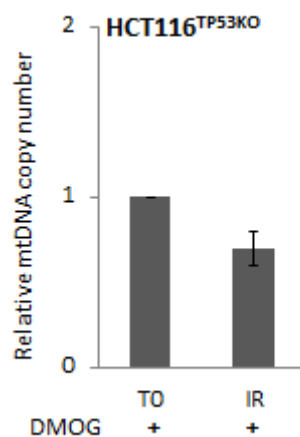


Fig. 59 Relative mtDNA copy number after γ -rays treatment in HCT116^{TP53KO} cells with HIF1 α stabilized by 1 μ M DMOG. Data are mean \pm SD (n=3, t-test, *P<0.05).

Overall, these data indicate that the hypoxic response prevails over the genotoxic one in terms of mitochondrial biogenesis activation that may be induced by irradiation *via* an indirect mechanism,

namely a re-positioning of MDM2 from p53 to HIF1 α . This would foster hydroxylated HIF1 α degradation upon p53 activation, preventing HIF1 α to inhibit mitochondrial biogenesis.

5.4 Role of HIF1 α in gamma rays-induced cellular senescence

Cellular senescence has emerged as a programmed cellular stress response that is induced due to the accumulation of damage. The activation of senescence induced by DNA damage leads to an irreversible arrest phenotype that is characterized by the activation of p53 or RB proteins. In this way, senescence can be seen as a tumor suppressor mechanism that prevents excessive cellular division, or division of damaged cells, and its induction may represent the goal of anticancer radiotherapy (Nardella 2011).

After irradiation, both RPE1 and HCT116 acquired the typical features that characterized senescent cell: increase in size, flattened and shaped morphology (Rodier 2011). The marker that is commonly used to assess the activation of senescence process is a cytochemical assay aimed at evaluating the activity of the lysosomal enzyme β -galactosidase (SA- β Gal). Senescence cells are characterized by an increased activity of this enzyme whose contribution to senescence has not been elucidated (Debacq-Chainiaux 2009). The positivity of the irradiated RPE1 and HCT116 cells to the β -galactosidase assay together with morphological changes showed that the genotoxic stress induced the activation of cellular senescence (Fig. 60).

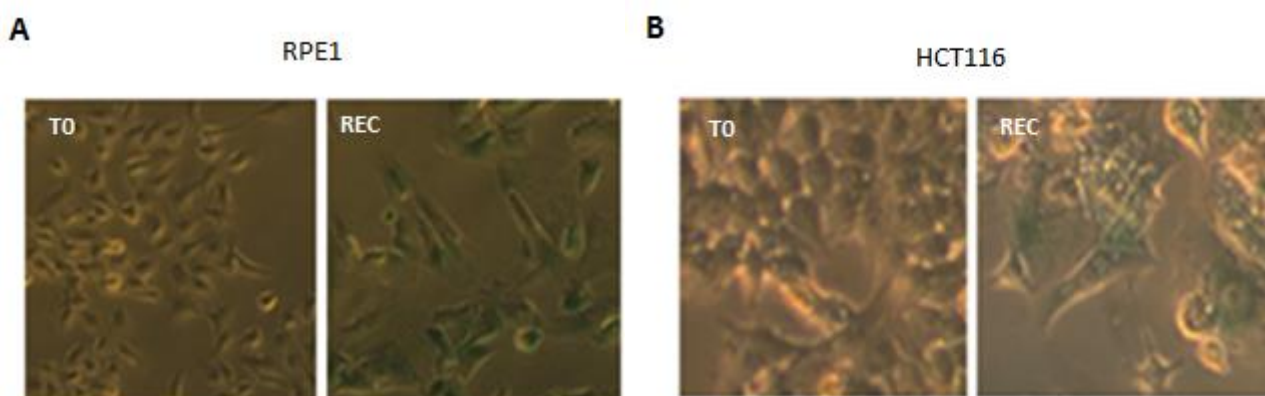


Fig. 60 Senescence-associated β -galactosidase staining in RPE1 and HCT116 irradiated. One representative experiment of 3 is shown. Magnification 10X

The pathways p53-p21 and pRB-p16^{INK4A} are the two effectors of senescence that determine the block of cell proliferation and morphological changes typical of senescent cells. It has been shown that these two pathways may interact or act independently in regulating senescence (Nardella 2011). The activation of genotoxic response in HCT116 and RPE1 cell was characterized by a stabilization of p53 and consequently by the increase of its target p21. To determine if also the pathway of pRB-p16 was involved in regulating the activation of senescence in these cell lines, the expression of p16 was evaluated (Fig. 61). Since this protein decreased after irradiation, the pathway pRB-p16 was not involved in activation of senescence response that it was regulated by p53 and p21.

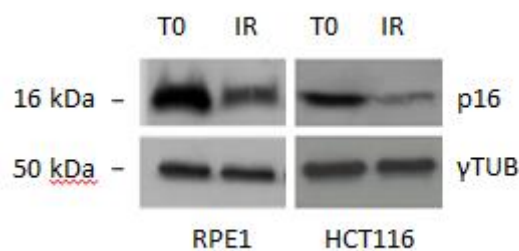


Fig. 61 Western blot analysis of p16 in RPE1 and HCT116 cell irradiated. Gamma-tubulin was used as a loading control. One representative experiment of 3 is shown.

In an opposite manner to p53, HIF1 α enhances proliferation and survival of tumors cells, and has a profound effect on the response to radiotherapy (Harada 2011).

Previously, it has been demonstrated that mitochondrial biogenesis is activated parallel to the genotoxic response, which in the presence of p53, determines the increased expression of the inhibitor of cyclin-kinase p21. HIF1 α acts contrary, represses the expression of PGC-1 β and then blocks the activation of mitochondrial biogenesis induced by ionizing radiation.

Interestingly, p53 stabilization did not increase after irradiation in DMOG-treated RPE1 and HCT116 cells, in the same fashion as its main target p21 and its regulator MDM2, whereas p16 was not shown to change (Fig. 62).

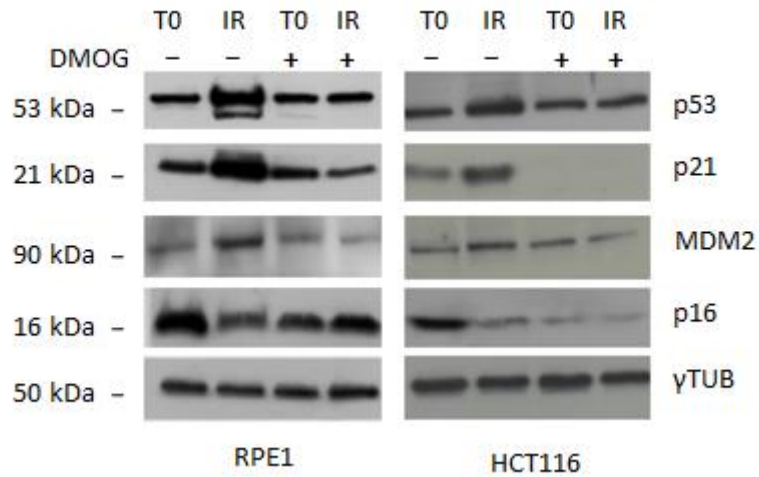


Fig. 62 Western blot analysis of p53, p21, MDM2 and p16 in RPE1 and HCT116 cells treated with DMOG and irradiated. γ -tubulin was used as a loading control.

The genotoxic stimulus was not able to activate p53 in presence of stabilized HIF1 α , as no binding of p53 could be detected on the p21 promoter in DMOG-RPE1 cells, and consequently no acetylation occurred, evaluated by the occupancy of histone H4 in the same regions of the promoter analyzed for the presence of p53 (Fig. 63)

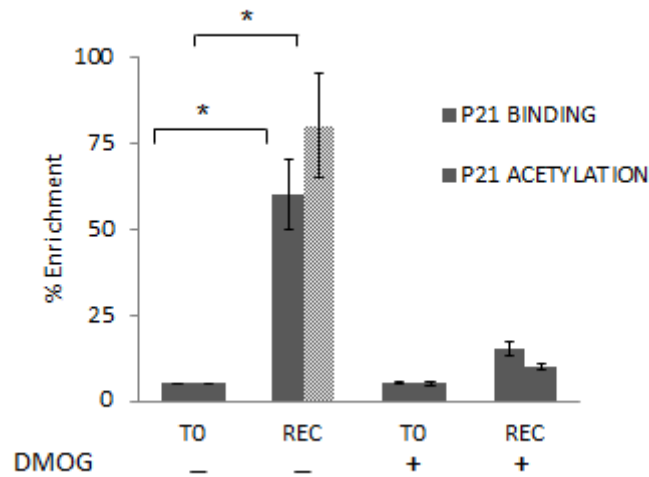


Fig. 63 P53 and histone H4 occupancy at the promoter of p21 in irradiated RPE1 cells, in presence or absence of stabilized HIF1 α by 1 μ M DMOG. Data are mean \pm SD (n=2, *P<0.05 vs TO).

Accordingly with the protein expression level of p21 and MDM2, other two target genes of p53: *BAX* and *GADD45A* were not increased in RPE1 after irradiation (Fig. 64).

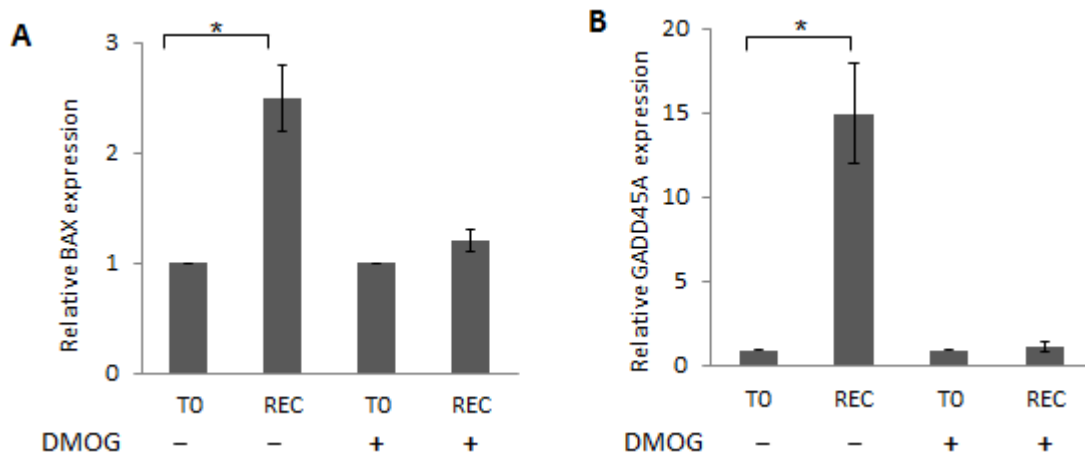


Fig. 64 Relative expression of p53-responsive genes *BAX* and *GADD45A* in RPE1 cells, in presence or absence of stabilized HIF1 α by 1 μ M DMOG, and irradiated. Data are mean \pm SD (n=3, *P<0.05 vs T0).

In both cell lines, RPE1 and HCT116, the non-stabilization of p53, and consequently of p21, would indicate that HIF1 α is able to block the process of senescence, induced by gamma radiation.

β -galactosidase assay confirmed that HIF1 α stabilization by DMOG was able to prevent cells to undergo senescence, as DMOG-treated cells did not show a different staining compared to controls after irradiation (Fig. 65).

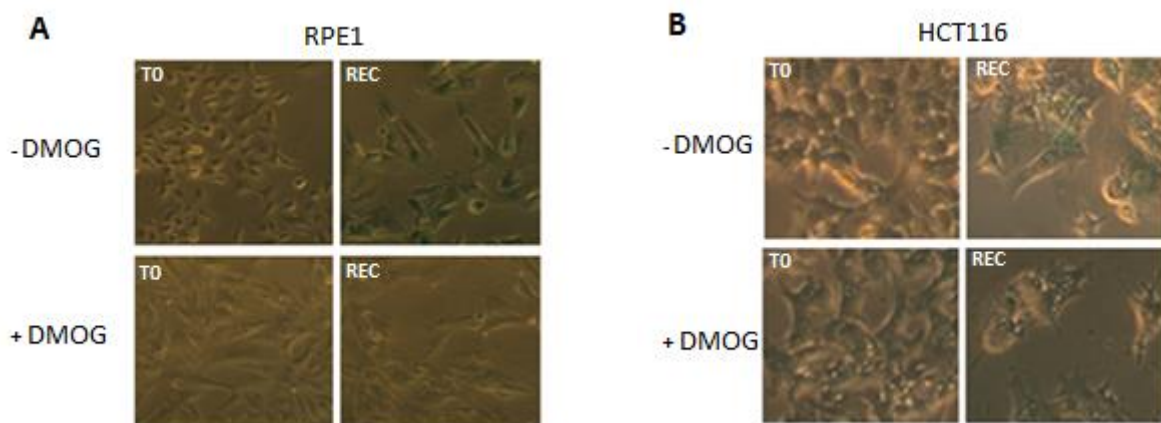


Fig. 65 Senescence-associated β -galactosidase staining in RPE1 and HCT116 irradiated and treated with DMOG. One representative experiment of 3 is shown. Magnification 10X.

The same effect was observed when DFO was used (Fig. 66).

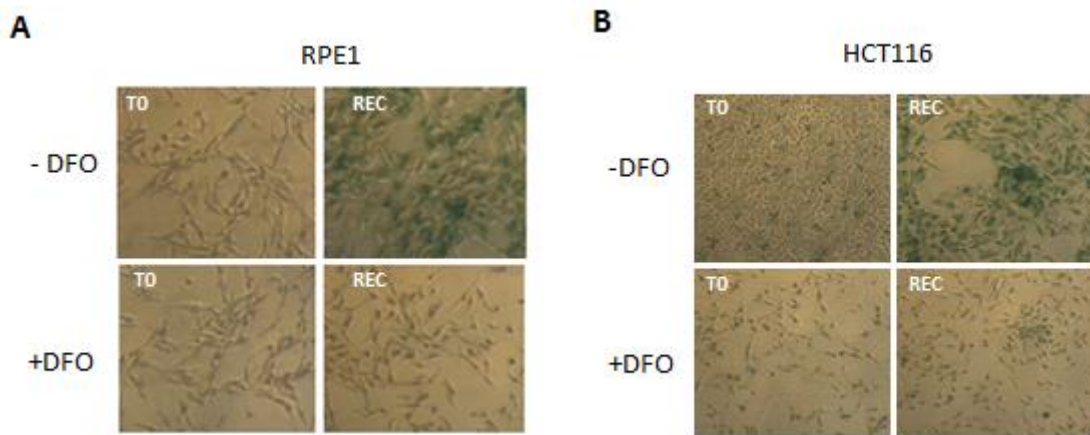


Fig. 66 β -gal staining of RPE1 and HCT116 cells irradiated and treated with 250nM DFO. One representative experiment of 3 is shown. Magnification: 10X.

Taken together, these data suggest that, along with mitochondrial biogenesis, HIF1 α stabilization was able to blunt the cell senescent response, suggesting the two processes to be concomitant.

5.5 Evaluating the mtDNA copy number as a predictive marker of HIF1 α stabilization after radiotherapy in vivo

Hypoxia is known to induce tumor radioresistance through the activation of HIF1 α . Consistent with these findings, there is clinical evidence that the size of the intratumoral hypoxic fraction and the level of HIF1 α correlate with a poor prognosis after radiation therapy (Harada 2011). Inhibition of HIF1 α activity could therefore represent an important component of anti-tumoral therapies (Semenza 2003). Strategies to quantify and image hypoxia in clinical tumors have received considerable attention because of the significant impact of hypoxia/HIF1 α activity on the effect of radiation therapy (Harada 2011).

In the previous experiments, it was shown how mitochondrial biogenesis is regulated by stabilization of HIF1 α . A collection of healthy tissue rectal biopsies taken from subject who had undergone radiation treatment for prostate cancer was evaluated, since γ -rays also hit the rectum lining. MtDNA copy number was measure in rectal epithelium before irradiation compared to biopsies taken two months after the end of therapy.

32 subjects were analyzed and mtDNA copy number was shown to be significantly higher in 16/32 (59%) subjects and decreased in only two sample (Fig. 67).

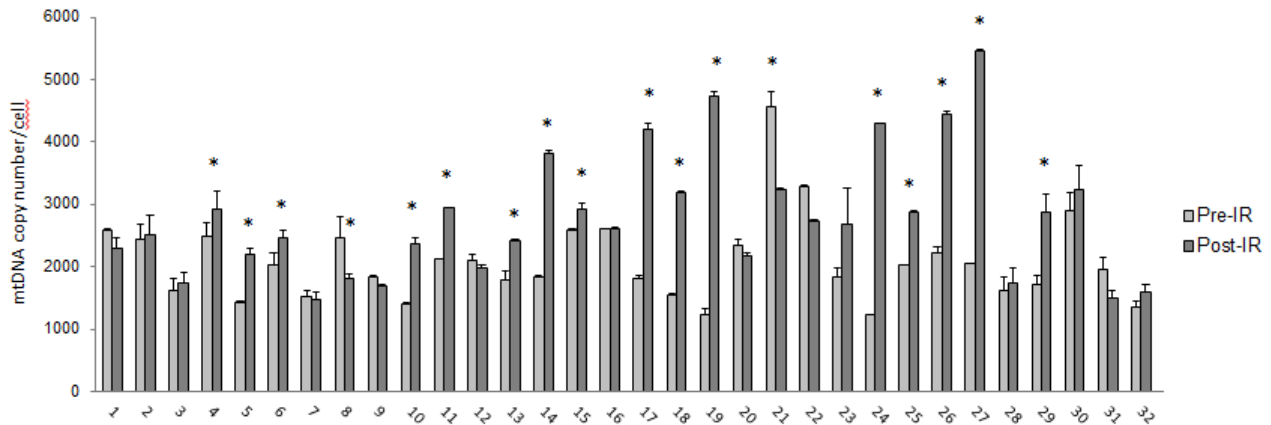


Fig. 67 Absolute mtDNA copy number in rectal biopsies of patients subjected to radiotherapy for prostate carcinoma, prior (pre-IR) and post-irradiation (post-IR). Data are mean \pm SEM (*P<0.05; paired t-test).

Considering all data together, the mtDNA copy number was significantly increased in all subjects analyzed (pre-IR vs post-IR, P<0.05), suggesting the radiation trigger had lasted long after the withdrawal of the stimulus (Fig. 68).

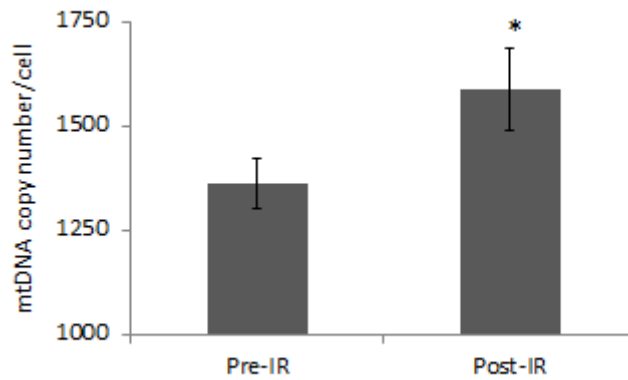


Fig.68 Median comparison of all pre- and post-irradiation biopsies (Wilcoxon Rank test, *P<0.05 vs Pre-IR).

The expression of HIF1 α was evaluated in all tissues pre e post irradiation. A tight correlation was found between HIF1 α stabilization and mtDNA copy number. In 8/10 cases in which the number of copies is the same or decrease, HIF1 α increase after irradiation, vice versa in 9/12 cases in which mtDNA increase after γ -rays treatment, HIF1 α does not change or decrease (Fig. 69).

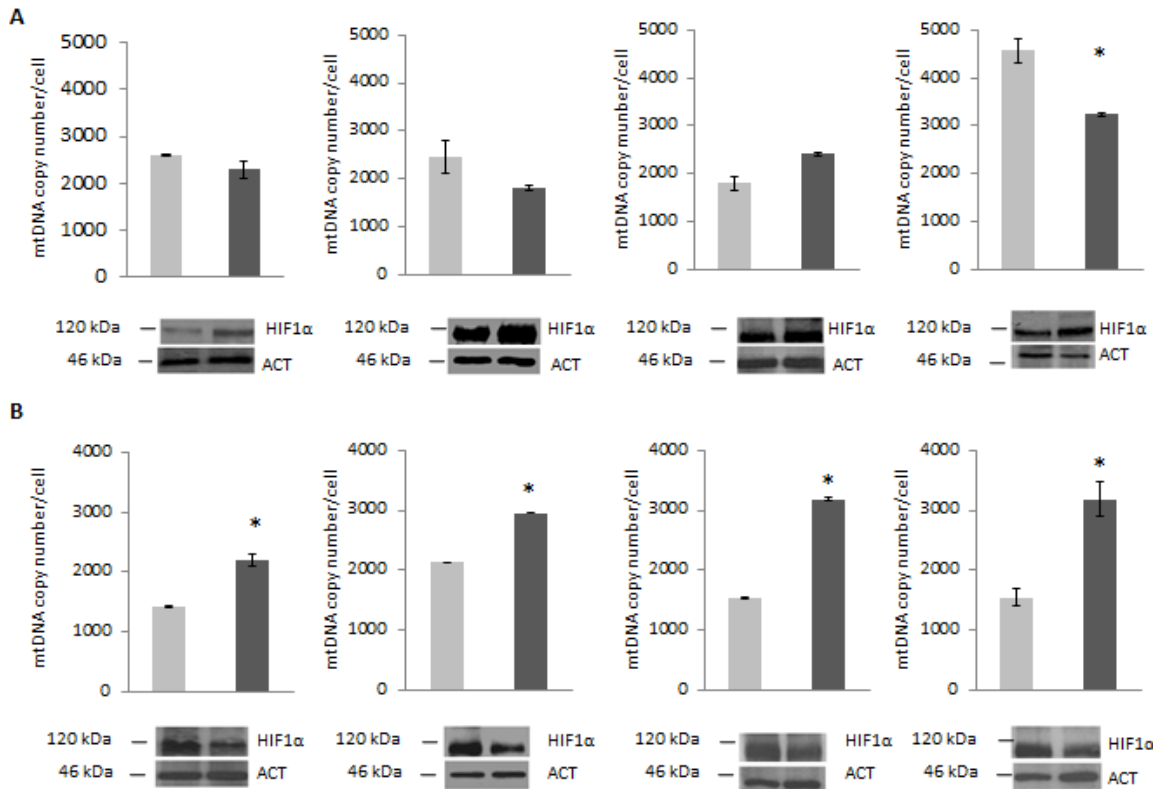


Fig. 69 (A) Western blot analysis of the expression of HIF1 α in representative cases in which the mtDNA copy number was found not to change or decreased after radiation treatment. **(B)** Western blot analysis of the expression of HIF1 α in representative cases in which mtDNA copy number increased after radiation treatment. Beta-actin (ACT) was used as a loading control. One representative blot of 3 is shown.

These data confirm the negative relationship between HIF1 α and mitochondrial biogenesis and suggest a HIF1 α regulated control of the γ -rays induced biogenesis.

6. DISCUSSION

This study demonstrates that γ -rays, in doses corresponding to those commonly used during anti-cancer therapy, potently induce a net mitochondrial biogenesis. Such induction is p53-independent and is blunted by HIF1 α stabilization, which occurs during the hypoxia response.

Recent transcriptomic, proteomic, functional and structural studies of mitochondria of cancer cells indicate that an impaired biogenesis and activity of the organelle is required for the development of some tumors (Formentini 2010). The decrease of mitochondrial activity in cancer cells may have multiple reasons, related either to the input of reducing equivalents to the electron transfer chain or to direct alterations of the mitochondrial respiratory complexes (Gasparre 2013). Interestingly certain tumor subtypes, identified as oncocytic, are characterized by abnormal biogenesis of non-functional mitochondria in their cells. These tumors are in most cases benign, having a low proliferative potential, and are not aggressive (Gasparre 2010).

A particular type of relapses after γ -rays was observed in patients with colorectal cancer, where oncocytic features were acquired in the recurring neoplasia after radiation therapy (Rouzbahman 2006, Ambrosini-Spaltro 2006) suggesting a potential connection between mitochondrial biogenesis and radiation treatment. An increase in mitochondrial mass and function had been previously observed in lung carcinoma cells after exposure to X-rays (Malakhova 2005). In the present thesis work it was demonstrated that also γ -rays are able to induced an increase of mitochondrial mass and a thorough characterization of mitochondrial changes that occur when a genotoxic stimulus is administered to cells was performed. In different cell line after irradiation, an increase of one of the master regulators of mitochondrial biogenesis, PGC-1 β was observed. In parallel, mitochondrial DNA replication, transcription as well as mitochondrial protein expression and mass were observed to increase. Simultaneously, one of the main effectors of the genotoxic response, p53, was stabilized. To date, a clear link between this phenotype and the canonical cellular responses to DNA damage has not been elucidated. The increased mitochondrial mass and function in irradiated cells was observed simultaneously to stabilization of p53 and increased expression of its target gene p21, positive staining for SA- β -Gal and enlarged cell size, that are all hallmark of cell senescence (Rodier 2011). Mitochondria are semi-autonomous organelles. Nuclear-encoded proteins are needed for their biogenesis, such as the DNA polymerase gamma or the fusion protein OPA1, yet checkpoints for mtDNA replication, for instance, do not seem to exist or are hypothesized to be different from those of nuclear DNA (Singh 2006). Moreover, the mitochondrial network fission and fusion are believed to be independent from cell division. Overall, mitochondria continue to

proliferate despite lack of cell division, in the senescent yet metabolically active G1 arrested cells. The mitochondrial biogenesis increase observed after γ -rays treatment, therefore, may not be an actively induced process, and it is surely not a compensatory effect since we showed mitochondrial function to be augmented in irradiated cells. This thesis results suggest a relation between mitochondrial biogenesis and cellular senescence. The increase of mitochondrial function may be an obligated condition for the activation of senescence, maintaining these cells metabolically active, and it is also possible that these processes are activated simultaneously by the same factor. It is well established that p53, the main effector of genotoxic response, regulates various aspect of mitochondrial biogenesis, but its role seems debatable. The physical interaction of tumor suppressor with mtDNA, TFAM, POLG and the coactivator PGC-1 α was reported (Yoshida 2003, Achanta 2005, Bakhanashvili 2008). Overall, these data suggest a positive control of p53 on mitochondrial biogenesis. Nevertheless, p53 has been recently called into play as negative regulator through its repressor activity at the promoters of murine homologues of the PGC-1 β family in the context of telomere dysfunction (Sahin 2011). After γ -rays treatment, an increased expression of coactivator PGC-1 β was observed in HCT116^{TP53KO} such as in same cells complemented with wild-type p53. Furthermore p53 did not bind PGC-1 β promoter in irradiated RPE1. Overall these data suggest that in human p53 does not act as negative regulator of mitochondrial biogenesis in the context of gamma rays treatment.

Although the presence of p53 is an obligatory condition for the activation of cell senescence induced by γ -rays, the tumor suppressor is not necessary for the increase of mitochondria in irradiated cells, in fact a net biogenesis like in RPE1 and HCT116 was observed also in cells knock-out for *TP53* and in osteosarcoma cell line (HPS11) whose *TP53* harbours a mutation in hemizyosity within the DNA binding domain that impair its transcriptional activity.

Interestingly, the effect of genotoxic stress in these cell lines was more detrimental, both HPS11 and HCT116^{TP53KO} did not survive beyond the fourth dose of radiation, likely because of their inability to undergo senescence, in fact the absence of functional p53 pathway prevent the transcriptional activation of p21. Therefore, mitochondrial biogenesis activation was observed in two different positive conditions in term of inhibition of tumor proliferation: senescence and cell death. Further experiments are necessary to identify whether the apoptotic pathway is activated in these cell.

These data also demonstrate that mitochondrial biogenesis and cellular senescence are not strictly correlated, but these two process may be possibly activated by a common effector, upstream to p53 in the DNA damage cascade response. It should be also interesting to evaluate whether a cell unable to trigger mitochondrial biogenesis after γ -rays treatment can activate cellular senescence.

Nonetheless, the influence of p53 over mitochondrial biogenesis may be indirect, via the previously demonstrated MDM2-mediated degradation of HIF1 α , the main effector of hypoxic response. MDM2 expression increased after irradiation, parallel to a time-dependent degradation of HIF1 α . Generally, MDM2 is involved in the negative regulation of the tumor suppressor p53. This occurs through two main mechanisms. First, the direct binding of MDM2 to the N-terminal and of p53 inhibits the transcriptional activation function of p53, second, MDM2 possesses E3 ubiquitin ligase activity that targets p53 for modification and subsequent degradation through the 26S proteasome. Although its role as an oncogene via suppression of p53 function remains clear, growing evidence argues for p53-independent effects, as well as the remarkable possibility that MDM2 has tumor suppressor functions in the appropriate context (Manfredi 2010). In this study one of these situations was demonstrated: in fact MDM2 was able to degrade HIF1 α , like observed in previous work (Ravi 2000).

It was observed that MDM2 expression increased after irradiation, parallel to stabilization of p53. It is therefore plausible to suppose that when p53 is activated and phosphorylated upon a genotoxic stimulus, such as γ -rays, MDM2 may not preside to its degradation and be re-directed towards HIF1 α , whose degradation would hence be fostered. This hypothesis is further justified by the increase in MDM2 protein observed also in HCT116 cells devoid of p53 and in HPS11, indicating that post-radiation MDM2 increase may also occur independently of p53 stabilization (Manfredi 2010), either through other members of the p53 family, such as p73 (Davis 2001) or through an NF κ B-mediated induction (Busuttill 2010), and contribute to HIF1 α degradation and mitochondrial biogenesis increase we observed in p53 knock out cells as well. It is well known that both HIF1 α and the mitochondrial respiratory chain are considered the two fundamental oxygen sensors of the cell. As O₂ tension decreases, in fact, HIF1 α stops becoming hydroxylated on essential proline residues and is hence stabilized. It may then act as a heterodimeric transcription factor to transcribe within the nucleus a large set of genes involved in the regulation of glycolysis and neoangiogenesis (Koh 2012, Semenza 2011). Since O₂ is also the major substrate for the electrons of the respiratory chain, the latter is shut off during hypoxia, and cells must rely on non-oxidative metabolism for ATP production. At normal oxygen condition, increased expression of MDM2 is sufficient to degrade HIF α , as previously demonstrated (Ravi 2000). This study demonstrates that the mechanisms are likely analogous to the O₂-dependent hydroxylation by PHDs, since a mutant HIF1 α did not respond to MDM2 degradation. Similar results were obtained when cells were treated with an inhibitor of PHDs.

Under normoxia, HIF1 α is rapidly degraded, whereas hypoxia leads to stabilization and accumulation of HIF1 α . However, under certain normoxic conditions, typical of cancer cells, HIF1 α

expression can be increased; for example, mutations in the von Hippel- Lindau protein stabilize HIF1 α protein and PI3K/AKT/mTOR activity stimulates translation of HIF1 α mRNA (Gillies 2008, Sun 2007). In this context the relation between genotoxic and hypoxic response may be different. When hypoxia was induced in parallel to a genotoxic stimulus, the former response prevailed over the latter. In fact, cells treated with HIF1 α specific stabilizer DMOG were prevented to undergo cell senescence when irradiated, as indicated by the unequivocal β -galactosidase marker and by the lack of p21 increase. Interestingly, p53 stabilization also appeared to be prevented, consequently there was no increase of its target genes, among which MDM2. In this condition, the absence of MDM2 the hypoxic response prevail over the genotoxic one, and after radiation treatment cells remained still able to replicate. Nonetheless, further investigation is warranted to understand in detail why the p53-p21 axis appears to be repressed upon HIF1 α stabilization.

In terms of mitochondria, it is most interesting that the γ -rays-induced biogenesis is also strongly blunted, in parallel to senescence, during hypoxia. HIF α stabilization blocked the expression of PGC-1 β , and consequently the increase of mitochondrial mass.

These findings therefore point to an indirect control of mitochondrial biogenesis by p53, whose role would be to allow, upon stabilization, MDM2 to be re-directed to HIF1 α , with a subsequent release of the basal inhibition by the latter over PGC-1 β , which appears to be the only master regulator of the PGC family involved in γ -rays induced biogenesis. These data also shed light on the controversial role of MDM2 in orchestrating the balance between genotoxic and hypoxic response (Sermeus 2011, Chen 2003). Although it has been suggested that MDM2 may either degrade or stabilize HIF1 α , the results point to the former hypothesis as the most likely, at least upon γ -rays treatment (Fig. 70).

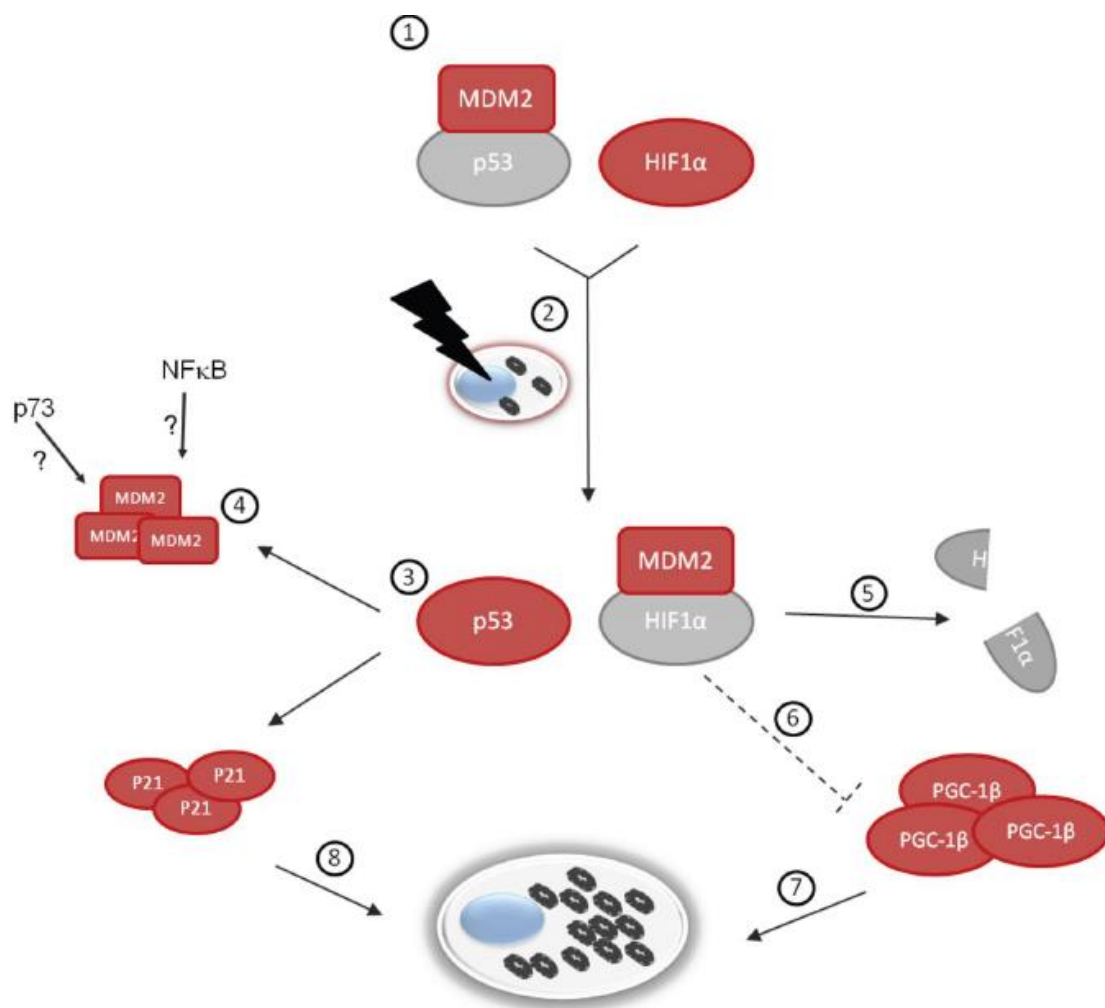


Fig. 70 In normal condition, MDM2 maintains low the expression of p53 (1), upon gamma radiation stimulus (2), the cell triggers the genotoxic response through P53 activation, this impaired the ability of MDM2 to interact with p53 and can be re-directed to HIF1 α (5) and turns to proteosomal degradation of HIF1 α , for which the P402, P564 and N803 HIF1 α residues are necessary. The HIF1 α directed repression of PGC1 β is therefore inhibited (6), which enables activation of mitochondrial biogenesis (7). The stabilization of p53 leads to activation of its target gene, MDM2 (3), that occurs also in absence of p53 (4) and p21. The last protein is necessary for the activation of senescence pathway (8).

The opposing relation between HIF1 α stabilization and mitochondrial biogenesis activation was also demonstrated *in vivo*. Rectal tissues from individuals who underwent radiotherapy for prostate cancer were shown to retain a ‘scar’ of activated mitochondrial biogenesis two months after the withdrawal of the γ -rays stimulus. This occurred only when local hypoxia had not set in, as shown by the decreased HIF1 α expression.

A significance of the increase of mitochondrial mass after irradiation should be deduced by analyses of oncocytic tumors. The irradiated cells presented a typical oncocytic phenotype: abnormal accumulation of mitochondria, low proliferation and destabilization of HIF1 α . The vast majority of oncocytomas are characterized by accumulation of non-functional mitochondria, due to the presence of disruptive mtDNA mutation. To date, there are no data relative to the presence of mutations in mitochondria that accumulate in tissues of patient that undergo radiotherapy and acquired an oncocytic phenotype (Rouzbahman 2006, Ambrosini-Spaltro 2006). After irradiation, cells analysed did not present mutations on the mitochondrial genome, but, interestingly, oncocytomas may develop also in absence of mtDNA mutation. A parotid oncocytoma were described in patients with FLCN mutation, causing the autosomal dominant syndromes Birt–Hogg–Dubè, (Pradella 2013), suggesting that there could be an alternative determinant to pathogenic mtDNA mutation in oncotic phenotype in cancer cells. Oncocytoma are consider a benign lesion, in fact these tumors are characterized by a low-grade of proliferation. This “senescent-like” phenotype is due to a chronic destabilization of HIF1 α , that explains the low aggressive tumor behaviour. It is therefore plausible to interfere regards the benign nature of oncocytic phenotypes occurs after radiation treatment. On the other hand, this thesis work provides an explanation for the reason why HIF1 α is an obligatory condition in oncocytic cell: first of all the activation of hypoxic response impair the increase of mitochondrial biogenesis and through its repressive role on genotoxic response blunts the cell-cycle inhibitor p21, as a consequence tumor cells maintain the capacity to proliferate.

7. CONCLUSION

Today, almost 100 years since the first clinical observation of the importance of hypoxia for radiotherapy, the role of hypoxia has been intensively explored with regard to both its influence on cancer progression and resistance to therapy. Different studies demonstrate that hypoxia is associated with poor prognosis after radiotherapy. For this reason, numerous clinical trials have explored the various means of modifying hypoxia and have demonstrate a significant survival benefit and no difference in the risk of developing distant metastases (Overgaard 2007). Therefore, it is important to develop imaging strategies for both hypoxia and HIF1 α activity (Harada 2011). The principles for measuring hypoxia in human tumors are mainly based on three different methods. The first includes measurement of the physical amount of oxygen in a tissue. The second is the use of hypoxic markers that are reduced under the presence of hypoxia and can subsequently be identified by various imaging methods such as immunohistochemistry or positron emission tomography. The third principle is more indirect because it is an identification of biologic processes, gene expression that are known to be caused by the presence of hypoxia. Most of this is associated with the hypoxia inducible factor-1 alpha cascade (hypoxia inducible factor-1 alpha and carbonic anhydrase IX) or other processes involved in hypoxia (Overgaard 2007).

In this study was demonstrate that mitochondrial biogenesis parameters like mitochondrial DNA copy number could be used for the prediction of hypoxic status of tissue after radiation treatment. γ -rays induce an increase of mitochondrial mass and function, in response to a genotoxic stress that pushes cells into senescence. Mitochondrial biogenesis is only indirectly regulated by p53, whose activation triggers a MDM2-mediated HIF1 α degradation, leading to the release of PGC-1 β inhibition by HIF1 α . On the other hand, this protein blunts the mitochondrial response to γ -rays as well as the induction of p21-mediated cell senescence, indicating prevalence of the hypoxic over the genotoxic response. Finally *in vivo*, post-radiotherapy mtDNA copy number increase well correlates with lack of HIF1 α increase in the tissue, concluding this may be a useful molecular tool to infer the trigger of a hypoxic response during radiotherapy, which may lead to failure of activation of cell senescence.

8. REFERENCES

- Achanta G, Sasaki R, Feng L, Carew JS, Lu W, Pelicano H, Keating MJ, Huang P (2005). Novel role of p53 in maintaining mitochondrial genetic stability through interaction with DNA Pol gamma. *EMBO J.*; 24: 3482-3492.
- Achison M, Hupp TR (2003). Hypoxia attenuates the p53 response to cellular damage. *Oncogene*. May 29;22(22):3431-40.
- Al-Ejeh F, Kumar R, Wiegman A, Lakhani SR, Brown MP, Khanna KK (2010). Harnessing the complexity of DNA-damage response pathways to improve cancer treatment outcomes. *Oncogene*. Nov 18;29(46):6085-98.
- Ambrosini-Spaltro, A, Salvi, F, Betts, CM, Frezza, GP, Piemontese, A, Del Prete, P et al., (2006) Oncocytic modifications in rectal adenocarcinomas after radio and chemotherapy. *Virchows Arch*. 206 448: 442-8.
- Bakhanashvili M, Grinberg S, Bonda E, Simon AJ, Moshitch-Moshkovitz S, Rahav G (2008). p53 in mitochondria enhances the accuracy of DNA synthesis. *Cell Death Differ.*; 15: 1865-1874
- Beausejour, CM, Krtolica, A, Galimi, F, Narita, M, Lowe, SW, Yaswen, P et al., (2003) Reversal of human cellular senescence: roles of the p53 and p16 pathways. *Embo J* 22: 4212-22.
- Benard G, Karbowski M (2009). Mitochondrial fusion and division: Regulation and role in cell viability. *Semin Cell Dev Biol*. May;20(3):365-74.
- Bensaad K, Tsuruta A, Selak MA, Vidal MN, Nakano K, Bartrons R, Gottlieb E, Vousden KH. (2006) TIGAR, a p53-inducible regulator of glycolysis and apoptosis. *Cell*. Jul 14;126(1):107-20.
- Bogenhagen DF, Rousseau D, Burke S (2008). The layered structure of human mitochondrial DNA nucleoids. *J Biol Chem*. Feb 8;283(6):3665-75.
- Bonawitz, ND, Clayton, DA and Shadel, GS (2006), Initiation and beyond: multiple functions of the human mitochondrial transcription machinery. *Mol Cell* 24: 813-25.
- Bonora E, Porcelli AM, Gasparre G (2006), et al. Defective oxidative phosphorylation in thyroid oncocytic carcinoma is associated with pathogenic mitochondrial DNA mutations affecting complexes I and III. *Cancer Res*;66(12):6087-96.

- Bradford MM (1976). A rapid and sensitive method for the quantitation of microgram quantities of protein utilizing the principle of protein-dye binding. *Anal Biochem*;72:248-54.
- Brown, JP, Wei, W and Sedivy, JM, (1997) Bypass of senescence after disruption of p21CIP1/WAF1 gene in normal diploid human fibroblasts. *Science* 277: 831-4.
- Busuttill, V, Droin, N, McCormick, L, Bernassola, F, Candi, E, Melino, G et al., (2010) NF-kappaB inhibits T-cell activation-induced, p73-dependent cell death by induction of MDM2. *Proc Natl Acad Sci U S A* 107: 18061-6.
- Butow RA, Avadhani NG (2004). Mitochondrial signaling: the retrograde response. *Mol Cell*. Apr 9;14(1):1-15.
- Campbell CT, Kolesar JE, Kaufman BA (2012). Mitochondrial transcription factor A regulates mitochondrial transcription initiation, DNA packaging, and genome copy number. *Biochim Biophys Acta*. Sep-Oct;1819(9-10):921-9.
- Campisi, J. & d'Adda di Fagagna, F (2007). Cellular senescence: when bad things happen to good cells. *Nature Rev. Mol. Cell Biol.* 8, 729–740
- Chatterjee A, Mambo E, Sidransky D (2006). Mitochondrial DNA mutations in human cancer. *Oncogene*. Aug 7;25(34):4663-74.
- Chen, D, Li, M, Luo, J and Gu, W, (2003) Direct interactions between HIF-1 alpha and Mdm2 modulate p53 function. *J Biol Chem* 278: 13595-8.
- Curtin NJ (2012). DNA repair dysregulation from cancer driver to therapeutic target. *Nat Rev Cancer*. Dec;12(12):801-17
- Dang CV(2012). Links between metabolism and cancer. *Genes Dev*. May 1;26(9):877-90
- Davis, PK and Dowdy, SF, (2001) p73. *Int J Biochem Cell Biol* 33: 935-9.
- Debacq-Chainiaux, F, Erusalimsky, JD, Campisi, J and Toussaint, O, (2009) Protocols to detect senescence-associated beta-galactosidase (SA-beta-gal) activity, a biomarker of senescent cells in culture and in vivo. *Nat Protoc* 4: 1798-806

- Dent P, Yacoub A, Contessa J, Caron R, Amorino G, Valerie K, Hagan MP, Grant S, Schmidt-Ullrich R (2003). Stress and radiation-induced activation of multiple intracellular signaling pathways. *Radiat Res.* Mar;159(3):283-300.
- Dimmer KS, Scorrano L (2006). (De)constructing mitochondria: what for? *Physiology (Bethesda)*. Aug;21:233-41.
- Falkenberg M, Larsson NG (2007), Gustafsson CM. DNA replication and transcription in mammalian mitochondria. *Annu Rev Biochem.*;76:679-99.
- Fernández-Silva P, Enriquez JA, Montoya J (2003). Replication and transcription of mammalian mitochondrial DNA. *Exp Physiol.* Jan;88(1):41-56.
- Formentini L, Martínez-Reyes I, Cuezva JM (2010). The mitochondrial bioenergetic capacity of carcinomas. *IUBMB Life.* Jul;62(7):554-60.
- Fu X, Wan S, Lyu YL, Liu LF, Qi H (2008). Etoposide induces ATM-dependent mitochondrial biogenesis through AMPK activation. *PLoS One.* Apr 23;3(4):e2009.
- Fuccio, L, Guido, A, Laterza, L, Eusebi, LH, Busutti, L, Bunkheila, F et al., (2011) Randomised clinical trial: preventive treatment with topical rectal beclomethasone dipropionate reduces post-radiation risk of bleeding in patients irradiated for prostate cancer. *Aliment Pharmacol Ther* 34: 628-37.
- Galluzzi L, Morselli E, Kepp O, Vitale I, Rigoni A, Vacchelli E, Michaud M, Zischka H, Castedo M, Kroemer G (2010). Mitochondrial gateways to cancer. *Mol Aspects Med.* Feb;31(1):1-20
- Gasparre G, Porcelli AM, Bonora E, Pennisi LF, Toller M, Iommarini L, Ghelli A, Moretti M, Betts CM, Martinelli GN, Ceroni AR, Curcio F, Carelli V, Rugolo M, Tallini G, Romeo G (2007). Disruptive mitochondrial DNA mutations in complex I subunits are markers of oncocytic phenotype in thyroid tumors. *Proc Natl Acad Sci U S A.* May 22;104(21):9001-6
- Gasparre, G, Bonora, E, Tallini, G and Romeo, G, (2010) Molecular features of thyroid oncocytic tumors. *Mol Cell Endocrinol* 321: 67-76.
- Gasparre G, Porcelli AM, Lenaz G, Romeo G (2013). Relevance of mitochondrial genetics and metabolism in cancer development. *Cold Spring Harb Perspect Biol.* Feb 1;5

Gillies RJ, Robey I, Gatenby RA (2008). Causes and consequences of increased glucose metabolism of cancers. *J Nucl Med*;49 Suppl 2:24S-42S.

Girnun GD (2012). The diverse role of the PPAR γ coactivator 1 family of transcriptional coactivators in cancer. *Semin Cell Dev Biol*. Jun;23(4):381-8.

Gisel, A, Panetta, M, Grillo, G, Licciulli, VF, Liuni, S, Saccone, C et al., (2004) DNafan: a software tool for automated extraction and analysis of user-defined sequence regions. *Bioinformatics* 20: 3676-9.

Gleyzer N, Vercauteren K, Scarpulla RC (2005). Control of mitochondrial transcription specificity factors (TFB1M and TFB2M) by nuclear respiratory factors (NRF-1 and NRF-2) and PGC-1 family coactivators. *Mol Cell Biol*. Feb;25(4):1354-66.

Grillo, G, Licciulli, F, Liuni, S, Sbisà, E and Pesole, G, (2003) PatSearch: A program for the detection of patterns and structural motifs in nucleotide sequences. *Nucleic Acids Res* 31: 3608-12.

Hanahan D, Weinberg RA (2011). Hallmarks of cancer: the next generation. *Cell*. Mar 4;144(5):646-74.

Harada H, Inoue M, Itasaka S, Hirota K, Morinibu A, Shinomiya K, Zeng L, Ou G, Zhu Y, Yoshimura M, McKenna WG, Muschel RJ, Hiraoka M (2012). Cancer cells that survive radiation therapy acquire HIF-1 activity and translocate towards tumour blood vessels. *Nat Commun*. Apr 17;3:783

Hayflick, L, (1965) The Limited in Vitro Lifetime of Human Diploid Cell Strains. *Exp Cell Res* 37: 614-36.

Hiroshi, Harada (2011), How Can We Overcome Tumor Hypoxia in Radiation Therapy? *J. Radiat. Res.*, 52, 545–556

Höckel M, Vaupel P (2001). Tumor hypoxia: definitions and current clinical, biologic, and molecular aspects. *J Natl Cancer Inst*. Feb 21;93(4):266-76.

Icard P, Lincet H (2012). A global view of the biochemical pathways involved in the regulation of the metabolism of cancer cells. *Biochim Biophys Acta*. Dec;1826(2):423-33

Jones RG, Thompson CB (2009). Tumor suppressors and cell metabolism: a recipe for cancer growth. *Genes Dev.* Mar 1;23(5):537-48.

Jung, YS, Qian, Y and Chen, X, (2010) Examination of the expanding pathways for the regulation of p21 expression and activity. *Cell Signal* 22: 1003-12.

Kasiviswanathan R, Collins TR, Copeland WC (2012). The interface of transcription and DNA replication in the mitochondria. *Biochim Biophys Acta.* Sep-Oct;1819(9-10):970-8

Keith B, Johnson RS, Simon MC (2011). HIF1 α and HIF2 α : sibling rivalry in hypoxic tumour growth and progression. *Nat Rev Cancer.* Dec 15;12(1):9-22.

Kim JJ, Tannock, (2005) Repopulation of cancer cells during therapy: an important cause of treatment failure. *Nat Rev Cancer.* Jul;5(7):516-25.

Kluza J, Marchetti P, Gallego MA, Lancel S, Fournier C, et al. (2004) Mitochondrial proliferation during apoptosis induced by anticancer agents: effects of doxorubicin and mitoxantrone on cancer and cardiac cells. *Oncogene* 23: 7018–7030.

Koh, MY and Powis, G, (2012) Passing the baton: the HIF switch. *Trends Biochem Sci* 37: 364-72

Kruse JP, Gu W. (2009), Modes of p53 regulation. *Cell.* May 15;137(4):609-22.

Kukat C, Wurm CA, Spåhr H, Falkenberg M, Larsson NG, Jakobs S. (2011) Super-resolution microscopy reveals that mammalian mitochondrial nucleoids have a uniform size and frequently contain a single copy of mtDNA. *Proc Natl Acad Sci U S A.* 2011 Aug 16;108(33):13534-9.

Liesa, M, Borda-d'Agua, B, Medina-Gomez, G, Lelliott, CJ, Paz, JC, Rojo, M et al.(2008), Mitochondrial fusion is increased by the nuclear coactivator PGC-1beta. *PLoS One* 3: e3613.

Lord CJ (2012), Ashworth A The DNA damage response and cancer therapy. *Nature.* Jan 18;481(7381):287-94.

Lunt SY, Vander Heiden MG (2011). Aerobic glycolysis: meeting the metabolic requirements of cell proliferation. *Annu Rev Cell Dev Biol.*;27:441-64

Luo L, Huang W, Tao R, Hu N, Xiao ZX, Luo Z (2013). ATM and LKB1 dependent activation of AMPK sensitizes cancer cells to etoposide-induced apoptosis. *Cancer Lett.* Jan 1;328(1):114-9

Malakhova, L, Bezlepkin, VG, Antipova, V, Ushakova, T, Fomenko, L, Sirota, N et al.(2005), The increase in mitochondrial DNA copy number in the tissues of gamma-irradiated mice. *Cell Mol Biol Lett* 10: 721-32.

Malka F, Lombès A, Rojo M (2006). Organization, dynamics and transmission of mitochondrial DNA: focus on vertebrate nucleoids. *Biochim Biophys Acta*. May-Jun;1763(5-6):463-72

Manfredi G, Yang L, Gajewski CD, Mattiazzi M (2002). Measurements of ATP in mammalian cells. *Methods*;26(4):317-26.

Manfredi JJ (2010). The Mdm2-p53 relationship evolves: Mdm2 swings both ways as an oncogene and a tumor suppressor. *Genes Dev*. Aug 1;24(15):1580-9.

Mannella CA (2008). Structural diversity of mitochondria: functional implications. *Ann N Y Acad Sci*. Dec;1147:171-9.

Matoba S, Kang JG, Patino WD, Wragg A, Boehm M, Gavrilova O, Hurley PJ, Bunz F, Hwang PM (2006). p53 regulates mitochondrial respiration. *Science*. Jun 16;312(5780):1650-3.

Meijer TW, Kaanders JH, Span PN, Bussink J(2012). Targeting hypoxia, HIF-1, and tumor glucose metabolism to improve radiotherapy efficacy. *Clin Cancer Res*. Oct 15;18(20):5585-94.

Moll UM, Petrenko O (2003). The MDM2-p53 interaction. *Mol Cancer Res*. Dec;1(14):1001-8.

Muller PA, Vousden KH (2013). p53 mutations in cancer. *Nat Cell Biol*. Jan;15(1):2-8

Nardella, C, Clohessy, JG, Alimonti, A and Pandolfi, PP, (2011) Pro-senescence therapy for cancer treatment. *Nat Rev Cancer* 11: 503-11.

Nunnari J, Suomalainen A (2012). Mitochondria: in sickness and in health. *Cell*. Mar 16;148(6):1145-59

Overgaard J (2007). Hypoxic radiosensitization: adored and ignored. *J Clin Oncol*. Sep 10;25(26):4066-74

Pandita, TK, Lieberman, HB, Lim, DS, Dhar, S, Zheng, W, Taya, Y et al. (2000), Ionizing radiation activates the ATM kinase throughout the cell cycle. *Oncogene* 19: 1386-91.

Porcelli AM, Ghelli A, Ceccarelli C, Lang M, Cenacchi G, Capristo M, Pennisi LF, Morra I, Ciccarelli E, Melcarne A, **Bartoletti-Stella** A, Salfi N, Tallini G, Martinuzzi A, Carelli V, Attimonelli M, Rugolo M, Romeo G, Gasparre G. The genetic and metabolic signature of oncogenic transformation implicates HIF1alpha destabilization. *Hum Mol Genet.* 2010 Mar 15;19(6):1019-32.

Pradella LM, Lang M, Kurelac I, Mariani E, Guerra F, Zuntini R, Tallini G, Mackay A, Reis-Filho JS, Seri M, Turchetti D, Gasparre G (2013). Where Birt-Hogg-Dubé meets Cowden Syndrome: mirrored genetic defects in two cases of syndromic oncogenic tumours. *Eur J Hum Genet.* Feb 6

Puigserver, P, Wu, Z, Park, CW, Graves, R, Wright, M and Spiegelman, BM (2008), A cold-inducible coactivator of nuclear receptors linked to adaptive thermogenesis. *Cell* 92: 829-39.

Ravi, R, Mookerjee, B, Bhujwala, ZM, Sutter, CH, Artemov, D, Zeng, Q et al., (2000) Regulation of tumor angiogenesis by p53-induced degradation of hypoxia-inducible factor 1alpha. *Genes Dev* 14: 34-44.

Reiman A, Lu X, Seabra L, Boora U, Nahorski MS, Wei W, Maher ER (2012). Gene expression and protein array studies of folliculin-regulated pathways. *Anticancer Res.* Nov;32(11):4663-70.

Rey S, Lee K, Wang CJ, Gupta K, Chen S, McMillan A, Bhise N, Levchenko A, Semenza GL (2009). Synergistic effect of HIF-1alpha gene therapy and HIF-1-activated bone marrow-derived angiogenic cells in a mouse model of limb ischemia. *Proc Natl Acad Sci U S A.* Dec 1;106(48):20399-404

Rodier F, Campisi J (2011). Four faces of cellular senescence. *J Cell Biol.* Feb 21;192(4):547-56.

Rouzbahman, M, Serra, S and Chetty, R (2006), Rectal adenocarcinoma with oncogenic features: possible relationship with preoperative chemoradiotherapy. *J Clin Pathol* 59: 1039-43.

Ryan MT, Hoogenraad NJ (2007). Mitochondrial-nuclear communications. *Annu Rev Biochem.*;76:701-22.

Sabin RJ, Anderson RM (2011). Cellular Senescence - its role in cancer and the response to ionizing radiation. *Genome Integr.* Aug 11;2(1):7

Sahin, E, Colla, S, Liesa, M, Moslehi, J, Muller, FL, Guo, M et al.(2011), Telomere dysfunction induces metabolic and mitochondrial compromise. *Nature* 470: 359-65.

- Salnikow, K., M. Costa, W. D. Figg, and M. V. Blagosklonny. (2000). Hyperinducibility of hypoxia-responsive genes without p53/p21-dependent checkpoint in aggressive prostate cancer. *Cancer Res.* 60:5630–5634.
- Scarpulla RC (2008). Nuclear Control of Respiratory Chain Expression by Nuclear Respiratory Factors and PGC-1-Related Coactivator. *Ann N Y Acad Sci.* December; 1147: 321–334.
- Scarpulla RC (2011). Metabolic control of mitochondrial biogenesis through the PGC-1 family regulatory network. *Biochim Biophys Acta.* Jul;1813(7):1269-78.
- Scarpulla RC, Vega RB, Kelly DP (2012). Transcriptional integration of mitochondrial biogenesis. *Trends Endocrinol Metab.* Sep;23(9):459-66.
- Schon EA, DiMauro S, Hirano M (2012). Human mitochondrial DNA: roles of inherited and somatic mutations. *Nat Rev Genet.* Dec;13(12):878-90.
- Semenza GL (2003). Targeting HIF-1 for cancer therapy. *Nat Rev Cancer.* Oct;3(10):721-32.
- Semenza, GL, (2007) Oxygen-dependent regulation of mitochondrial respiration by hypoxia inducible factor 1. *Biochem J* 405: 1-9.
- Semenza, GL, (2009) Regulation of oxygen homeostasis by hypoxia-inducible factor 1. *Physiology (Bethesda)* 24: 97-106.
- Semenza, GL, (2011) Oxygen sensing, homeostasis, and disease. *N Engl J Med* 365: 537-47.
- Semenza GL (2012). Cancer-stromal cell interactions mediated by hypoxia-inducible factors promote angiogenesis, lymphangiogenesis, and metastasis. *Oncogene.* Dec 10.
- Sermeus, A and Michiels, C, (2011) Reciprocal influence of the p53 and the hypoxic pathways. *Cell Death Dis* 2: e164.
- Silbergeld DL, Mayberg MR, Berger MS, Ali-Osman F, Kelly WA, Shaw CM (1993). Pituitary oncocytomas: clinical features, characteristics in cell culture, and treatment recommendations. *J Neurooncol*;16(1):39-46.

Singh, KK, (2006) Mitochondria damage checkpoint, aging, and cancer. *Ann N Y Acad Sci* 1067: 182-90.

Sun HL, Liu YN, Huang YT, Pan SL, Huang DY, Guh JH (2007), et al. YC-1 inhibits HIF-1 expression in prostate cancer cells: contribution of Akt/NF-kappaB signaling to HIF-1alpha accumulation during hypoxia. *Oncogene*;26:3941–51

Suzuki M, Boothman (2008). Stress-induced premature senescence (SIPS)-influence of SIPS on radiotherapy. *J Radiat Res*, 49(2):105-112

Trounce IA, Kim YL, Jun AS, Wallace DC (1996). Assessment of mitochondrial oxidative phosphorylation in patient muscle biopsies, lymphoblasts, and transmitochondrial cell lines. *Methods Enzymol*;264:484-509

Vafai SB, Mootha VK (2012). Mitochondrial disorders as windows into an ancient organelle. *Nature*. Nov 15;491(7424):374-83

Vander Heiden MG (2009), Cantley LC, Thompson CB Understanding the Warburg effect: the metabolic requirements of cell proliferation. *Science*. May 22;324(5930):1029-33.

Wallace, DC, (2005) A mitochondrial paradigm of metabolic and degenerative diseases, aging, and cancer: a dawn for evolutionary medicine. *Annu Rev Genet* 39: 359-407.

Wallace DC (2005). The mitochondrial genome in human adaptive radiation and disease: on the road to therapeutics and performance enhancement. *Gene*. Jul 18;354:169-80.

Wallace DC, Fan W, Procaccio V(2010). Mitochondrial energetics and therapeutics. *Annu Rev Pathol.*;5:297-348.

Wallace DC (2007). Why do we still have a maternally inherited mitochondrial DNA? Insights from evolutionary medicine. *Annu Rev Biochem.*;76:781-821.

Wallace, DC, (2012) Mitochondria and cancer. *Nat Rev Cancer* 12: 685-98.

Wang B, Xiao Z, Ko HL, Ren EC (2010). The p53 response element and transcriptional repression. *Cell Cycle*. Mar 1;9(5):870-9.

Westermann B (2008). Molecular machinery of mitochondrial fusion and fission. *J Biol Chem*. May 16;283(20):13501-5

Wong LJ (2010). Molecular genetics of mitochondrial disorders. *Dev Disabil Res Rev.* Jun;16(2):154-62.

Yoshida Y, Izumi H, Torigoe T, Ishiguchi H, Itoh H, Kang D, Kohno K (2003). P53 physically interacts with mitochondrial transcription factor A and differentially regulates binding to damaged DNA. *Cancer Res.* Jul 1;63(13):3729-34.

Youle RJ, van der Bliek AM (2012). Mitochondrial fission, fusion, and stress. *Science.* Aug 31;337(6098):1062-5
Chan DC. Mitochondrial fusion and fission in mammals. *Annu Rev Cell Dev Biol.* 2006;22:79-99.

Youlyouz-Marfak, I, Gachard, N, Le Cloennec, C, Najjar, I, Baran-Marszak, F, Reminieras, L et al.(2008), Identification of a novel p53-dependent activation pathway of STAT1 by antitumour genotoxic agents. *Cell Death Differ* 15: 376-85.

Zanna C, Ghelli A, Porcelli AM, Martinuzzi A, Carelli V, Rugolo M (2005). Caspase-independent death of Leber's hereditary optic neuropathy cybrids is driven by energetic failure and mediated by AIF and Endonuclease G. *Apoptosis*;10(5):997-1007.

Zhang, H, Gao, P, Fukuda, R, Kumar, G, Krishnamachary, B, Zeller, KI et al. (2007), HIF-1 inhibits mitochondrial biogenesis and cellular respiration in VHL-deficient renal cell carcinoma by repression of C-MYC activity. *Cancer Cell* 11: 407-20.

9. APPENDIX A

Primer *TP53* sequencing

	PRIMER FW	PRIMER RV
Exon 2/3	5'-ATCCCCACTTTTCCTTGC-3'	5'-AGCCCAACCCTTGTCCCTAC-3'
Exon 4	5'-CCTGGTCCTCTCTGACTGCTCT-3'	5'-CAGGCATTGAAGTCTCATGG-3'
Exon 5	5'-CTGTCTCCTTCCTCTTCTACAG-3'	5'-AACCAGCCCTGTCGTCTCT-3'
Exon 6	5'-CAGGCCTCTGATTCCTCACT-3'	5'-CTTAACCCCTCCTCCCAGAC-3'
Exon 7	5'-CTCATCTTGGGCCTGTGT-3'	5'-TGGAAGAAATCGGTAAGAGGTG-3'
Exon 8	5'-GGGACAGGTAGGACCTGATTT-3'	5'-ATAACTGCACCCTTGGTCTCC-3'
Exon 9	5'-GGGACAGGTAGGACCTGATTT-3'	5'-TCAGGCAAAGTCATAGAACCA-3'
Exon 10	5'-AACTTGAACCATCTTTAACTCAGC-3'	5'-GGAATCCTATGGCTTTCCAAC-3'
Exon 11	5'-GTCATCTCTCCTCCCTGCTTC-3'	5'-CACAACAAAACACCAGTGCAG-3'

Primer Real-time PCR

	PRIMER FW	PRIMER RV
PGC-1β	5'-AGTCAACGGCCTTGTGTTAAGAG-3'	5'-ACAACCTTCGGCTCTGAGACTG-3'
HIF1α	5'-TTTTTCAAGCAGTAGGAATTGGGA-3'	5'-GTAATGTAGTAGCTGCATGATC-3'
P21	5'-CCGAAGTCAGTTCCTTGTGG -3'	5'-CATGGGTTCTGACGGACAT -3'
BAX	5'-AGCAAACCTGGTGCTCAAGG-3'	5'-TCTTGGATCCAGCCCAAC-3'
GADD45A	5'-GAGAGCAGAAGACCGAAAGG-3'	5'-TGACTCAGGGCTTTGCTGA-3'
MT-ND5	5'-ATCCTTCTTGCTCATCAGTTG-3'	5'-GGCTATTTGTTGTGGGTCTC-3'

Primer Chromatin Immunoprecipitation

	PRIMER FW	PRIMER RV
PGC-1β REp53	5'-CACTCCCAAGTTTGGCCTC -3'	5'-AGCACTAAGGACTTGAATTCTC-3'
P21 RE_p53	5'-GTGGCTCTGATTGGCTTTCTG -3'	5'-CTGAAAACAGGCAGCCCAAG -3'

10.PUBLICATION

Porcelli AM, Ghelli A, Ceccarelli C, Lang M, Cenacchi G, Capristo M, Pennisi LF, Morra I, Ciccarelli E, Melcarne A, **Bartoletti-Stella** A, Salfi N, Tallini G, Martinuzzi A, Carelli V, Attimonelli M, Rugolo M, Romeo G, Gasparre G. The genetic and metabolic signature of oncocytic transformation implicates HIF1alpha destabilization. *Hum Mol Genet.* 2010 Mar 15;19(6):1019-32.

Bartoletti-Stella A, Salfi NC, Ceccarelli C, Attimonelli M, Romeo G, Gasparre G. Mitochondrial DNA mutations in oncocytic adnexal lacrimal glands of the conjunctiva. *Arch Ophthalmol.* 2011 May;129(5):664-6.